PREPARATION AND CHARACTERIZATION OF TiO_2 WORKING ELECTRODE AND COUNTER ELECTRODE FOR DYE SENSITIZED SOLAR CELL

SOMPHOP MORADA

A THESIS SUBMITTED IN PARTIAL FULFILLMENT OF THE REQUIREMENTS FOR THE DEGREE OF MASTER OF SCIENCE

MAJOR IN CHEMISTRY FACULTY OF SCIENCE

UBON RATCHATHANI UNIVERSITY

YEAR 2013

UBON RATCHATHANI UNIVERSITY

THESIS APPROVAL

MASTER OF SCIENCE

MAJOR IN CHEMISTRY FACULTY OF SCIENCE

TITLE PREPARATION AND CHARACTERIZATION OF TiO_2 WORKING ELECTRODE AND COUNTER ELECTRODE FOR DYE SENSITIZED SOLAR CELL

AUTHOR MR.SOMPHOP MORADA

EXAMINATION COMMITTEE

DR. MANTHANA JARIYABOON	CHAIRPERSON
ASST. PROF. DR. TAWEESAK SUDYOADSUK	MEMBER
DR. TINNAGON KEAWIN	MEMBER
ASST. PROF. DR. SIRIPORN JUNGSUTTIWONG	MEMBER
ASSOC. PROF. DR. VINICH PROMARAK	MEMBER

ADVISOR

T. Sudyoadsuk
....

(ASST. PROF. DR. TAWEESAK SUDYOADSUK)

....	H. Juthamas ....
(ASSOC. PROF. DR. UTITH INPRASIT)	(DR. JUTHAMAS HONGTHONG)
DEAN, FACULTY OF SCIENCE	ACTING FOR VICE PRESIDENT
	FOR ACADEMIC AFFAIRS

ACADEMIC YEAR 2013

ACKNOWLEDGMENTS

This work was carried out at Center for Organic Electronic and Alternative Energy (COEA) during September 2010 - March 2014. I would like to thank Asst. Prof. Dr. Taweesak Sudyoadsuk, my supervisor, for his excellent suggestions, supervision, and understanding throughout my study. I wish to acknowledge Dr. Manthana Jariyaboon, Dr. Tinnagon Keawin and Asst. Prof. Dr. Siriporn Jungsuttiwong for constructive comments and suggestion. I would also like to thank many people who contributed their time, instrumentation, and advice to this project. In particular, Asst. Prof. Dr. Aranya Pimmongkol for SEM experiment, Asst. Prof. Dr. Anuson Niyompan for XRD experiment, Assoc. Prof. Dr. Vinich Promarak for providing ideas and special guidelines.

Thanks so much to Center of Excellence for Innovation in Chemistry (PERCH-CIC) and Ubon Ratchathani University for financial support. My sincere thankful the Department of Chemistry, Faculty of Science, Ubon Ratchathani University for providing a wonderful academic environment during the course work.

I would also like to thank Dr. Tanika Khanasa, Dr. Kanokkorn Sirithip, Mrs. A-monrat Tankthong and Mr. Sakravee Punsay for synthesis of organic dye molecules. I feel thankful to my friends, sisters and brothers particularly Dr. Narid Prachumrak, Dr. Pongsathorn Tongkasee, Mr. Theerawat Naowanont and Miss. Niparat Tidutit. Most of all, I feel appreciate and grateful to my beloved family for their inculcation and encouragement that found me to be a fortitude person.

S. Morada

(Mr. Somphop Morada)

Researcher

บทคัดย่อ

ชื่อเรื่อง : การเตรียมและพิสูจน์เอกลักษณ์ขั้วไฟฟ้าทำงานไททาเนียมไดออกไซด์และขั้วไฟฟ้าเคาน์เตอร์สำหรับเซลล์แสงอาทิตย์ชนิดสีย้อมไวแสง

โดย : สมภพ มรดา

ชื่อปริญญา : วิทยาศาสตรมหาบัณฑิต

สาขาวิชา : เคมี

ประธานกรรมการที่ปรึกษา : ผู้ช่วยศาสตราจารย์ ดร.ทวีศักดิ์ สุดยอดสุข

ศัพท์สำคัญ : ขั้วไฟฟ้าทำงานไททาเนียมไดออกไซด์ / ขั้วไฟฟ้าช่วยงาน / เซลล์แสงอาทิตย์ชนิดสีย้อมไวแสง

ประสิทธิภาพการเปลี่ยนพลังงานแสงเป็นพลังงานไฟฟ้าของเซลล์แสงอาทิตย์ชนิดสีย้อมไวแสงสามารถพัฒนาได้ โดยการศึกษาสมบัติโฟโตโวลทาอิกของสีย้อมไวแสง งานวิจัยนี้มุ่งศึกษาสภาวะที่เหมาะสมสำหรับการขึ้นรูปเซลล์แสงอาทิตย์ชนิดสีย้อมไวแสงได้เลือกใช้ความหนาแผ่นประสาน 30 ไมโครเมตร ความหนาชั้นฟิล์มไททาเนียมไดออกไซด์ 11 ไมโครเมตร ปริมาณโลหะแพลทินัม 8 ไมโครกรัมต่อตารางเซนติเมตร การปรับสภาพด้วยไททาเนียมเททระคลอไรด์สำหรับสร้างเซลล์แสงอาทิตย์ชนิดสีย้อมไวแสงที่มีประสิทธิภาพที่ดี

ศึกษาสมบัติโฟโตโวทาอิกของสีย้อมอินทรีย์ TPA (2D-D-p-A) และDPA (D-D-p-A) ถูกตรวจพิสูจน์ พบว่าค่าความหนาแน่นกระแสไฟฟ้า และประสิทธิภาพการเปลี่ยนแปลงพลังงานแสงเป็นพลังงานไฟฟ้าเพิ่มขึ้น เมื่อเพิ่มจำนวนหมู่ให้อิเล็กตรอนด้วยหมู่คาร์บาโซล และแถบการดูดกลืนแสงกว้างขึ้น โดยขยับไปทางคลื่นแสงสีแดง เมื่อมีการเพิ่มความยาวคอลจูเกตด้วยหมู่ไธโอฟีน เซลล์แสงอาทิตย์ชนิดสีย้อมไวแสงที่ใช้สีย้อม DPA3 และ TPA3 แสดงประสิทธิภาพการเปลี่ยนพลังงานแสงเป็นพลังงานไฟฟ้าคิดเป็นร้อยละ 76 และร้อยละ 84 ตามลำดับ โดยเฉพาะเซลล์แสงอาทิตย์ที่ใช้สีย้อม CCT3A คิดเป็นร้อยละ 94 เมื่อเปรียบเทียบกับประสิทธิภาพที่ได้จากสีย้อมมาตรฐาน N3

ABSTRACT

TITLE : PREPARATION AND CHARACTERIZATION OF TiO_2 WORKING ELECTRODE AND COUNTER ELECTRODE FOR DYE SENSITIZED SOLAR CELL

BY : SOMPHOP MORADA

DEGREE : MASTER OF SCIENCE

MAJOR : CHEMISTRY

CHAIR : ASST. PROF. TAWEESAK SUDYOADSUK, Ph.D.

KEYWORDS : TIO_2 WORKING ELECTRODE / COUNTER ELECTRODE / DYE SENSITIZED SOLAR CELL

The power conversion efficiency (%PCE) of DSSC devices can be improved by development of novel sensitizer which have good photovoltaic characteristic. This research has focused on the optimization condition for fabrication of dye-sensitized solar cell. A 30 μm sealant thickness, 11 μm TiO_2 film thicknesses, 8 $\mu g/cm^2$ platinum loading, $TiCl_4$ treatment and device masking were applied to obtain the good photovoltaic characteristic of DSSC devices. This method was applied to evaluated photovoltaic characteristic of novel organic dye.

The photovoltaic properties of DSSC device based on TPA (2D-D-p-A) and DPA (D-D-p-A) organic dyes were investigated. The J_{sc} and %PCE of DSSC devices increased when increased the carbazole electron donor unit. The bathochromically red shift and broad extended the IPCE spectra were observed when extend the conjugate lengths with thiophene unit. The DSSC device based on DPA3 and TPA3 dye exhibited the %PCE of 76% and 84%, respectively, particularly DSSC devices base on CCT3A dye, which 94% compared with the standard N3 dyes.

CONTENTS

CONTENTS (CONTINUED)

CONTENTS (CONTINUED)

LIST OF TABLES

LIST OF FIGURES

LIST OF FIGURES (CONTINUED)

FIGURE **PAGES**

LIST OF FIGURES (CONTINUED)

FIGURE **PAGES**

LIST OF ABBREVIATIONS

ABBREVIATION	FULL WORD
A	Ampere
AcN	Acetronitrites
AM	Air mass
CB	Conduction band
CE	Counter electrode
DMSO	Dimethylsulphoxide
DSSCs	Dye sensitized solar cells
eV	Electron volt
FF	Fill factor
FTO	Fluorine doped tin oxide
G	Global
GBL	Gamma-butyrolactone
h	Hour/hours
HOMO	Highest occupied molecular orbital
HTM	Hole transporting materials
I	Current (A)
Ils	Ionic liquids
IPCE	Incident photon to current conversion efficiency
IR	Infrared
I_{sc}	Short circuit current
J_{sc}	Short circuit current density
J_{max}	Maximum current density
LHE	Light harvesting efficiency
LUMO	Lowest unoccupied molecular orbital

LIST OF ABBREVIATIONS (CONTINUED)

ABBREVIATION	FULL WORD
M	Molar concentration
mA	Milliampare
min	Minutes
mg/mL	Milligram per milliliter
mmol	Millimoles
mol	Mole
nm	Nanometers
NMP	*N*-methyl-2-pyrrolidone
ppm	Parts per million
Pt	Platinum
PV	Photovolatics
s	Second
R_{ct}	Charge transfer resistance
R_s	Series resistance
UV	Ultra violet
V	Voltage (V)
V_{max}	Maximum voltage
V_{oc}	Open circuit voltage
W	Watt
WE	Working electrode
Wp	Watt peak

LIST OF ABBREVIATIONS (CONTINUED)

ABBREVIATION	FULL WORD
Å	Angstrom (10^{-10}m)
^{o}C	Degree of celsius
ε	Molar extinction coefficients
η	Overall light to electric power conversion efficiency (%PCE)
μm	Micrometers
%v/v	Percentage volume by volume
λ	Wavelength (nm)
S^{+}	Excited dye
$S^{\bullet}$	Original state

CHAPTER 1

INTRODUCTION

This chapter describes the photovoltaic technology, dye-sensitized solar cells technology and the objective of this work.

1.1 Photovoltaic technology

Advancement in technology and global economic growth has led to a boom in energy demand over the past years. There is high consumption and need for more energy.

Presently, the energy economy is still highly dependent on three forms of fossil fuels - oil, natural gases and coal with percentages of 36.4%, 23.5% and 27.8%, respectively. However, in the near future there will be a replacement of fossil fuels as the world's primary energy resource. With an annual consumption of 82.5 millionbarrels/years, oil might run out in around 40 years at current reserves-to-production (R/P) ratio. A better synopsis is for natural gases that can last for 60 years and coal being the most abundant for 150 years [1].

Meanwhile, there is increasing awareness that environmental pollution arises from the combustion of these fossil fuels. This necessitates urgent promotion of alternatives in renewable energy sources to cover the substantial deficit left by fossil fuels. Figure 1.1 shows all the available technologies for producing renewable energy.

(a) (b) (c)

Figure 1.1 The renewable energy: (a) solar cell, (b) biomass and (c) wind technology [2-4].

However, photovoltaic or solar technology is a hot topic in current research. One simple reason is that the Earth receives 1.2 x 10^{17} W insolation or 3 x 10^{24} J of energy per year from the Sun and this means covering only 0.13% of the Earth's surface with solar cells with an efficiency of 10% would satisfy our present needs. Figure 1.2 shows the isoflux contour plots, the worldwide solar radiation measurements could give an indication of solar insolation across the world. The unit are in MJ/m^2 and give the solar insolation falling on a horizontal surface per day.

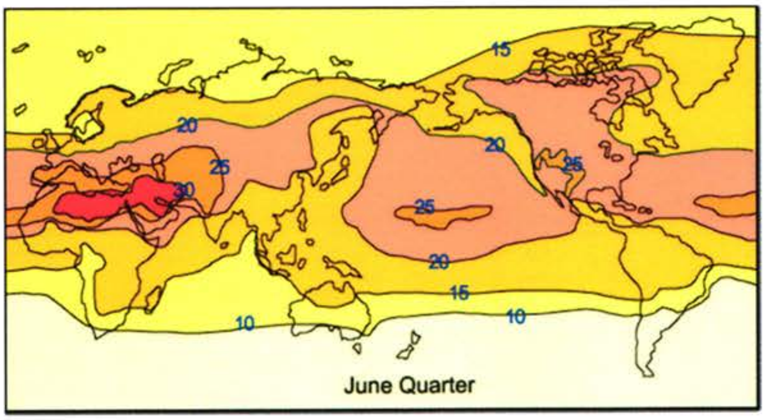

Figure 1.2 The average quarterly global isoflux contour plots for each quarter in the year [5].

Apart from the abundance of potentially exploitable solar energy, photovoltaic cells also have other competitive advantages such as little need for maintenance, off-grid operation and silence, which are ideal for usage in remote sites or mobile applications. Therefore, the world strategies energy perspective on how various solar technologies has been suffice to global energy demand. The photovoltaic cells are a promising technology to capture the sunlight and turn it into electric power. The photovoltaic cell is also sometimes called "solar cell".

The solar cell production has grown at 30% per annum over the past 30 years. A selling price of \$2/Wp. The conventional cell of today, the first generation solar cells was based on a crystalline silicon (c-Si) technology (Figure 1.3). A second generation of solar cells, based on thin film technologies includes amorphous silicon (a-Si), CIGS and CdTe. The advantages of such solar cells include ease of manufacturing, a wider range of applications with attractive appearance, and possibilities of using flexible substrates [6].

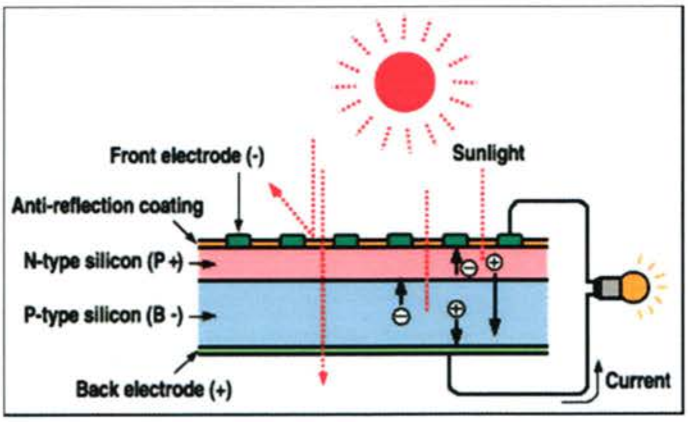

Figure 1.3 Schematic basic composition of single-junction silicon solar cell [7].

However, both the first and second generation solar cells are based on single-junction devices and the fabrication process was requires high energy intensive (high temperature and high vacuum processes) [8]. Therefore, the photovoltaic sell price was very expensive. The theoretical maximum efficiency for such cells is 31% - the so-called Shockley-Queissar limit.

These limitations were overcomed by third-generation solar cells technologies. That is utilizing the nano-scale properties of devices. In principle, sunlight can be converted to electricity at efficiency close to the Carnot limit of around 94%. The primary goal for the third generation solar cells is to produce electricity at a price that is competitive with conventional fossil fuel sources: that is, less than $0.5/Wp [9].

1.2 Dye-sensitized Solar cells

In 1991 O'Regan and Grätzel published a breakthrough of an alternative solar harvesting device, yielding a solar energy conversion to electricity of 7%, based on a sensitizer and mesoscopic inorganic semiconductor (see Figure 1.4). The sensitized nanocrystalline photovoltaic device was new comer name the dye-sensitized solar cells (DSSCs) [10].

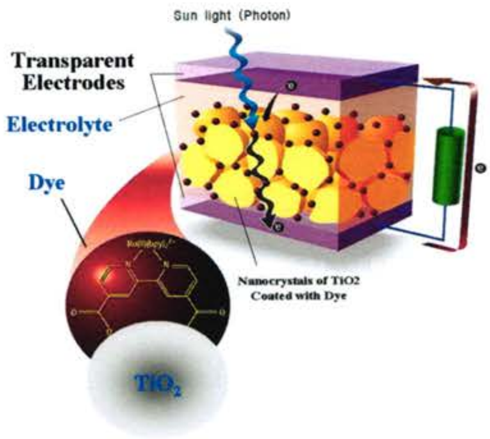

Figure 1.4 Schematic basic compositions of DSSCs [11].

With the discovery of the N3 dye and the later panchromatic "black dye", the power to electricity conversion efficiency was pushed well over 10% [12-13]. An interesting modification to this classic system was replacing the electrolyte with a solid hole conductor, yielding an all-solid state dye-sensitized device [14-17]. Recent achievements of long time stability under accelerated experiments with quasi-solid molten salt (ionic liquid) [18-19], polymer gel [20-21] electrolyte greatly promoted the practical application of this third generation photovoltaic technology and put it currently right at the start of commercialization stage. Therefore, DSSCs are interesting choices for a third generation technology. Figure 1.5 shows development chart of photovoltaic technology as recorded by the national renewable energy laboratory [22].

1.3 Objectives of this thesis

The objectives of this work are as follow;

(1) To investigation the fabricated condition of DSSC devices.

(2) To characterization physical properties and photovoltaic characteristic of DSSCs

(3) To characterization photovoltaic characteristic of novel organic dye.

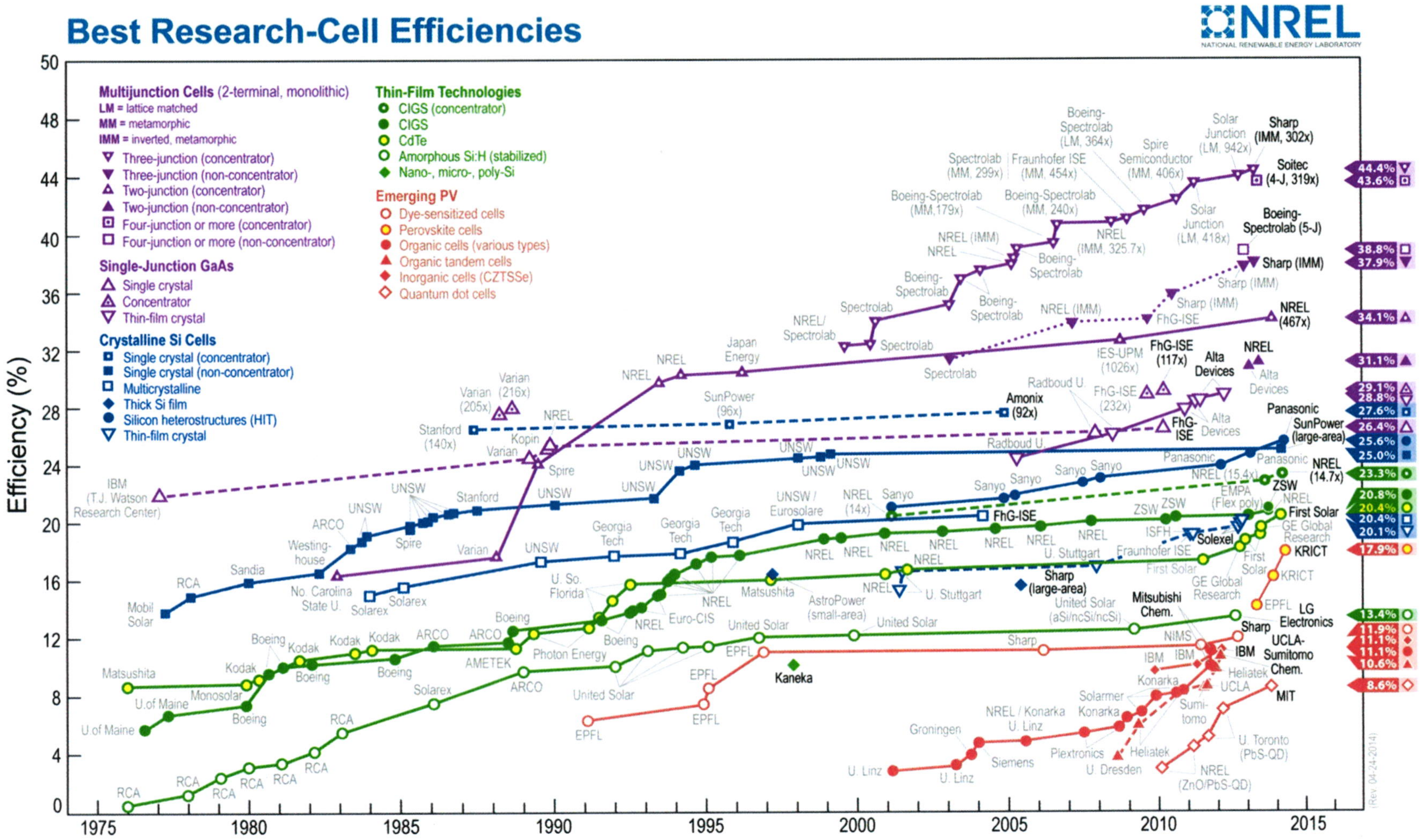

Figure 1.5 The development chart in conversion efficiencies of photovoltaic device [22]

CHAPTER 2

THE THEORY AND LITERATURE REVIEWS

The theoretically and literature reviews of device fabrication of dye sensitized solar cells were described in this chapter.

2.1 The DSSCs configuration and component

The dye-sensitized solar cell (DSSCs) generate electric power from light without suffering any permanent chemical transformation. The DSSCs main components consist of working electrode, a counter electrode and a liquid redox electrolyte (see Figure 2.1).

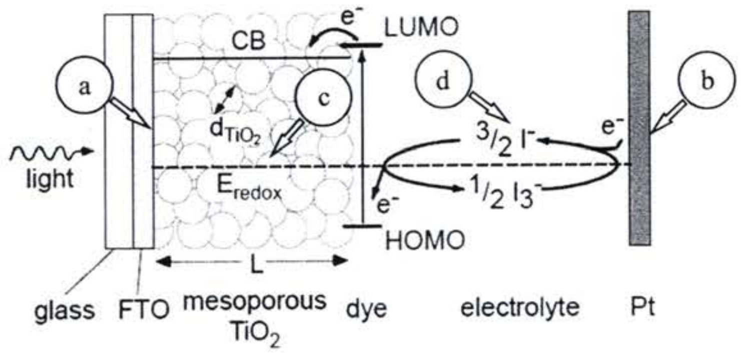

Figure 2.1 The schematic drawing of the DSSCs key components. The configuration consist of (a) Working electrode (WE): porous TiO_2 attached to a fluorine doped tin oxide (FTO), (b) Counter electrode (CE): platinum nano particle attached to a fluorine doped tin oxide (FTO), (c) Light absorbing layer: adsorbed sensitizing dye/ chromophore and (d) Redox system: liquid electrolyte containing the iodide/tri-iodide (I^-/I_3^-) [23].

Figure 2.1 shows the schematic drawing of basic composition of DSSCs, commonly in four parts. The working electrode (WE) usually is nanocrystalline semiconductor such as TiO_2, although alternative wide band gap oxides such as ZnO. A monolayer of the sensitizer is attached to the surface of the semiconductor. Photoexcitation of the sensitizer results in the injection of an electron into the conduction band of the semiconductor.

The counter electrode (CE) usually is fluorine-doped tin oxide (FTO) glass coated with platinum to afford more reversible electron transfer. It is the interfaced where the oxidized species in the electrolyte (or holes) is reduced and an equally important component of DSSCs.

The chromophore are the key component to light harvesting of the sun light. In addition, chromophore in some time calls the sensitizers or dye. The best chromophore relates to some basic criteria. The HOMO potential of the dye should be sufficiently positive to match the potential of the electrolyte redox potential for efficient dye regeneration. The LUMO potential of the dye should be sufficiently negative to match the potential of the conduction band edge of the semiconductor (TiO_2) and the broadening the absorption light in the visible to near infrared region [24].

The electrolyte was combined with two redox mediators such as I^-/I_3^-, usually dissolved in an organic solvent. The electrolyte was operated in series of transport the positive and negative charges to regenerate the dye. The electron donation to the chromophore by iodide is compensated by the reduction of tri-iodide at the counter electrode and the circuit is completed by electron migration through the external load.

2.2 The basic principle of DSSCs operation

The DSSC devices are brought together to generate electric power from light without suffering any permanent chemical transformation. Figure 2.2 shows a scheme of dynamics processes involved in such a DSSCs device. The conceptual of basic operation start with sunlight enters the cell through the transparent FTO top contact, striking the dye on the surface of the TiO_2. Photons striking the dye with enough energy to be absorbed create an excited state of the dye, from which an electron can be "injected" directly into the conduction band of the TiO_2. From there it moves by diffusion (as a result of an electron concentration gradient) to the clear anode on top. Meanwhile, the dye molecule has lost an electron and the molecule will decompose if another electron is not provided. The dye strips one from iodide in electrolyte below the TiO_2, oxidizing it into triiodide. This reaction occurs quite quickly compared to the time that it takes for the injected electron to recombine with the oxidized dye molecule, preventing this recombination reaction that would effectively short circuit the solar cell. The triiodide then recovers its missing electron by mechanically diffusing to the bottom of the cell, where the counter electrode re-introduces the electrons after flowing through the external circuit [25, 26].

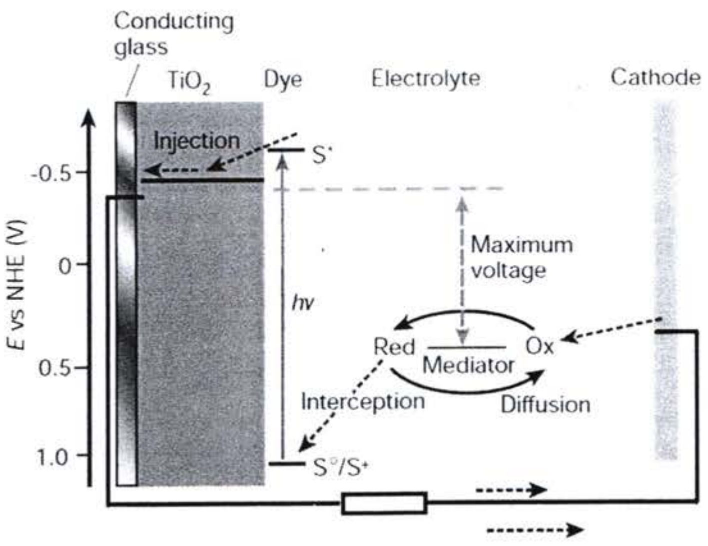

Figure 2.2 The schematic operation of DSSCs [8].

Upon illumination, the sensitizer is photo excited (1) and electron injection is ultrafast from S* to TiO_2 (2) on the sub pico-second time scale (intramolecular relaxation of dye excited states might complicate the injection process and change the timescale, where they are rapidly (less than 10 fs) thermalized by lattice collisions and phonon emissions. The nanosecond ranged relaxation of S^* (3) is rather slow compared to injection, ensuring the injection efficiency to be unity. The ground state of the sensitizer is then recuperated by I^- in the microsecond domain (4), effectively annihilating S^+ and intercepting the recombination of electron in TiO_2 with S^+ (5) that happens in the millisecond time range. This is followed by the two most important processes electron percolation across the nanocrystalline film and the redox capture of the electron by the oxidized relay (back reaction, 6), I_3^-, within milliseconds or even seconds. The similarity in time constants of both processes induces a practical issue on achieving high conversion efficiencies in DSSCs [27, 28].

$S|TiO_2 + h\nu$	$\longrightarrow$	$S^{\bullet}| TiO_2$	Photo excitation	(1)
$S^{\bullet}| TiO_2$	$\longrightarrow$	$S^{+}| TiO_2 + e^{-}_{cb}(TiO_2)$	Charge injection	(2)
$S^{\bullet}| TiO_2$	$\longrightarrow$	$S|TiO_2 + h\nu'$	Relaxation	(3)
$2S^{+}|TiO_2 + 3I^{-}$	$\longrightarrow$	$2S|TiO_2 + I_3^{-}$	Regeneration	(4)
$S^{+}| TiO_2 + e^{-}(TiO_2)$	$\longrightarrow$	$S|TiO_2$	Recombination	(5)
$2e^{-}(TiO_2) + I_3^{-}$	$\longrightarrow$	$3I_2^{-}$	Back reaction	(6)

2.3 The properties of sun light and simulate sun light

2.3.1 The solar radiation at the earth surface

The earth continuously receives about 174 x 10^{15} W of incoming solar irradiation at the upper atmosphere. When it meets the atmosphere, 6% of the irradiation is reflected and 16% is absorbed. The sun ray outside the earth's atmosphere travel parallel to each other. The interaction of solar radiation with earth's atmosphere is shown in Figure 2.3.

As the sunlight travels through the atmosphere, chemicals interact with the sunlight and absorb certain wavelengths. Perhaps the best-known example is the stripping of ultraviolet light by ozone in the upper atmosphere, which dramatically reduces the amount of short-wavelength light reaching the Earth's surface. A more active component of this process is water vapor, which results in a wide variety of absorption bands at many wavelengths, while molecular nitrogen, oxygen and carbon dioxide add to this process.

The atomic and molecular oxygen and nitrogen absorb very short wave radiation effectively blocking radiation with wavelengths <190 nm. When molecular oxygen in the atmosphere absorbs short wave ultraviolet radiation, leads to the production of ozone. Ozone strongly absorbs longer wavelength ultraviolet in the band from 200 - 300 nm and weakly absorbs visible radiation. The water vapor, carbon dioxide, and to a lesser extent, oxygen, selectively absorb in the near infrared. These effects were several impacts on the solar radiation at the Earth's surface. The major effects for photovoltaic applications are reduced power of the solar radiation due to absorption, scattering and reflection by water vapour, clouds and pollution. It is loss of solar radiation and changing terrestrial solar spectrum at earth surface [29].

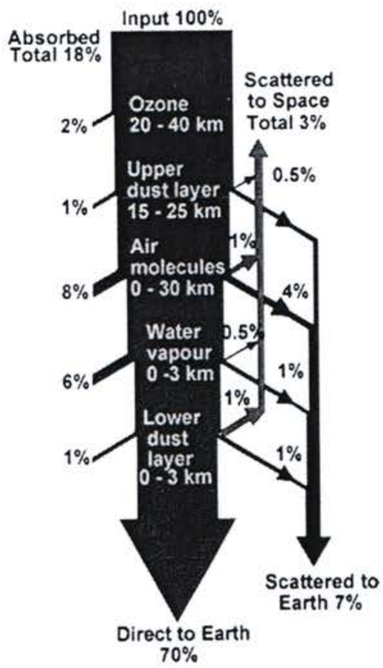

Figure 2.3 The interaction of solar radiation at the earth atmosphere [29].

2.3.2 Air Mass

The Air Mass is the path length which light takes through the atmosphere normalized to the shortest possible path length (that is, when the sun is directly overhead). The Air Mass quantifies the reduction in the power of light as it passes through the atmosphere and is absorbs by air and dust. The Air Mass (AM) is defined as

$$\mathrm{AM} = \frac{1}{\cos(\theta)} \tag{7}$$

Where θ is the angle from the vertical (zenith angle). The AM 1 is that the sun directly overhead. The air mass number is thus dependent on the sun's elevation path through the sky and therefore varies with time of day and with the passing seasons of the year, and with the latitude of the observer. The schematic diagram of solar air mass is shown in Figure 2.4.

The estimation of air mass coefficient are considered to be effectively concentrated into around the bottom 9 km, i.e. essentially all the atmospheric effects are due to the atmospheric mass in the lower half of the Troposphere. This is a useful and simple model when considering the atmospheric effects on solar intensity [30, 31].

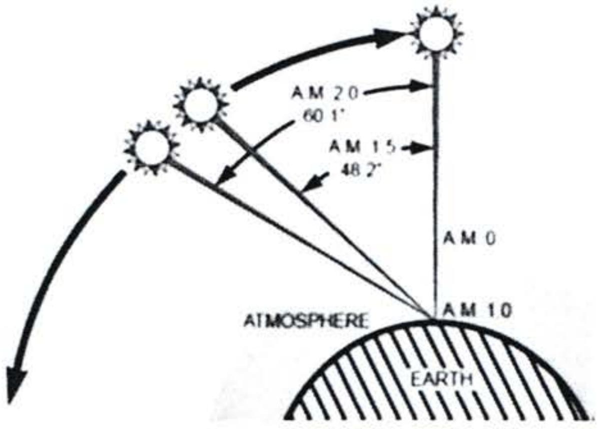

Figure 2.4 The schematic diagram of solar air mass [30].

2.3.3 Standard solar spectrum and solar irradiation

The efficiency of a solar cell is sensitive to variations in both the power and the spectrum of the incident light. To facilitate an accurate comparison between solar cells measured at different times and locations, a standard spectrum and power density has been defined for both radiations outside the earth's atmosphere and at the earth's surface.

The standard spectrum outside the earth's atmosphere is called AM 0, because at no stage does the light pass through the atmosphere. This spectrum is typical by used to predict the expected performance of cells in space.

The standard spectrum at the earth's surface is usually used AM 1.5G, which the G stands for global and includes both direct and diffuse radiation. The most widely used standard spectra are those published by the Committee Internationale d'Eclaraige (CIE), the world authority on radiometric and photometric nomenclature and standards. The American Society for Testing and Materials (ASTM) publish three spectra, AM 0 AM 1.5 direct and AM 1.5 global for a 37° tilted surface [5, 30, 31].

Figure 2.5 shows typical of AM 1.5 in standard direct and global spectra. These curves are from the data in ASTM standards, E891 in direct spectrum and E892 for global, a turbidity of 0.27 and a tilt of 37° facing the sun and a ground albedo of 0.2. The standard AM 1.5G spectrum (radiation at sea level) has been normalized to give 1 kW/m^2 [32].

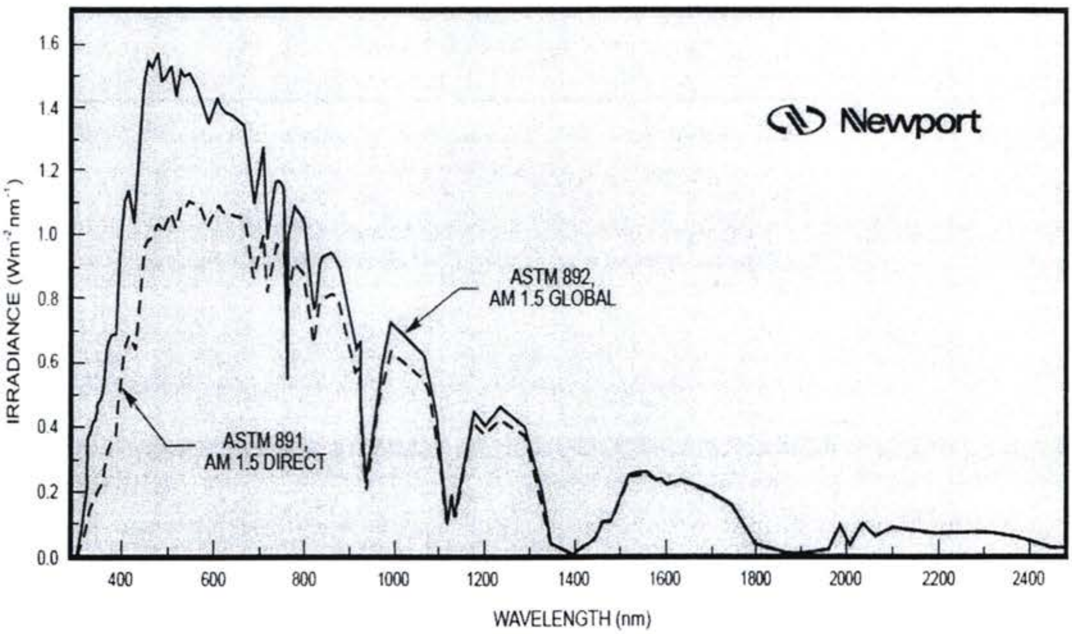

Figure 2.5 Standard spectra for AM 1.5 [32].

2.4 The evaluation of photovoltaic characteristic

2.4.1 Overall power conversion efficiency of DSSCs

The overall power conversion efficiency of the photovoltaic cell (%PCE) was investigated by current-voltage (*J-V*) measurement. The measurement are monitored under illumination white light irradiation by varying an external load from zero load (short circuit condition) to infinite load (open-circuit condition). The photovoltaic characteristic are illustrated by a *J-V* curve (Figure 2.6). The power conversion efficiency is defined as

$$\%\mathrm{PCE} = \eta = \frac{\mathrm{P_{out}}}{\mathrm{P_{in}}} = \frac{J_{sc} \times V_{oc} \times \mathrm{FF}}{\mathrm{P_{in}}} \tag{8}$$

The maximum power is generated when the product of the maximum current density (J_{max}) and maximum voltage (V_{max}), since the electrical power is given by current (J_{sc}) times voltage (V_{oc}), i.e P = IV. The degree of the squared shape of the curve is given by the fill factor (FF), the ratio of current (J_{max}) and voltage (V_{max}) at the maximum power point by short circuit current density (J_{sc}) and open circuit voltage (V_{oc}) [25, 33-34]. The fill factor is defined as

$$FF = \frac{J_{max} \text{ x } V_{max}}{J_{sc} \text{ x } V_{oc}} \tag{9}$$

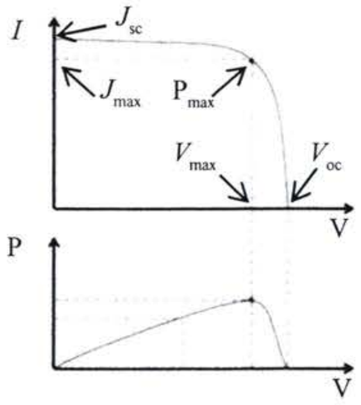

Figure 2.6 The current-voltage and power-voltage characteristics of photovoltaic cell [34].

2.4.2 Incident photon to current conversion efficiency of DSSCs

Quantum efficiency (QE) is the ratio of the number of charge carriers collected by the solar cell to the number of photons of a given energy shining on the solar cell. The QE relates to the response of a solar cell to the various wavelengths in the spectrum of light shining on the cell. The QE is also sometimes called IPCE, which stands for Incident Photon to electron Conversion Efficiency [25, 35-36]. The IPCE reveals how efficient the numbers of absorbed photons are converted into current as a specific wavelength. The IPCE is defined as

$$IPCE(\%) = \frac{I_{sc}}{I_0} \times \frac{1240}{\lambda} x100 \tag{10}$$

Where I_{sc} is short circuit current, I_0 is illuminate current of incidents light (Silicon photo diode measurement base), λ is the wavelength of the incident light. The IPCE are related trough the Light harvesting efficiency (LHE) of device. If the amount of dye present on the surface is enough to yield close to 100% LHE, the IPCE will be equal. Therefore, the IPCE are powerful tool to explore the sensitizer absorption behavior and significantly to design the sensitizer molecule. Figure 2.7 shows the spectral response of the photocurrent of the N3 and the black dye sensitizers. Both dyes show very high IPCE values in the visible range. However, the response of the black dye extends 100 nm farther into the IR than that of N3.

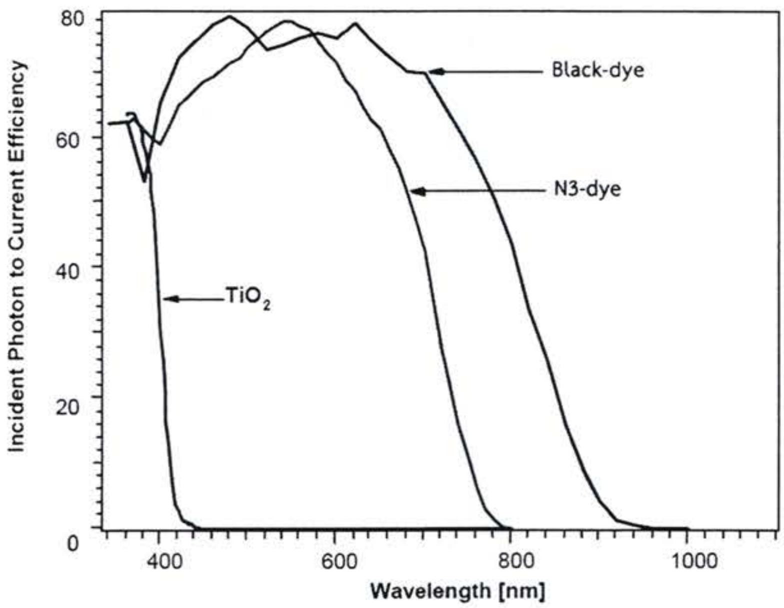

Figure 2.7 The IPCE spectra obtained with the N3 and the black dye as sensitizer [34].

2.5 The literature survey

2.5.1 Preparation of the infrastructure of DSSCs

2.5.1.1 Preparation of the working electrode of DSSCs

The photovoltaic effect takes advantage of the fact that photons falling on a semiconductor can create electron hole pairs, and at a junction between two different materials, this effect can set up an electric potential difference across the interface. Figure 2.8 shows first type of the regenerative cell, which converts light to electric power leaving no net chemical change behind. Photons exceed generate the electron hole pairs, which are separates by the electric field present in the space-charge layer. The negative charge carriers move through the bulk of the semiconductor to the current collector and the external circuit. The positive holes are driven to the surface where they are scavenged by the reduced form of the redox relay molecule (R), oxidizing it: $h^+ + R \rightarrow O$ The oxidized form Ox is reduced back to Red by the electrons that reenter the cell from the external circuit [8].

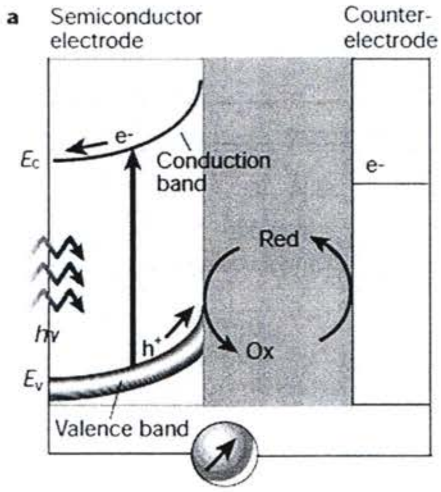

Figure 2.8 The schematic drawing principle of operation of photo-electrochemical cells base on n-type semiconductors [25].

The heart of the system is a wide band gap oxide semiconductor which is placed in contact with a redox electrolyte or an organic hole conductor. The material of choice has been TiO_2 (anatase), although alternative wide band gap oxides such as ZnO and Nb_2O_5 have also given promising results. The overall device generates electric power from light without suffering any permanent chemical transformation. Accelerated endurance tests have shown that ruthenium based charge transfer sensitizers can sustain 100 million turnovers without decomposition, corresponding to 20 years of cell operation under natural light conditions. The DSSCs have maintained their performance over 14,000 h of continuous light soaking [26].

The astounding photo electrochemical performance of nanocrystalline semiconductor junctions is illustrated in Figure 2.9, which compare the photo-response of an electrode made of single-crystal anatase, one of the crystal forms of TiO_2, with that of a mesoporous TiO_2 film. The electrodes are sensitized by the ruthenium complex cis-$RuL_2(SCN)_2$ (L is 2,28-bipyridyl-4-48-dicarboxylate), which is adsorbed as a monomolecular film at the titania surface. The electrolyte consisted of a solution of 0.3 M LiI and 0.03 M I_2 in acetonitrile. The IPCE value obtained with the single-crystal electrode is only 0.13% near 530 nm, where the sensitizer has an absorption maximum, whereas it reaches 88% with the nanocrystalline electrode more than 600 times as great [8].

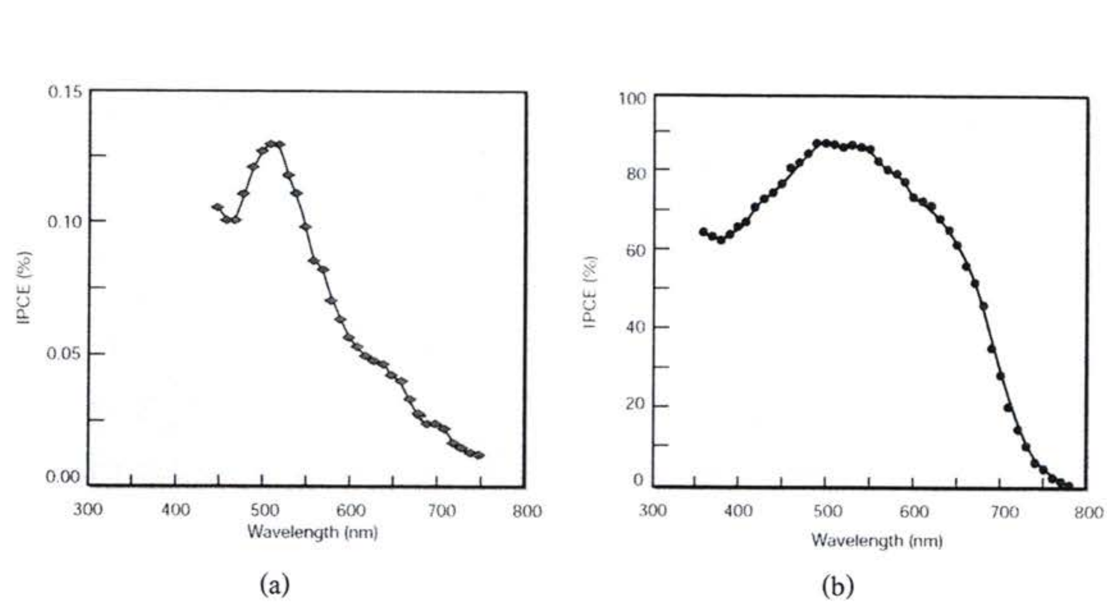

Figure 2.9 The incident photon to current conversion efficiency of (a) bare TiO_2 electrodes and (b) TiO_2 with sensitized by the surface anchored with ruthenium complex [8].

Consequently, titanium dioxide became the semiconductor of choice. The TiO_2 has many advantages for sensitized photochemistry and photo electrochemistry: it is a low cost, widely available, non-toxic and biocompatible material, and as such is even uses in health care products as well as domestic applications such as paint pigmentation.

However, the mesoporous TiO_2 for DSSCs working electrode are require: (a) the inherent conductivity of the film is very low, (b) small size of the nanocrystalline particles do not support a built-in electrical field and (c) the electrolyte penetrates the porous film all the way to the back contact making the semiconductor/electrolyte interface essentially three dimensional. Therefore, controlling the nanocrystalline structure of TiO_2 powders is very important for the application to DSSCs because the efficiency of DSSCs is considerable influenced on the change of the TiO_2 nanostructures. The nanoporous structure permits the specific surface concentration of the sensitizing dye to be sufficiently high for total absorption of the incident light, necessary for efficient solar energy conversion, since the area of the monomolecular distribution of adsorbate is 2 - 3 orders of magnitude higher than the geometric area of the substrate [37].

Figure 2.10 shows the surface of mesoporous TiO_2 film prepared from a colloidal suspension processed and by the conventional sol-gel method [33]. The comparison the surface morphology of TiO_2 film, the result indicates that. The TiO_2 films from sol-gel chemical methods, which evidently provides a much more reproducible and controlled particle size, porous, high surface area texture.

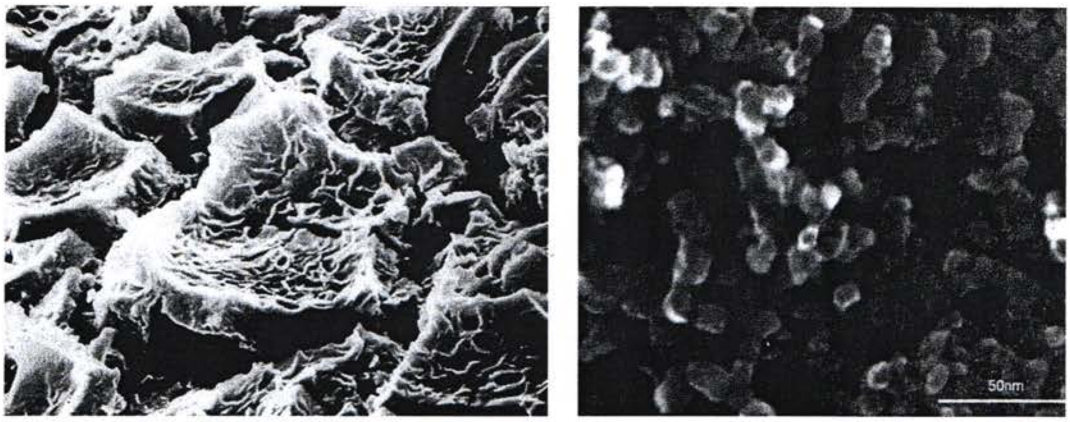

(a) (b)

Figure 2.10 The scanning electron micrograph of a meso-porous anatase TiO_2 film surface: (a) colloidal suspension and (b) hydrothermally technique [8, 33].

Figure 2.11 shows the schematic flow chart of hydrothermal technique. That are involves the hydrolysis of the titanium alkoxide precursor producing an amorphous precipitate followed by peptisation in acid or alkaline water to produce a sol, which is a subject to hydrothermal Ostwald ripening in an autoclave. This method yield was 20 nm TiO_2 nano-particles with anatase or a mixture of anatase and rutile phase. This technique are ease to control the particle size, hence of nanostructure and porosity of the resultant semiconductor substrate [12].

The sol-gel chemical methods, since it is compatible with screen printing technology, while commercially, available titania powders produced by a pyrolysis route from a chloride precursor have been successfully employed. It anticipates future production requirements. Therefore, the available commercial titanium dioxide powder was used to make screen-printing pastes i.e. P25, ST21 and ST41 [38-41].

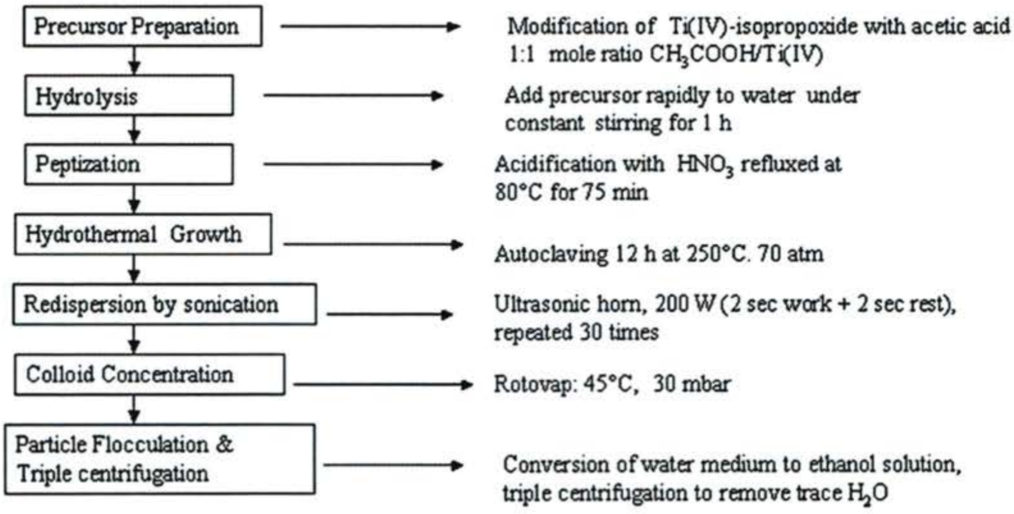

Figure 2.11 Flow chart of preparation TiO_2 particle from hydrothermally technique [12].

Figure 2.12 shows the photograph and transmittance spectra of screen printed commercial available nanocrystalline TiO_2 layers. The measurements was performed with cover glass plates, which were attached on the surface of TiO_2 layer, and the pores in nanocrystalline-TiO_2 layers were filled with butoxyacetonitrile to decrease the light scattering effect [40].

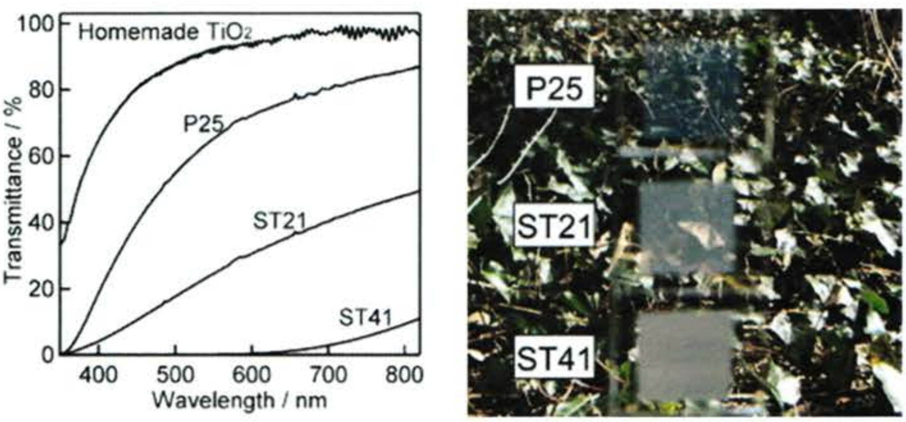

(a) (b)

Figure 2.12 (a) transmittance spectra and (b) photograph of screen-printing paste prepared form commercial available TiO_2 powder [40].

The paste composition was influent on properties of screen-printing paste. The TRITON™ X with a carboxylic terminal group as a dispersant was employed to prepare nc-TiO_2 photoanode films. It was found that simply introducing TRITON™ X-based surfactants with an octyl phenol ethoxylate (OPE) backbone and various chain ends the [nc-TiO_2/ethyl cellulose/terpineol] paste is helpful to increase the powder loading and make it possible to produce nc-TiO_2 films with higher surface uniformity and particle density after sintering process [42]. The screen-printed nanoporous TiO_2 thin films with large size pores due to the addition of PS balls, cellulosic polymer (PEG Mw 20,000) [41-44]. The TiO_2 pastes prepare by varying the proportion of TiO_2 powder, α-terpineol, and ethyl cellulose in their composition. The paste compositions with PEG MW 20,000 use as the binder and pore-forming agent. The viscosity and rheology of paste was control by ethylcellulose. Moreover, acetylacetone and 4-hydroxy-benzoic acid can effectively prevent the aggregation of TiO_2 nanoparticles and improve the mechanical stability of film [44]. The paste prepared with 26% TiO_2 powder, 15% ethyl cellulose gel and 59% α-terpineol found to appropriate for application in DSSCs [45].

Figure 2.13 shows step-by-step preparation the TiO_2 screen-printing past process, which prepared form the commercially available TiO_2 powder. A specific advantage of the procedure is fabricating the nanocrystalline layers without cracking and peeling-off for the photoactive electrodes [40].

The nanoparticle TiO_2 films need to be deposits immediately after paste preparation to avoid agglomeration of the material. Storage paste may be feasible only under controlled conditions as it is more sensitive to environmental conditions than powder storage, resulting to the formation of large aggregates of TiO_2 nanoparticles. Large aggregates of TiO_2 nanoparticles enhance porosity but reduce active surface area for dye adsorption and also reduce the transparency of the film, which enhance evaporation of acetyl acetone and water, thereby reducing cracks. The development of cracks on the film's surface results to a decrease in the efficiency of the cell [46].

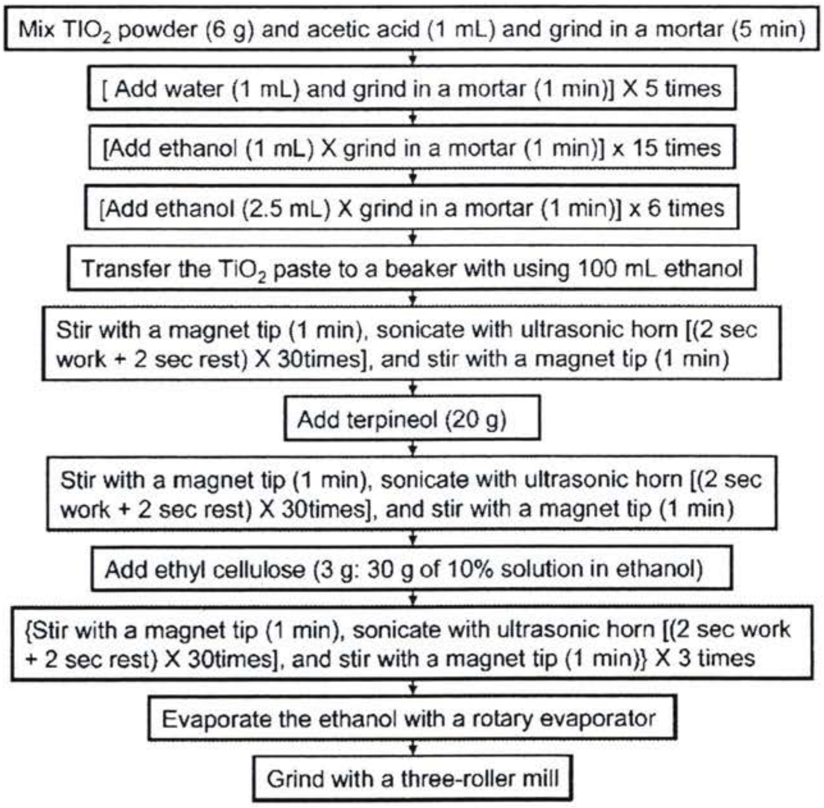

Figure 2.13 Flow chart of paste preparation from commercially available TiO_2 powder [40].

Figure 2.14 shows schematic drawing conceptual of screen printing technique. In addition, the screen characteristics are described specific properties i.e. screen net materials, mesh count (number of fabric line per square inch), mesh open (percentage of open surface), fabric thickness and theoretical paste volume. The deposition of paste was conducted under the following conditions: squeegee speed, distance between screen and substrate, applied squeegee pressure and squeegee angle.

The extremely promising for up-scaling and industrial production, screen-printing is a reliable and cost effective low technology method currently used as deposition technique for thick films of particulate and polymeric materials for use in superconducting, photovoltaic, and electronic devices and sensors.

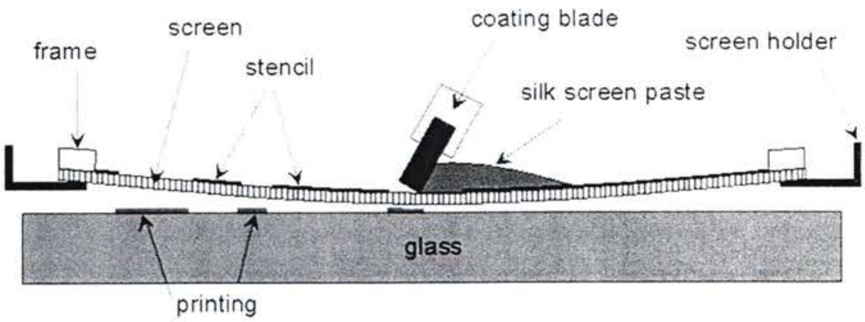

Figure 2.14 The schematic conceptual of screen printing technique [47].

Figure 2.15 shows the photograph of available commercial DSSCs test cell glass plate supplied by pilot production laboratory. The DSSCs made easy with the test cell kit supplied by Solaronix, Switzerland (Figure 2.15(a)). The available as a laser pre-cut plate of 28 separate electrodes, supplied by Dyesol, Australia. The transparency and opaque TiO_2 coated working electrode was coated by a suite of high quality pastes, containing TiO_2 load of 20 nm (Figure 2.15(b)) and 350-450 nm nano-particulate paste, respectively. The complete Solaronix spot cell kit, which allows scientists and enthusiasts to easily make their own cells. Ready-to-use electrodes and sealing materials allow the experimenter to focus on the chemistry of dyes and electrolytes (Figure 2.15(c)). The homemade education cell kit in ECN laboratory, Netherlands was shown in Figure 2.15(d) [48-50].

In the pilot manufacturing production plant of DSSCs, screen printer is typically used for screen of an electrical conductor to form a busbar, a catalyst paste to form the counter electrode and a semiconductor paste to form the working electrode (see Figure 2.15(e)). The flexible nature of this piece of equipment allows users to experiment with application of other cell components such as electrolytes and sealants. Figure 2.15(f) shows the photograph of screen-printing technology, which controllable squeegee speed and pressure, allow for precise repeatable prints for both small and large production runs.

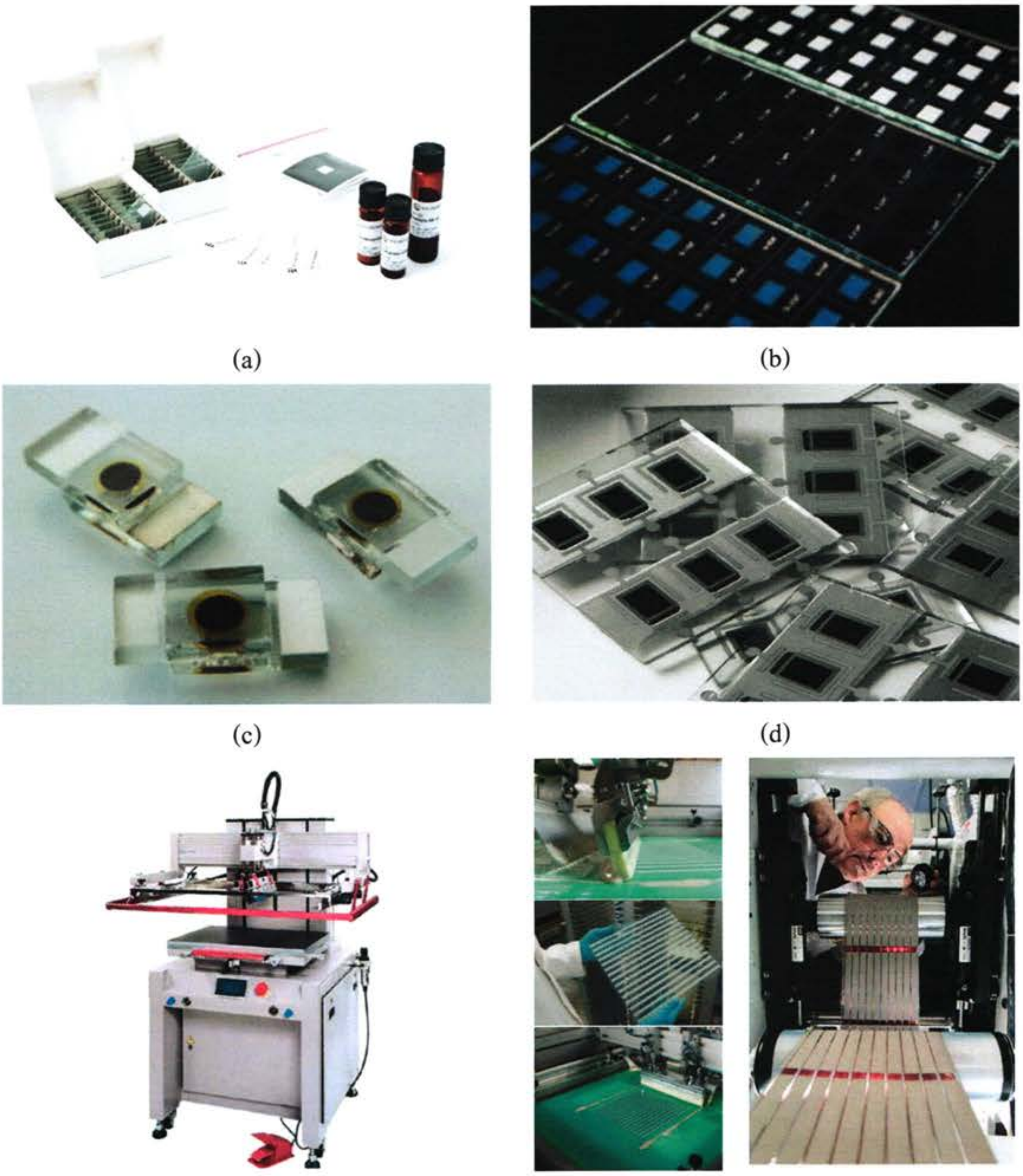

Figure 2.15 A photograph of the DSSCs working electrode technology. (a) Solaronix education kits, (b) Dyesol pre-cut test-cell glass plate, (c) Solaronix spot cell kit, (d) ECN lab's homemade test cell, (e) semi-automate screen printer and (f) screen printing process and a piece of TiO_2 green on conducting glass substrate [48-50].

2.5.1.2 Preparation of the counter electrode of DSSCs

The task of the counter electrode (CE) is the reduction of the redox species used as a mediator in regenerating the sensitizer after electron injection, collection of the holes from the hole conducting material in solid-state DSSCs. At present, several different kinds of CEs has been introduced, for example: platinized transparent, carbon, and conductive polymer.

However, Platinum-loaded on the conducting glass has already been widely used as the standard for DSSCs counter electrodes. The reactions at the CE depend on the type of redox shuttle used to transfer charge between the photo-electrode and the CE. In many cases the iodide triiodide couple has been employed as the redox mediator. The kinetics of reduction of triiodide at the CEs have been studied with a symmetric two electrode system and the mass transfer limitation on the photocurrent. The electrochemical potential of CE was determine by the catalytic activity.

The catalytic activity was expressed in terms of the exchange current density (J_0), which is calculated from the charge-transfer resistance (R_{ct}) using the $R_{ct} = RT/nFJ_0$, which R, T, n, and F are the gas constant, temperature, number of electrons transferred in the elementary electrode reaction (n = 2) and Faraday constant, respectively [51].

Several methodologies to produce the platinized counter electrode were reported one has self-assembly deposit method. The Pt hydrosol was prepared by adding the acrylic solution in precursor solution, ageing and nitrogen gas bubbled was flow to reduction the platinum ions. Solution of dodecanethiol and stearic acid were transferred to FTO surface, which used to generate the monolayer of dodecanethiol. Follow the last step by immersed in platinum colloidal solution the nanoparticles were covalently coordinated to the thiol group. The time of self-assembly of platinum nanoparticles was about 4 day [52].

Hydrogen reduction combine with screen print method, the H_2PtCl_6 as a precursor mixed as antimony doped tin dioxide powders, After evaporating the solvent, the impregnated platinum precursor was reduced by preheated hydrogen at 120 °C during 60 min. Afterwards each 1 g of catalytic powder was mixed with 8 g of binder (α-terpineol+10 wt.% ethyl cellulose 45cP). The mixture was stirred at 8,000 rpm for 25 min. The cell area was 2.5 cm^2. After film deposition, the master plats were dried at 150 °C and annealed at 630 °C [53].

Figure 2.16 show a SEM photograph of platinum counter electrodes surface prepared by the electro deposition method. The platinum colloid was prepared by the reaction between H_2PtCl_6 and NaH_2Cyt. The conductive glass sheet was immersed in dodecanethiol ethanol solution for 10 min. The 2 volt direct current was applied and follow with sintered at 450°C for 30 min. Using such a counter electrode, DSSCs showed 6.40% of overall energy conversion efficiency [54].

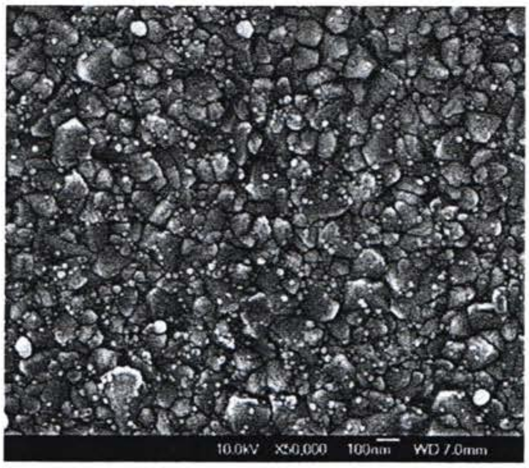

Figure 2.16 The SEM photograph of platinum counter electrodes surface prepared by electro deposition technique [54].

The Pt counter electrode was prepared by the sputtering method. The Pt film's thickness was controlled by deposition time. It was found that the counter electrodes sheet resistance (Rs) decreased as the Pt film thickness increased (Figure 2.17). however, when the Pt film thickness exceeds 100 nm, there has no significant effect on the conductivity improvement [55-56]. Usually, the Pt counter electrode for DSSCs was prepared by the thermal decomposition method of H_2PtCl_6 solution. The Pt solution was deposited on FTO substrates by several techniques such as spin coating, drop casting and screen-printing.

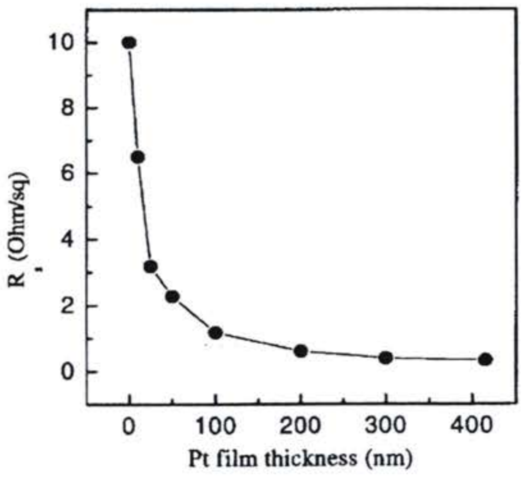

Figure 2.17 The dependence of sheet resistance of platinized counter electrodes on Platinum film thickness [56].

2.5.1.3 Preparation of the electrolyte of DSSCs

The electrolyte is one of key components for DSSCs, effect on the conversion efficiency and stability of the solar cells. The electrolytes can be classified into 3 groups: liquid electrolyte, Ionic liquid electrolyte and quasi - solid state in term of gel, polymer, inoraganic and organic hole conductor electrolyte [57-58].

(1) Liquid Electrolytes

The essential constituents of liquid electrolytes are organic solvent, redox couple such as $3I^-/I^-_3$ and additives. The organic solvent is a basic component in liquid electrolytes, an environment for iodide/triiodide ions' dissolution and diffusion. The physical characteristics of organic solvent including donor number, dielectric constants, and viscosity was affect to the photovoltaic performance of DSSCs.

Figure 2.18 shows the relation between donor number of solvent shows obvious influence on the open circuit voltage (V_{oc}) and short circuit current density (J_{sc}). The donor number was variation by change type and ratio of mix solvent: 1: AcN, 2: 10 % THF/90 % AcN, 3: 20 % THF/80 % AcN, 4: 30 % THF/70 % AcN, 5: 50 % THF/50 % AcN, 6: 70 % THF/30 % AcN, 7:10 % DMSO/90 % AcN, 8: 20 % DMSO/80 % AcN, 9: 50 % DMSO/50 % AcN, 10: DMSO, 11: 50 % DMF/50 %AcN, 12: DMF, 13: 10 % NMP/90 % AcN, 14: 20 % NMP/80 % AcN, 15: 30 % NMP/70 % AcN. Electrolyte contains 0.6 M DMPII, 0.1 M LiI, 0.05 M I_2 [59].

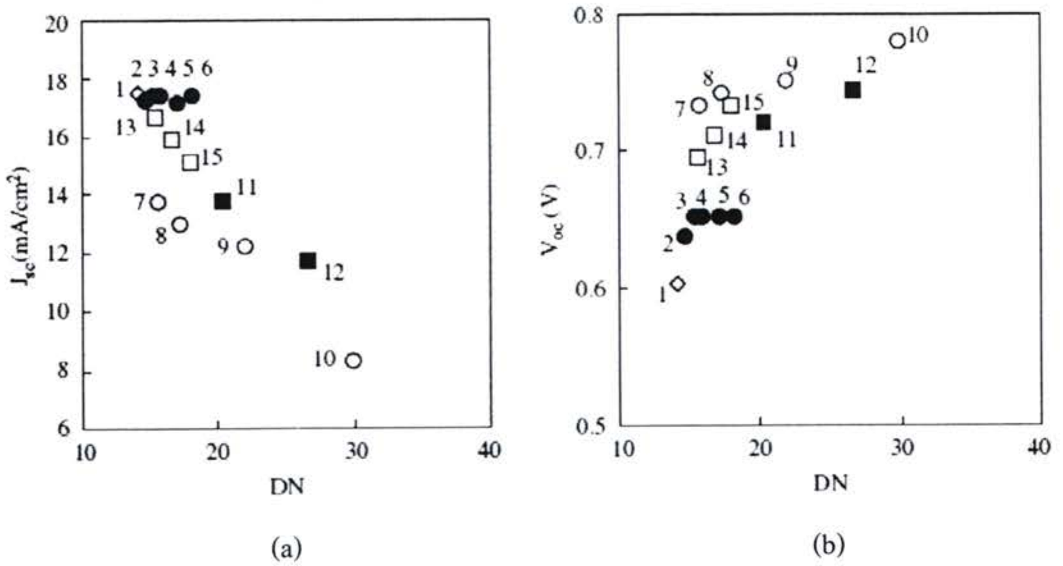

Figure 2.18 Dependence of (a) J_{sc} and (b) V_{oc} of DSSCs on the donor number of solvents [59].

The additives such as specific cation and compounds are normally introduced into the liquid electrolytes; to enhance the photovoltaic parameters in DSSCs. Two kinds of additives are typically employed in liquid electrolytes for DSSCs. (1) alkali cations or guanidium cations mainly devoted to the enhancement of short circuit photocurrents (J_{sc}). The adsorption of specific cation in the electrolytes onto the TiO_2 surface could shift the conduction band of the TiO_2 towards more positive potentials, thus affecting the electron injection dynamics of the excited state of dye molecules [59]. (2) Nitrogen-containing heterocyclic compound, most frequently 4-tert-butylpyridine (4-TBP) is another class additives in DSSCs electrolyte, mainly dedicated to the improvement of the V_{oc}.

In contrast to the specific cation, Lewis bases, such as 4-TBP, instead are expected to deprotonate the TiO_2 surface, therefore causing a negative shift of the conduction band of the TiO_2. The effect of 4-TBP has been extensively investigated over the past several years, and several mechanisms have been put forward. It has been proposed that the dramatic increase of the V_{oc} arising from the introduction of the 4-TBP can be attributed to either the suppression of the dark current at TiO_2/electrolyte interface or the negative shift of the conduction band in the TiO_2 film or a combination of both [60].

(2) Ionic Liquid Electrolytes

Ionic liquids (ILs) are materials which consist only of ions and which are liquid below 100 °C. The ionic liquids was used in many difference such as catalysis, extraction processes, protein synthesis, cellulose processing, electroplating batteries, double layer capacitors, electrochromic windows and dye solar cells (DSSCs) [60]. Table 2.1 was listed the photovoltaic performance of DSSCs based on ionic liquid electrolyte of different composition.

Table 2.1 The partial literatures reported on the DSSCs with ILs electrolytes [61].

Electrolyzes Composition	Dye	PCE (%)	Stability
Binary ILs (PMII/EMIDCN) with I^-/I_3^-	Z907	6.6	N/A
IL with $SeCN^-/(SeCN)^{3-}$, Iodine-free	Z907	7.5	N/A
Binary ILs (PMII/EMIB$(CN)_4$) with I^-/I_3^-	K77	7.60	1,000 h at 60 °C, decay 9%
Binary ILs (PMII/G.CI) with I^-/I_3^-	D149	3.88	N/A
Binary ILs (BMII/BMISO$_3$CF$_3$) with I^-/I_3^-	N3	4.11	576 h at 25 °C, decay < 5%

(3) Solid - State electrolytes

There are two kinds of solid-state electrolytes DSSCs, one uses hole transport materials (HTMs) as medium and the other uses a solid state electrolyte containing redox couple as medium. Familiar large band gap HTMs such as SiC and GaN are not suitably used in DSSCs since the high temperature deposition process for these materials will certainly degrade conduction band the sensitized dyes on the surface of nanocrystalline TiO_2 [62].

It was found that a kind of inorganic HTM based on copper compounds such as CuI, CuBr, or CuSCN could be used in DSSCs. These copper-based materials can be casted from solution or vacuum deposition to form a complete hole-transporting layer, the CuI and CuSCN share good conductivity in excess of 10 - 2 S/cm, which facilitates their hole conducting ability. For example, DSSCs based on CuI HTM obtained as high as 2.4% light to electricity power conversion efficiency under irradiation of AM 1.5G, 100 mW/cm^2 [63-65].

However, stability is quite poor, even lower than the traditional organic photovoltaic cell, which is also a common problem existing in DSSCs based on this kind of inorganic HTMs. Therefore, It was paid the attention to organic HTMs. Organic HTMs have already been widely used in organic solar cells, organic thin film transistors, and organic light emitting diodes. Compared with inorganic HTMs, organic HTMs possess the advantages of plentiful sources, easy preparation, and low cost.

Table 2.2 lists the photovoltaic performance of DSSCs based on typical inorganic and organic HTMs. The solid-state DSSCs based on organic HTM 2,2',7,7'-tetrakis (N,N-di-p-methoxyphenylamine) 9,9'-spirobifluorene (OMeTAD) was reported, although overall light-to-electricity conversion efficiency of this DSSCs only reached 0.74% under irradiation of 9.4 $mWcm^{-2}$. It is a pioneer for fabricating DSSCs with organic HTMs by improving the dye adsorption in the presence of silver ions in the dye solution. The efficiency of solid-state DSSCs employing spiro-OMeTAD was enhanced to 3.2%, which is the highest level of the solid state DSSCs by utilizing an organic transport material up to now. However, the overall light to electricity power conversion efficiencies of these DSSCs lower than that of the DSSCs based on liquid electrolytes.

Table 2.2 The performance of solid-state DSSCs utilizing different HTMs [59].

Type of hole transport materials	Materials	PCE (%)
Inorganic HTM	CuI	2.4 – 3.8
	CuSCN	1.50
	$4CuBr_3S(C_4H_9)_2$	0.60
Organic HTM	OMeTAD	0.74 - 2.56
	Spiro-OMeTAD	3.20
	Pentacene	0.80
	Polyaniline	1.15

The quasi-solid state, or gel state, is a particular state of matter, neither liquid, solid, conversely both liquid and solid. Generally, a quasi-solid-state electrolyte is defined as a system which consists of a polymer network (polymer host) swollen with liquid electrolytes. The quasi-solid-state electrolytes are usually prepared by incorporating a large amount of a liquid electrolyte into organic monomer or polymer matrix, forming a stable gel with a network structure via a physical or chemical method. Quasi-solid-state electrolytes show better long-term stability than liquid electrolytes do and have the merits of liquid electrolytes including high ionic conductivity and excellent interfacial contact property. Table 2.3 shows the photovoltaic performance of DSSCs based on different gelators and ionic liquid electrolytes.

Table 2.3 The quasi-solid state DSSCs with different gelators and ionic liquid electrolytes [61].

Electrolyzes Composition	Gelator	Dye	PCE (%)
HMII, I_2 et al.	Low-molecular-weight gelator	N719	5.01
I_2, MPII, NMBI	PVDF-HFP	Z907	5.30
I_2 and NMBI in MPII	Silica Nanoparticles	Z907	6.10
I_2, GuSCN, NMBI in PMII/EMINCS (13:7,v/v)	Low-molecular-weight gelator	K-19	6.3
EMImI, I_2, LiI, TBP in EMITFSA	PVDF-HFP	N3	2.4
TMS-PMII/I_2 in 10:1 ratio	Self-gelation	N3	3.2
I_2, LiI, TBP in MPII	Agarose	N719	2.93
I_2, LiI, TBP, DMPII in EMIDCA	Agarose	N719	3.89
EMII, LiI, I_2, and TBP in EMITFSI	Nanoparticles	N3	4.57

In addition, the iodide/triiodide has been demonstrated as the most efficient redox couple for regeneration of the oxidized dye, its severe corrosion for many sealing materials, especially metals, causes a difficult assembling and sealing for a large area DSSCs and poor long-term stability of DSSCs. Therefore, redox couples such as Br^-/Br_2, SCN^-/SCN_2, $SeCN^-/SeCN_2$ bipyridine cobalt(III/II) complexes was investigate. The unmatchable energy with sensitized dyes or their intrinsic low diffusion coefficients in electrolyte, these redox couples show lower conversion efficiencies than the iodide/triiodide redox couple [59].

2.5.1.4 Preparation of the dye or sensitizer of DSSCs

The ideal to design molecular of sensitizer for a single junction photovoltaic cell converting standard global AM 1.5 sunlight to electricity should absorb all light below a threshold wavelength of about 920 nm. In addition, it must also carry attachment groups such as carboxylate or phosphonate to firmly graft it to the semiconductor oxide surface. Upon excitation it should inject electrons into the solid with a quantum yield of unity. The energy level of the excited state should be well matched to the lower bound of the conduction band of the oxide to minimize energetic losses during the electron transfer reaction. Its redox potential should be sufficiently high that it can be regenerated via electron donation from the redoxn electrolyte or the hole conductor. Finally, it should be stable enough to sustain about 10^8 turnover cycles corresponding to about 20 years of exposure to natural light [33].

The efficiencies of the sensitizers are related to some basic criteria. The HOMO potential of the dye should be sufficiently positive compared to the electrolyte redox potential for efficient dye regeneration. The LUMO potential of the dye should be sufficiently negative to match the potential of the conduction band edge of the TiO_2 and the light absorption in the visible region should be efficient. However, by broadening the absorption spectra, the difference in the potentials of the HOMO and the LUMO energy levels is decreased. If the HOMO and LUMO energy levels are too close in potential, the driving force for electron injection into the semiconductor or regeneration of the dye from the electrolyte could be hindered. The sensitizer should also exhibit small reorganization energy for excited and ground state, in order to minimize free energy losses in primary and secondary electron transfer step [68].

There have been two kinds of dyes, namely, metal-complexes and metal-free complexes or organic dyes. Up to now, several Ru(III) polypyridyl complexes have achieved light-to-electricity power conversion efficiencies (%PCE) more over 10% in standard global air mass 1.5 and shown favorable stabilities [12-13]. Ruthenium complexes such as the N3, N719 and black dye have been intensively investigated and show record solar energy to electricity conversion efficiencies of 11% (Figure 2.19) [33].

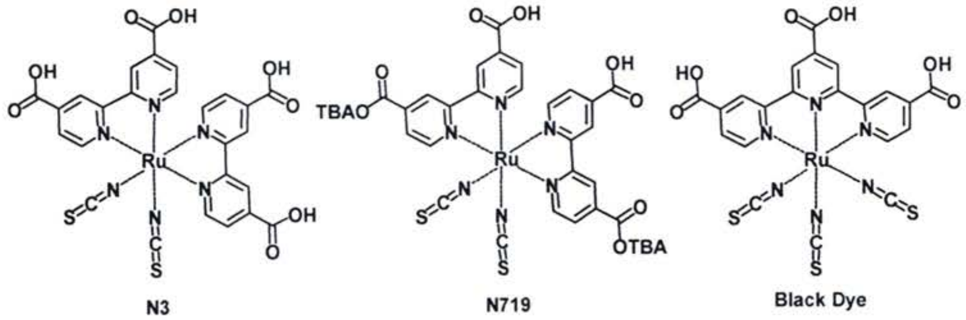

Figure 2.19 The chemical structures of commercialize ruthenium based metal dye [33].

Although Ru complexes show high power conversion efficiencies, the problem of costs and environmental issues will limit the large-scale application of this type of solar cells. Compared with Ru dyes, metal-free organic dyes have many advantages such as high molar absorption coefficient, wide variety of the structures, facile modification, no concern with the noble metal resource, and environment friendly dyes.

However, many organic dyes still present moderately conversion efficiency in DSSCs. There are two major factors for the efficiency: one is due to the sharp and narrow absorption band of organic dyes; the other is the aggregation of dyes on the semiconductor surface. Organic dyes have some advantages over conventional ruthenium based chromophore as photosensitizers. For instance, they exhibit high molar extinction coefficients and are easily modified due to relatively short synthetic routes and especially low cost starting materials. The high extinction coefficients of the organic dyes are suitable for thin TiO_2 films required in solid state devices where mass transport and insufficiently pore filling limit the photovoltaic performance.

The interest in metal-free organic sensitizers has grown in the last few years. Sayama and coworker was published a merocyanine dye (Mb(18)-N), which gave an efficiency of 4.2% [69]. Before this milestone, the organic dyes for DSSCs performed relatively low efficiencies (%PCE < 1.3%). This finding opens new roads for exploring new dye types. In recent years, a great deal of research aimed at finding highly efficient and stable organic sensitizers has been carried out. A number of coumarin, indoline, and triphenylamine-based organic sensitizers have been intensively investigated and some of them have reached efficiencies in the range of 3 - 8% (Figure 2.20).

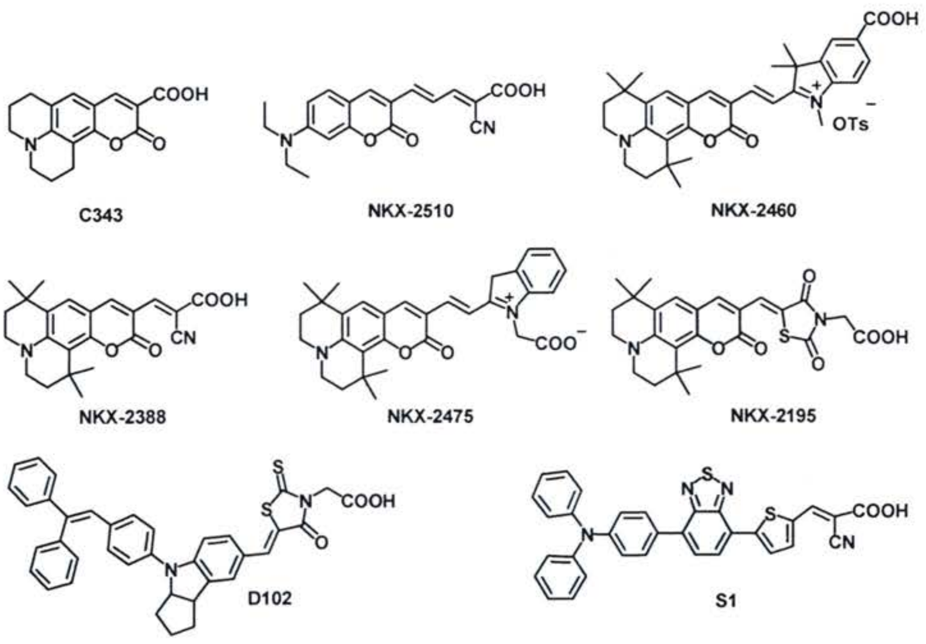

Figure 2.20 The chemical structures of coumarin, indoline and triphenylamine organic dyes [70].

2.5.2 Device assembly for DSSCs

Generally, DSSCs test cells was designed in sandwich type cell, the shape of device look like sandwich or hamburger structure (Figure 2.21). The algorithm of cell assembly step, when the electrodes are put together, the active sides of the anode and the cathode will be facing each other. In other words, the stained titania will face the platinum counter electrode. The gap left between the two glass plates will be filling with electrolyte.

Depending on the objective, durability of test cell and measurement speed. It was classify to two types of test cell. First, approach an "open cell" because the inner part of the solar cell is exposed to air. The resulting devices won't last as long as in a sealed configuration. The second approach is called "close cell", devices are sealed together with a gasket so that the electrolyte is confined in the cavity by capillary effect. This type is popular used in laboratory research and pilot plant scale [72].

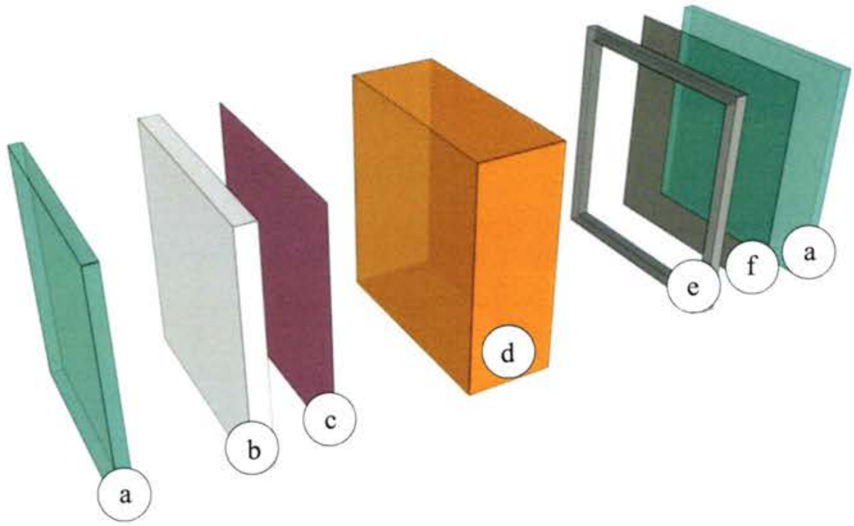

Figure 2.21 The layout of DSSCs in sandwich type cell design. The DSSCs configurations consist of (a) conductive substrate, (b) Titanium dioxide, (c) sensitizer/dye, (d) electrolyte, (e) sealing gasket and (f) platinum catalyst [71].

The fabrication process of the close cell DSSCs test cell, the TiO_2 working electrode should be use right after preparation. The sealant gasket was carefully place around the TiO_2 film, which dimensions of the gasket and the stained titania shall match but not overlap. The Pt counter electrode was faced down on top of the gasket, which the alignment of conductive sides of both electrodes was face to face. Apply heat and pressure all over the gasket with the help of a hot press at about softening temperature of sealing materials. The hot melt material should glue the electrodes together, which hot-melt material should match the refractive index of the glass and look completely transparent all over the gasket surface.

The gap between the two electrodes can now be fills with electrolyte. Use a syringe or dropper to flush the electrolyte from one hole, through the cell by capillary effect. Complete filling can be confirms by a visual examination. Wipe off any excess electrolyte left around the filling holes and clean the glass with an acetone wetted paper towel. A small glass cap will be seal on top of each hole with another piece of sealing film. Apply heat and pressure on both seals at softening temperature of sealing materials. The resulting DSSCs test cell is now ready for use [72].

Seigo Ito and coworker was purposed a step to fabrication of DSSCs with solar to electric power conversion efficiency over 10%. The dye covered TiO_2 electrode and Pt counter electrode were assembled into a sandwich type cell and sealed with a hot melt gasket of 25 μm thickness made of the Dupont ionomer Surlyn 1702 (see Figure 2.22). The size of the TiO_2 electrodes used was 0.16 cm^2. The aperture of the Surlyn frame was 2 mm larger than that of the TiO_2 area and its width was 1 mm. The hole in the counter electrode was sealed by a film of Bynel using a hot iron bar (protectively covered by a fluorine polymer film). A drop of the electrolyte was put on the hole in the back of the counter electrode. It was introduced into the cell via vacuum backfilling. Finally, the hole was sealed using a hot melt ionomer film (Dupont Bynel 4702, 35-μm) and cover glass [12].

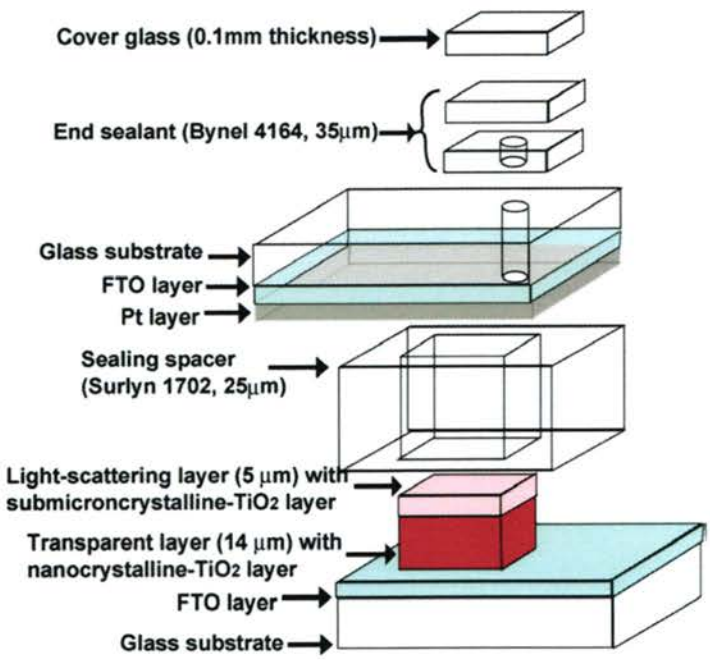

Figures 2.22 The photograph of layer by layer DSSCs configuration [12].

CHAPTER 3

EXPERIMENTAL

The chapter is divided into six parts including list of materials, list of chemical and reagents, list of equipment, preparation of DSSCs components, DSSC devices assembly, physical properties and device measurement.

3.1 List of materials.

The dye sensitized solar cell (DSSCs) devices were fabricated by using appropriate amounts of following commercial materials, as shown in Table 3.1.

Table 3.1 List of commercial materials.

Materials	Company	Material data specification note
Surlyn®-30	DYESOL®	30 μm film thickness, 110-130°C Temperature for sealing
TCO 30-8	SOLARONIX®	Soda lime glass, 3.0 mm thickness, FTO conducting layer
		~ 8Ω/sq surface resistivity
		> 65% from 500 – 1,000 nm Transmission
TCO 22-15	SOLARONIX®	Soda lime glass, 2.2 mm thickness, FTO conducting layer
		~ 15Ω/sq surface resistivity
		> 80% from 500 – 800 nm Transmission

All organic dyes were synthesized by Mr. Sakravee Punsay and Mrs. Tanika Khanasa under supervision of Assoc. Prof. Dr. Vinich Promarak.

3.2 List of chemical and reagents

The reagents were obtained from various suppliers as shown in Table 3.2. All reagents used were of analytical grade and unless indicated.

Table 3.2 List of chemical and reagents.

Chemical and Reagents	**Purity (%)**	**Company**
3-methoxypropionitrile	98.0	Sigma - Aldrich
4-tert-butylpyridine (TBP)	96.0	Sigma - Aldrich
Chloroplatinic acid hexahydrate (H_2PtCl_6. $6H_2O$)	99.9	Sigma - Aldrich
Guanidine thiocyanate (CH_6N_4S)	97.0	Sigma - Aldrich
Iodine (I_2)	99.9	Sigma - Aldrich
Titanium tetrachloride ($TiCl_4$) 0.09 M	20.0	Sigma - Aldrich
Ethanol (CH_3CH_2OH)	99.7	Acros Organics
Lithium iodide pure analysis (LiI)	99.5	BDH
Nitric acid (HNO_3)	65.0	EMSURE®ISO
Hydrochloric acid (HCl)	37.0	Carlo Erba
Isopropanol ($(CH_3)_2CHOH$)	99.5	Carlo Erba
EL-HSE-TEL (High Stability Electrolyte batch#2372)	N/A	DYESOL™

3.3 List of equipment

The equipment used in this work were summarized in Table 3.3.

Table 3.3 List of equipments.

Apparatus/Instruments	**Model**
X-ray diffractometer	Phillip X'Pert-MDP
Scanning electron microscope	JEOL JSM-5410 LV
Solar Simulator	Newport 96000 (150 W Xe lamp)
Source Meter	Keithley 2400
Pico ammeter	Keithley 6485
Monochromator	Oriel Cornerstone™ 130 1/8 m
Silicon photodiode	Newport 818UV low power detector 190 – 1100 nm
	BS 520 (Bunnkoukeiki. Co., Ltd.)
Furnace	Intelmats® FT12005
Ultrasonic bath	Bransonic® B2200E-3
Vacuum Oven	Isotemp® vacuum oven 282A
Screen printing net	polyester; mesh count (230T mesh/inch)

3.4 Preparation of DSSCs components

Figure 3.1 shows the schematic diagram of the DSSCs fabrication process. The working electrode and counter electrode were prepared by using screen printing and drop casting technique, respectively. The working and counter electrode were assembled into a sandwich type cell and sealed with a hot-melt gasket of Dupont ionomer Surlyn 17025.

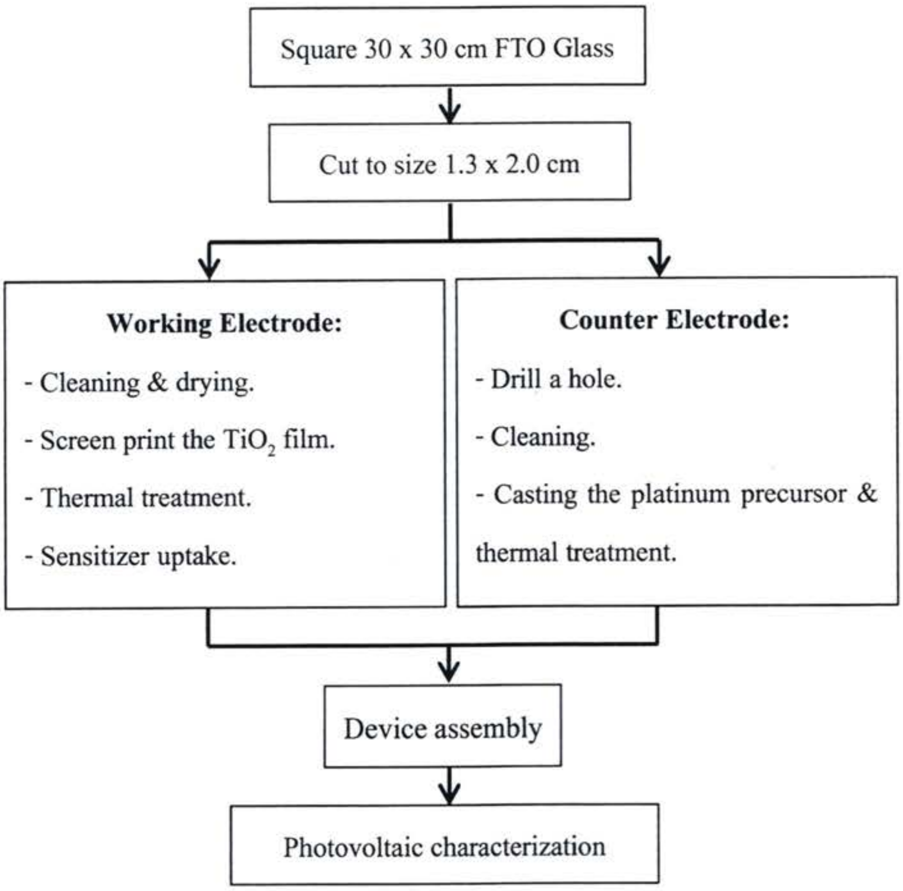

Figure 3.1 Flow chart of the fabrication and characterization of DSSCs device.

3.4.1 Preparation the conducting glass substrate

Figure 3.2 show the schematic shape of conducting glass for dye sensitized solar cell. A size of FTO glass used in this work is 1.3 cm x 2.0 cm (see Figure 3.2(a)). The FTO glass was drilled to make a hole with diameter of 1 mm, which used for fill the electrolyze solution in final process (see Figure 3.2(b)).

(a) (b)

Figure 3.2 The FTO glass used as (a) working and (b) counter electrode.

3.4.2 Cleaning conducting glass substrate

The substrates (working and counter electrode) were cleaned in order to avoid contamination. The cleaning procedure was (a) 20 %v/v nitric acid, (b) cleaning detergent, (c) deionized water, (d) acetone and (e) isopropanol. The residues metal on FTO surface were cleaned with 20%v/v nitric acid in ultrasonic bath followed by a trough rinse in deionized (DI) water. Then subsequently ultrasonicated in acetone to remove organic contaminate on the substrate surface. Afterwards rinse with isopropanol, a piece of glass was dried and stored in a closed box to protect them from dust.

3.4.3 Preparation the counter electrodes

The cleaned FTO was coated the platinum catalytic layer by thermal decomposition technique. The organic contaminate on FTO surface was removed by heating in air for 15 min at 400 °C. The platinum precursor solution (2 mgPt/mL in isopropanol) was droped on the cleaned FTO glass. Then, the Pt coated FTO glass was dried in an ambient air and subsequently heated at 385 °C for 20 min.

3.4.4 Preparation the TiO_2 working electrode

The cleaned FTO was coated with the nanocrystalline TiO_2 by screen printing technique. The electrodes were gradually heated under an air flow at 325 °C for 5 min, at 375 °C for 5 min, at 450 °C for 15 min and 500 °C for 30 min (see Figure 3.3). The binder and additives in paste were removed during the sintering process. After the sintering process, the active area of the TiO_2 was measured by a digital camera. The TiO_2 film was re-heated again at 450 °C for 30 min. At the 80 °C in cooling process, the TiO_2 working electrode was immersed in a dye solution and kept at room temperature to complete the sensitizer uptake.

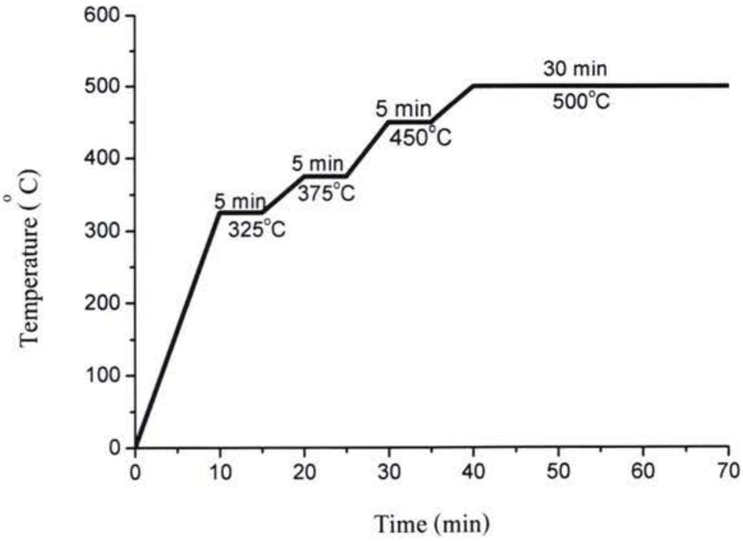

Figure 3.3 The temperature programs of the working electrode heat treatment.

3.5 The DSSC devices assembly

The dye-covered TiO_2 electrode and Pt-counter electrode were assembled in sandwich type cell and sealed with a hot melt sealant gasket, which was adapted from Seigo Ito [12]. The assembly process started with an attachment sealant gasket to the working electrode. The aperture of the sealant frame was 2 mm larger than that of the TiO_2 area and width was 1 mm.

Figure 3.4 The photograph of the electrolyte filling machine. (a) entrance of vacuum pressure valve and (b) release pressure knop.

Then platinum counter electrodes was placed on top of the anode electrode. The cell was sealed by apply heating and pressure. A drop of the electrolyte was filled to cavity in the backside of the counter electrode by Electrolyte Filling Machine (EFM see Figure 3.4), the hole was sealed by using a sealant film and a cover glass. The cathodes and anode contact of DSSC devices was established. The FTO surface was contacted with copper foil and painted with silver paint. Finally, the electric wires were soldered on the copper film to ensure the electric contact. A photograph of complete of DSSC devices and schematic drawings cross section of the DSSC devices are shown in Figure 3.5

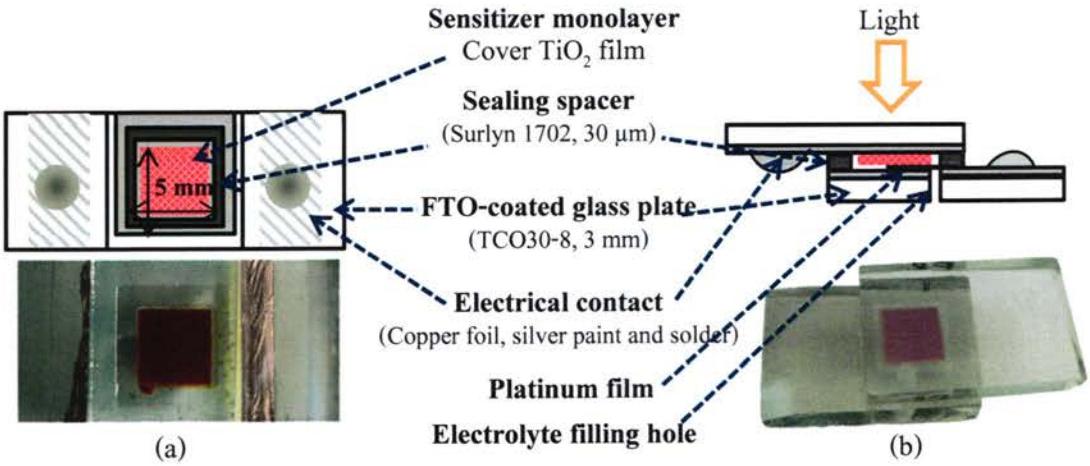

Figure 3.5 The photograph and schematic drawings cross section of the DSSCs test cell. (a) top view and (b) side view.

3.6 The DSSCs characterization

3.6.1 The *J-V* measurement

The photovoltaic properties of DSSCs were determined by current voltage workstation. The measurements were performed under the white illuminate light source (AM 1.5G) conditions. Figure 3.6 shows the key equipment of the *J-V* test station. These station was run a *J-V* measurement and calculated critical parameters such as short circuit current (I_{sc}), short circuit current density (J_{sc}), open circuit voltage (V_{oc}), fill factor (FF), maximum output power (P_{max}), solar light to electric power conversion efficiency (%PCE), and other standard photovoltaic cell parameters.

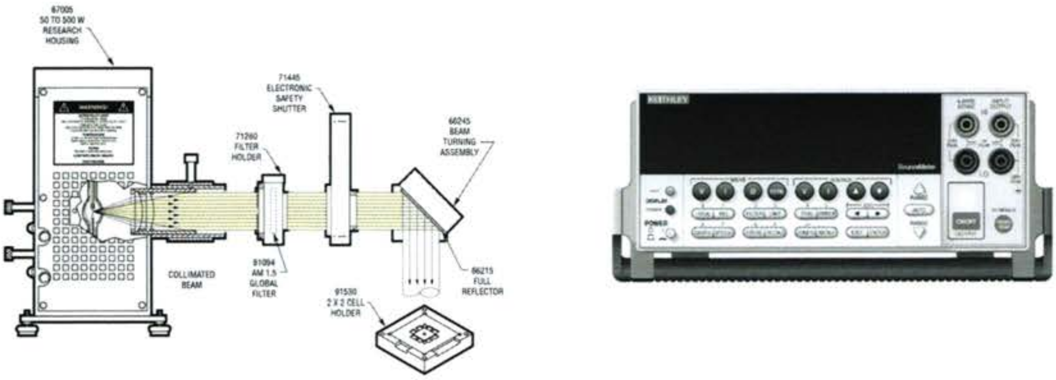

(a) (b)

Figure 3.6 The key equipment of *J-V* tester: (a) 96000 Oriel solar simulators and (b) front panel of 2400 Keithley source meter [32].

The *J-V* Tester configuration consist of Newport's Oriel 2 x 2 inch a 150 W xenon arc lamp 96000 solar simulator, the band pass filters to adjust the band pass spectral output and heat absorbing, source meter (Keithley model 2400) and computer control (see Figure 3.7). In this work, the photovoltaic characteristic of DSSCs was measured comparing to N3 dye and the photovoltaic characteristic value was reported in term of average value in three replicate (n=3).

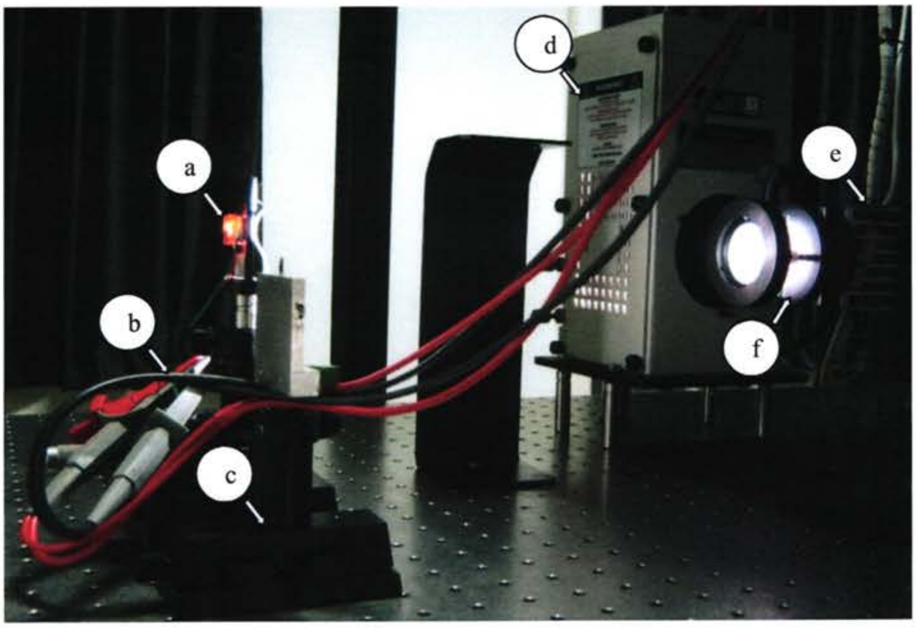

Figure 3.7 The photograph of *J-V* workstation. The key component of hardware configuration consist of (a) photovoltaic cell, (b) four point probe clamp and solid wire, (c) sample holder with high performance modular ball bearing linear and rotation stages, (d) solar simulator (Newport Oriel 96000), (e) beam turning (Newport 66245) and (f) multiple filter holder and optional filters.

3.6.2 The IPCE measurement

The incident photon to current conversion efficiency (IPCE) is defined as the number of electrons generated by light in the external circuit divided as a specific wavelength by the number of incident photons. In practice, this is achieved by using a monochromator as a tool to generate specific monochromatic light. The measurements processes were compared the spectral response of the silicon-photodiode and dye-sensitized solar cell devices.

The systems was based on a light source (Newport 96000 150 W Xenon arc lamp), monochromator (Newport Oriel Cornerstone™ 130 1/8 m), picoammeter (Keithley 6485), and computer control (Figure 3.8).

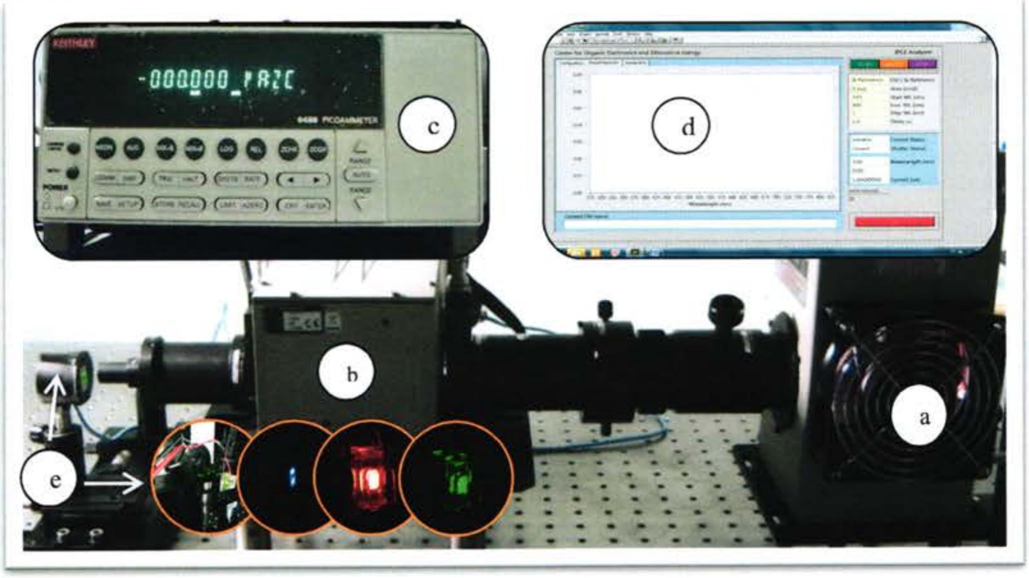

Figure 3.8 The photograph of IPCE tester. The key components consist of (a) Oriel 96000 solar simulator, (b) Oriel Cornerstone™ 130 1/8 m monochromator, (c) Keithley 6485 picoammeter, (d) front panel of software control and (e) photovoltaic cell.

3.6.3 The X-ray diffraction (XRD) measurement

The XRD was performed to determine crystal phase and crystallite size of TiO_2. The characterization was conducted by using a Phillip X'Pert - MDP, X - ray diffractometer with Cu K-α radiation (λ = 1.5418 Å) with Ni filter (Figure 3.9(a)). The operation was performed at 40 kV and 35 mA. The spectra were scanned in the 2θ range of 20 - 90° at a rate of 0.02°/s.

3.6.4 The scanning electron microscopy (SEM) measurement

The surface morphology and thickness of TiO_2 film were measured by using a scanning electron microscope (JEOL JSM - 5410 LV) (Figure 3.9(b)). The operation was performed at an acceleration voltage of 15 - 20 kV.

(a) (b)

Figure 3.9 The photograph of (a) JSM - 5410 LV scanning electron microscope and (b) Philips X'pert MDP X - ray diffractometer.

CHAPTER 4

RESULTS AND DISCUSSION

This chapter is divided into two parts including the optimization of fabrication process of dye-sensitized solar cell based on N3 dye, which was described in section 4.1. The photovoltaic characteristic of organic dye-sensitized solar cell fabricated by optimization procedure was reported in section 4.2.

4.1 DEVICE FABRICATION AND PHOTOVOLTAIC CHARACTERIZATION OF DYE SENSITIZED SOLAR CELL

4.1.1 The effect of sealant thickness

The redox couple was a basic factor in dye-sensitized solar cell (DSSCs). The part length between electrodes; working electrode and counter electrode was affected on the diffusion and ion migration of redox mediator ($3I^-/I_3^-$) in the electrolyte.

In order to study the effect of electrolyte layer thickness, the electrolyte layer was controlled by sealant film thickness. The thickness was varied by changing type of sealant materials. The sealant materials used in this study were Surlyn® - 30, Para film M and EVA film. The thickness of sealant material was measured by scanning electron microscope (SEM) as shown in Figure 4.1.

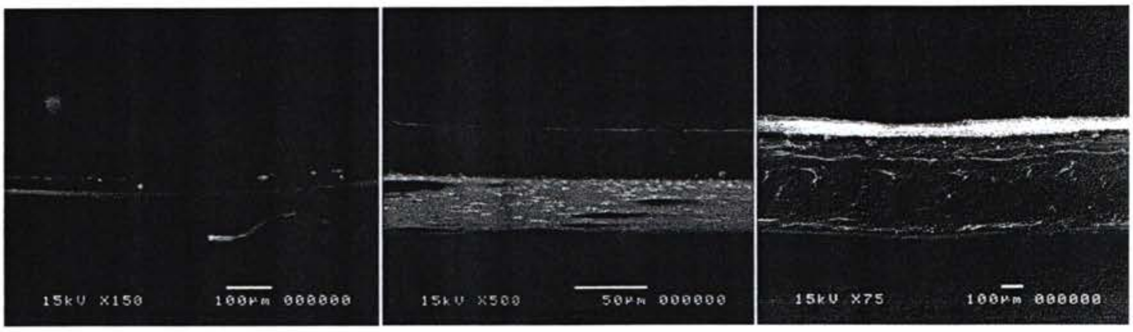

(a) (b) (c)

Figure 4.1 The cross section SEM photograph of sealant materials. (a) Surlyn® 30, (b) Para film M and (c) EVA film.

Table 4.1 The short circuit current density of DSSC devices as a function of sealant thickness.

Sealant Materials	**Average thickness (μm)**	**J_{sc} (mA/cm²)**
Surlyn® - 30	30	25.49±0.49
Para film M	140	19.20±1.08
EVA film	520	5.99±0.57

Table 4.1 shows the relationships between short circuit current density (J_{sc}) and thickness of sealant. The short circuits current density (J_{sc}) decreased when increased the sealant thickness. This result can be described by diffusion and ion migration in electrolyte. The ion migration in steady state operation processes sometime called the mass transport [73-74]. The mass transport and charge transfer rates of redox couple ($3I^-/I_3^-$) were represented in term of ionic conductivity and charge transfer resistance. The charge transfer resistance or electrolyte resistance (R_e) which one fraction of the series resistance (R_s), was depended on distance (d) between the two electrodes, the electrolyte conductivity (σ) and the electrode cross section (A) [75]. The electrolyte resistance (R_e) is defined as

$$R_e = \frac{d}{\sigma A} \tag{11}$$

The migration in steady state operation particularly in electrolyte systems with relatively low ionic conductivity display relatively low I_3^- diffusion coefficients, which can affect to noticeable limitation of low photocurrents [73, 75-76].

The Surlyn® film 30 μm of thickness was chosen as a sealant in this work.

4.1.2 The effect of TiO_2 film thickness

Generally, the photo-anode of DSSCs device consists of a nano-porous layer of titanium dioxide (TiO_2) nanoparticles, which monolayer sensitizer was adsorbed on their surface. In this work, two types of the commercial TiO_2 paste supplied by Solaronix® were used to make a TiO_2 working electrode. The transparent nanocrystalline titanium dioxide paste (Ti-Nanoxide T20/SP) contained 18%wt of 20 nm TiO_2 anatase particles. The result of TiO_2 layer after sintering was transparent, as shown in Figure 4.2(a). The reflective nanocrystalline titanium dioxide paste (Ti-Nanoxide R/SP) was contained 20%wt of optically dispersing TiO_2 mixed with small particle. The result of TiO_2 layer after sintering was opaque and reflective, as shown in Figure 4.2(b). The screen printing step was performed by screening of Ti-Nanoxide T/SP to make the photo absorbers layer and followed by Ti-Nanoxide R/SP in final layer to make the light scattering layer.

(a) (b)

Figure 4.2 The photograph of monolayer N3 sensitizer on titanium dioxide film coated FTO conducting glass surface, (a) Ti-Nanoxide T20/sp and (b) Ti-Nanoxide R/sp.

Figure 4.3 shows the X-ray diffraction patterns of the Ti-Nanoxide 20/SP and Ti-Nanoxide R/SP particle on the working electrode. The results indicated that the major phase of TiO_2 is anatase.

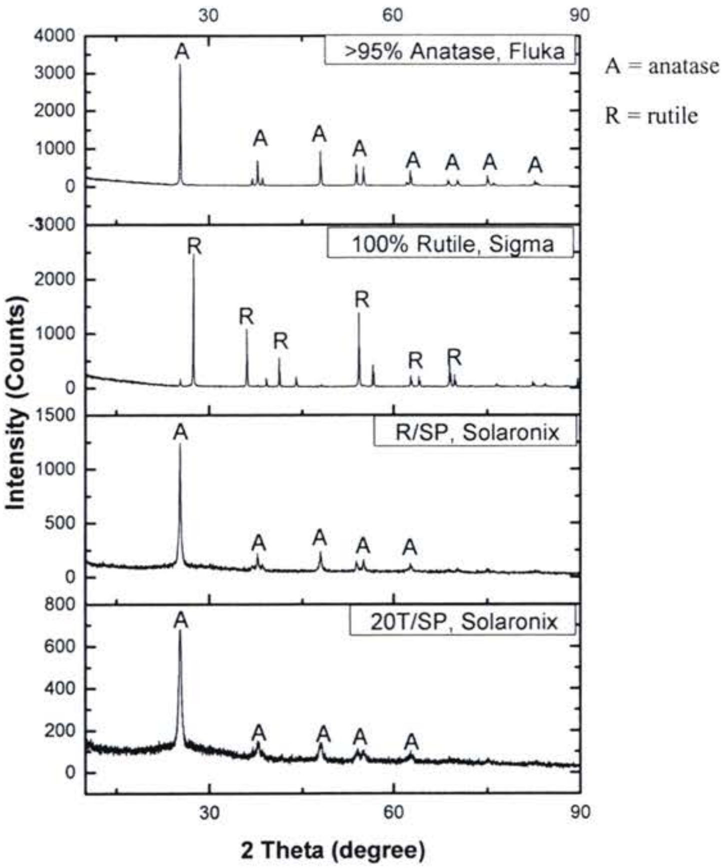

Figure 4.3 The X-ray diffraction pattern of TiO_2 particle.

Figure 4.4 shows the SEM cross section photograph of TiO_2 film on the FTO glass. The thickness as a number of screen printing time are listed in Table 4.2.

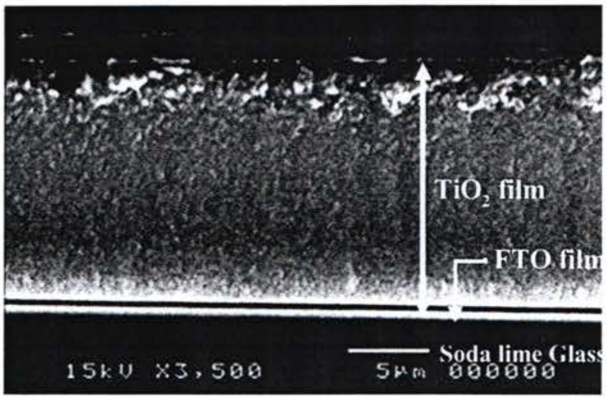

Figure 4.4 The SEM image of the TiO_2 film coated on the FTO glass.

Table 4.2 The thickness of TiO_2 film with difference screen printing time.

Coating time	**Details of screen printing step**	**Thickness (μm)**
2 time :	(1 layer Transparent past + 1 layer reflective paste)	5
3 time :	(2 layer Transparent past + 1 layer reflective paste)	11
4 time :	(3 layer Transparent past + 1 layer reflective paste)	16
5 time :	(4 layer Transparent past + 1 layer reflective paste)	18

Table 4.3 shows the current voltage (*J-V*) characteristic as a function of TiO_2 thickness. When the thickness of TiO_2 was increased from 5 μm to 11 μm, the current density of DSSCs increased from 9.07 to 10.40 mA/cm^2 and the power of conversion efficiency (%PCE) increase from 3.5% to 4.2%. The result shows that the power conversion efficiency increased when thickness of TiO_2 increased. This result can be explained by there are more light harvested of sensitizer on TiO_2 film. When TiO_2 film thickness was increased, the amount of TiO_2 particle also increased. Consequently, could absorbed more dye molecules leading to an enhancement the photocurrent of the DSSCs [26, 75, 77, 78].

Table 4.3 The photovoltaic characteristic of DSSC devices as a function of TiO_2 film thickness.

Thickness (μm)	J_{sc} **(mA/cm^2)**	V_{oc} **(V)**	**FF**	**PCE (%)**
5	9.07±1.30	0.64±0.02	0.61±0.03	3.5±0.4
11	10.40±1.31	0.64±0.02	0.63±0.01	4.2±0.7
16	8.77±0.26	0.57±0.04	0.49±0.15	2.5±1.0
18	8.50±1.31	0.42±0.29	0.41±0.16	1.8±1.7

However, the current density and power of conversion efficiency (%PCE) decreased when thickness of TiO_2 increased greater than 11 μm.

The optimal TiO_2 film thickness was 11 μm. The screen print step was 3 time which 2 layer Ti-Nanoxide T/SP as transparent layer and follow with 1 layer Ti-Nanoxide T/SP as reflective layer.

4.1.3 The effect of $TiCl_4$ treatment

Generally, the working electrode of DSSCs are requires at least one transparent conductive glass coated with nanocrystalline TiO_2 film. It was remained of the bare FTO surface around active area which electrolyte directly contract to the FTO glass surface. Therefore, the influence of the interfacial TiO_2 thin layer on the photovoltaic characteristic of DSSCs device was investigated. The TiO_2 thin layer was constructed by immersed FTO glass substrate in 40 mM titanium tetrachloride ($TiCl_4$) solution at 70°C for 30 min. After drying at room temperature, the TiO_2 paste was screen printed on $TiCl_4$ treated FTO substrate. The TiO_2 layer was sintered at 550°C.

Table 4.4 exhibits the influence of $TiCl_4$ treatment on the photovoltaic properties. The short circuit current density (J_{sc}) and fill factor of $TiCl_4$ treatment DSSCs have greater than DSSCs without treatments. The results indicated that, the DSSCs working electrode with $TiCl_4$ treatment was enhanced bonding strength between TiO_2 particle and FTO surface and suppressed the dark current [12, 79].

Table 4.4 The photovoltaic characteristic of DSSC devices with and without $TiCl_4$ treatment.

FTO conductive glass	J_{sc} (mA/cm^2)	V_{oc} (V)	FF	PCE (%)
without $TiCl_4$ treatment	9.55±1.76	0.69±0.01	0.59±0.01	3.9±0.8
with $TiCl_4$ treatment	11.14±0.51	0.69±0.01	0.62±0.01	4.8±0.1

In conclusion, the working electrode with $TiCl_4$ treatment was applied to increase the photocurrent of the DSSC devices.

4.1.4 The effect of device masking

The DSSCs device requires at least one transparent conductive glass substrate. An overestimation indirect light (absorption, reflection, and scattering et al.) from areas surrounding the active part of the photovoltaic cell are critical point in accurate characteristic of cell performance data. Therefore, the influence of shading or device masking on the photovoltaic characteristic was investigated. The current – voltage of DSSCs device was measured in with and without mask. The aperture area of mask was square 5 mm x 5 mm.

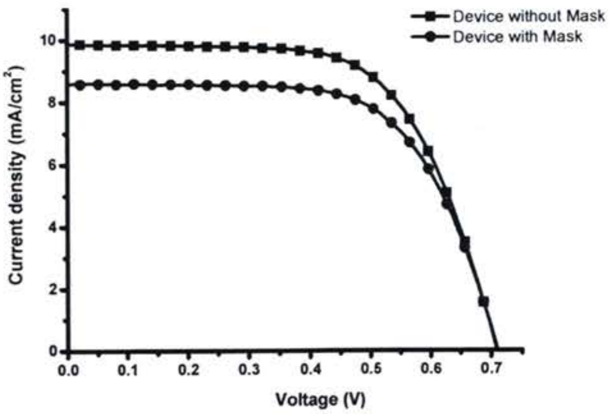

Figure 4.5 The *J-V* curves of DSSCs device measured with and without mask.

Figure 4.5 shows the *J-V* curve of DSSCs device measured with and without mask. The photovoltaic characteristics are listed in Table 4.5. The short circuit current density (J_{sc}) of DSSCs device without mask was greater than that of device with solid mask. The overestimation of J_{sc} was increased around 15% in the device without solid mask.

Table 4.5 The photovoltaic characteristic of DSSC devices with and without device masking

DSSCs test cell device	J_{sc} (mA/cm^2)	V_{oc} (V)	FF	PCE (%)
with mask	8.35±1.64	0.71±0.03	0.65±0.01	3.8±0.5
without mask	9.86±1.12	0.72±0.04	0.64±0.01	4.5±0.3

The phenomena were explained by the lighting collections in measurement condition. The optical artifacts such as light piping reflect, light striking and scattering from surrounding the active area by surface of FTO conducting glass are major of uncertainty light source. Therefore, the lighting condition has been avoided any diffuse or stray light hitting the device which may artificially increase device output. The solid mask should be used to correct the accurately define of the illuminated cell area in the case of a well collimate light beam. It is provided more accurate cell characteristic data [75, 80-81].

The square 0.25 cm^2 of aperture area masks was placed on the DSSCs device to accuracy the photovoltaic characteristic measurement.

4.1.5 The effect of platinum loading

The Pt film on counter electrodes was usually used as the conter electrode of DSSC device, due to its superior electrocatalytic reduction for redox couple (I^-/I_3^-) in electrolyte. Therefore, the influence of the Pt loading on photovoltaic characteristic of DSSCs device was investigated. The platinum film on DSSCs counter electrode was prepared by drop casting of platinum precursor on a cleaned FTO conductive glass and following by thermal treatment. The content of Pt was controlled by vary the volume, deposition time and concentration of platinum precursor. In this research, the concentration of platinum precursor of 2 mgPt/mL was prepared from chloroplatinic acid hexahydrate ($H_2PtCl_6.6H_2O$) in ethanolic solution.

Table 4.6 The photovoltaic characteristic of DSSC devices as a function of platinum loading

Pt content (μg/cm^2)	J_{sc} (mA/cm^2)	V_{oc} (V)	FF	PCE (%)
0.8	18.16±1.37	0.63±0.03	0.32±0.03	3.7±0.80
8.0	20.03±2.34	0.76±0.00	0.53±0.03	8.0±0.40
88.0	15.62±3.03	0.76±0.02	0.51±0.06	6.1±1.00

Table 4.6 shows the relationship between the Pt loading and *J-V* characteristics of DSSCs device. When a FTO glass was laminated with a low Pt loading (0.8 μg/cm^2), the J_{sc}, V_{oc}, FF and %PCE of the DSSCs were 18 mA/cm^2, 630 mV, 0.32 and 3.7% respectively.

The moderately Pt loading (8.0μg/cm^2) gave the J_{sc}, V_{oc}, FF and %PCE of 20.03 mA/cm^2, 760 mV, 0.53 and 8.0%, respectively. The results indicated that catalytic reactivity increased with increased the Pt loading. It is no significant difference in V_{oc} and FF value between 8.0 and 88.0 μg/cm^2 Pt loading. However, the J_{sc} and %PCE of DSSC devices dramatically decreased as high Pt content of 88.0 μg/cm^2 [54, 55, 56, 82].

The platinum counter electrode of DSSCs device was prepared by drop casting combined with thermal decomposition technique. This preparation method was simple, feasible in lab scale and low cost. The optimal platinum loading was 0.8 μg/cm^2.

4.1.6 Method validation

The fabrication process of DSSC devices consists of the electrolyte layer thickness, thickness of TiO_2 film, $TiCl_4$ treatment, device masking, and platinum loading. The methods validation of the optimal conditions was investigated by statistically variation of *J-V* characteristic.

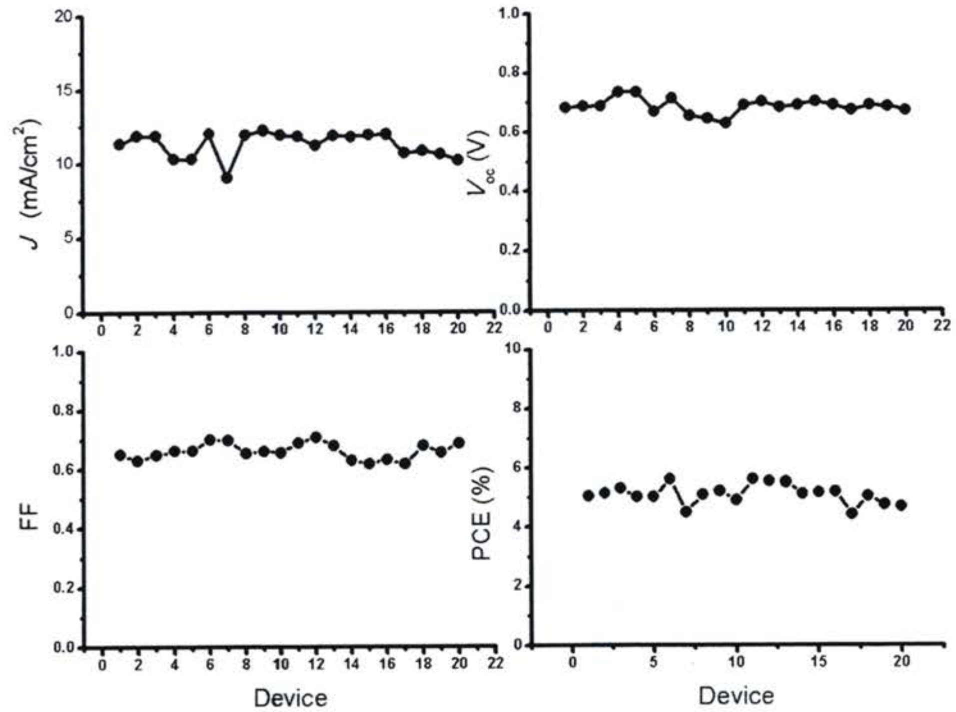

Figure 4.6 The *J–V* of DSSC devices in same process.

The repeatability of the DSSCs assembly process was evaluated based on fabrication of the DSSC device under the optimal condition in one batch (20 cells). The J_{sc}, V_{oc}, FF and %PCE distribution value of DSSC devices are shown in Figure 4.6.

The light-to-electric power conversion efficiency (%PCE) of 15 cells in 20 cells was greater than 5% and the best cell has %PCE of 5.6%. The average %PCE was 5.1%, the relative standard deviation (%RSD) was 0.33% and repeatability was over 75%. The results indicated that repeatability of optimal fabrication process was precise and suffice for evaluate photovoltaic characteristic of the novel organic dye.

4.2 PHOTOVOLATIC CHARACTERIZATION OF ORGANIC DYES FOR DYE SENSITIZED SOLAR CELLS

4.2.1 Photovoltaic characterization of carbazole triphenylamine dye for DSSCs

4.2.1.1 Target dye molecular and aim

Due to the promising donor ability of phenylamine, we has designed the target dyes with triphenylamine co-operate with two carbazole for the purpose of prevent dye aggregation and increasing donor ability, oligothiophene (thiophene 1-3 units) as π-conjugated bridge and cyanoacrylic acid as electron accepter for 2D-D-π-A sensitizer. The chemical structures of TPA1-3 dye are shown in Figure 4.7.

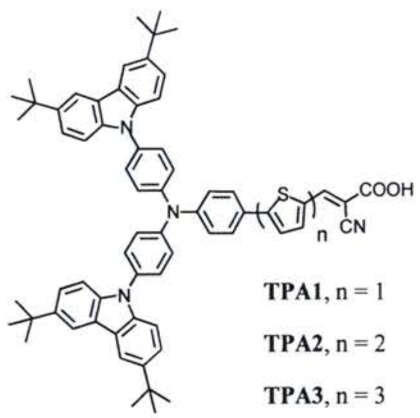

TPA1, n = 1

TPA2, n = 2

TPA3, n = 3

Figure 4.7 The chemical structure of target dyes (TPA1-3).

The TPA1-3 dyes have been designed by Assoc. Prof. Dr.Vinich Promarak, The compound were synthesized and characterized by Dr. Tanika Khanasa. The physical properties of TPA1-3 dye are listed in Table 4.7 [83].

Therefore, the objectives of this part are to fabrication DSSC devices based on the organic (TPA1-3) dyes and evaluated their photovoltaic characteristic performance.

Table 4.7 The physical properties of TPA1-3 dye [83].

Physical Properties	**N3**	**TPA1**	**TPA2**	**TPA3**
Chemical formula	$C_{26}H_{16}N_6O_8RuS_2$	$C_{66}H_{64}N_4O_2S$	$C_{70}H_{66}N_4O_2S_2$	$C_{74}H_{68}N_4O_2S_3$
Molecular weight (g/mole)	705.64	792.12	1059.43	1141.55
$Abs_{max}^{(a)}$ (nm)	530	458	455	464
Molar absorptivity$^{(a)}$ ($M^{-1}cm^{-1}$)	14,500	25,225	29,322	33,926
$Abs_{max}^{(b)}$ (nm)	-	436	442	450
$T_{5d}^{(c)}$ (^{o}C)	-	284	285	353
HOMO$^{(d)}$ (eV)	-5.52	-5.22	-5.20	-5.16
LUMO$^{(e)}$ (eV)	-3.84	-2.97	-2.99	-3.03

$^{(a)}$ Absorption measured in CH_2Cl_2 solution. $^{(b)}$ Absorption of the dyes adsorbed on TiO_2 film. $^{(c)}$ Measured by TGA at heating rate of $10^{o}C$/min under N_2. $^{(d)}$ Calculated using the empirical equation: HOMO = $-(4.44 + E^{ox}_{onset})$. $^{(e)}$ Calculated from LUMO = HOMO + E_g.

4.2.1.2 Photovoltaic characteristic of DSSC devices based on TPA1-3 dyes

The photovoltaic characteristic of the DSSC devices base on TPA1-3 dyes were measured under simulated sunlight AM 1.5G irradiation (100 mW/cm^2). The DSSC devices were fabricated under the conditions as described in section 4.1. The photograph of completed DSSC devices based on TPA1-3 dye and dye solution are shown in Figure 4.8(a) and Figure 4.8(b), respectively.

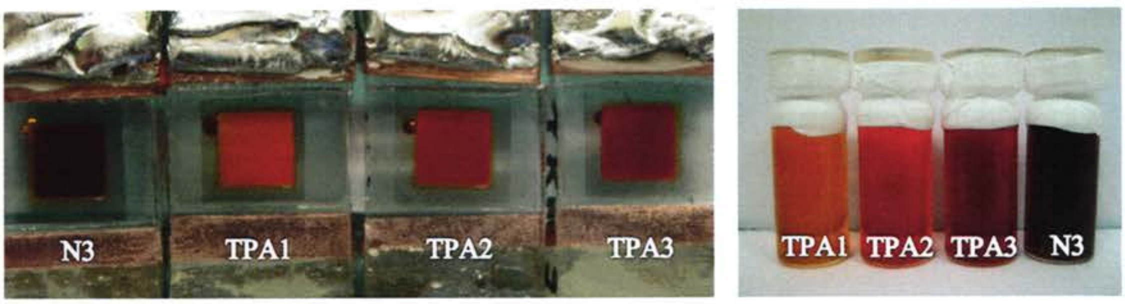

(a) (b)

Figure 4.8 The photograph of (a) DSSC devices and (b) dye solution based on TPA1-3 dye.

The J-V curves and the incident photon to current conversion efficiencies (IPCE) of all dyes are shown in Figure 4.9(a) and Figure 4.9(b), respectively. The photovoltaic characteristics of DSSC devices base on TPA1-3 dye are listed in Table 4.8.

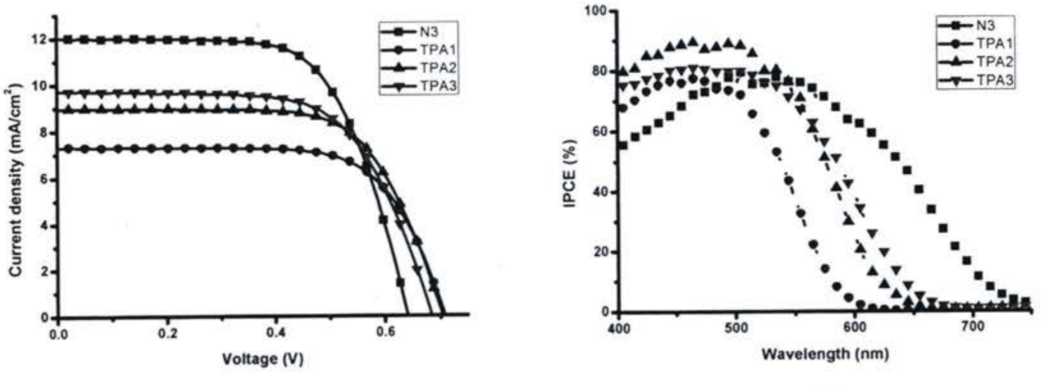

(a) (b)

Figure 4.9 (a) the J-V characteristics and (b) photocurrent action spectra of DSSCs device based on TPA1-3 sensitizer measured under irradiance of 100 mW/cm^2 AM 1.5G.

Under standard simulated sunlight irradiation (AM 1.5G, 100 mW/cm^2), the DSSC devices base on TPA3 dye showed the highest photovoltaic character among three dyes and gave a J_{sc}, V_{oc}, FF and %PCE of 9.73 mA/cm^2, 0.68 V, 0.65 and 4.3%, respectively.

Table 4.8 The photovoltaic characteristic of DSSC devices base on TPA1-3 dye.

Sensitizer	J_{sc} (mA/cm^2)	V_{oc} (V)	**FF**	**PCE** (%)
TPA1	7.31±0.36	0.71±0.02	0.69±0.02	3.6±0.2
TPA2	9.02±0.06	0.71±0.01	0.68±0.00	4.3±0.1
TPA3	9.73±0.32	0.68±0.01	0.65±0.01	4.3±0.1
N3	12.03±0.19	0.64±0.01	0.66±0.00	5.1±0.1

In addition, the larger J_{sc} and %PCE of DSSC devices with TPA3 (2D-D-π-A) dye demonstrates the beneficial influence of the red shifted absorption spectrum and the broadening of the IPCE spectrum. The result indicate that additional of carbazole groups as electron donors and tert-butyl groups as a molecular blocking, which shielding the TiO_2 surface from I^-/I_3^- in the electrolyte was enhance the light harvesting and reducing charge recombination or dark reaction, resulting in larger photo current and power conversion efficiency of the DSSC devices. However, the lower efficiency of device base on TPA1 dye was attributed by two manners, firstly poorer of spectral response in photocurrent action spectra, and secondly lower dye content on TiO_2 film, which rationalized by the steric hindrance of the donor moiety around the carboxylic acid anchoring group [83].

The IPEC spectra of the DSSC devices based on TPA1-3 dyes lie in blue/green regions and show maximum IPCE larger than N3 dye. The TPA2 based device with two thiophene units exhibit the best maximum IPCE of 86%. This observation deviates from expectation on the basis of the ε values of their absorption spectra. The DSSC devices with TPA3 dyes were exhibit the broadest spectra among three dyes, which almost reach to 750 nm. It is an indicated the high performance of photon absorption, resulting in high photocurrent and power conversion efficiency. The DSSC devices base on TPA3 dye was shown the excellent photovoltaic character which comparing to 84% with N3 dye. In contrast, the slightly lower IPCE value of DSSC devices base on TPA3 dyes compared with that DSSC devices base on TPA2 dyes is probably due to extended π-conjugation elongation of TPA3 dye, which may lead to decreased electron injection yield. Moreover, the IPCE values of all DSSC devices base on synthesized dyes were higher than that of the N3 dye due to the larger molar extinction coefficients of these organic dyes. However, the N3 dye showed a broader IPCE spectrum, which is consistent with its wider absorption spectrum [83].

It was found that the DSSC devices base on TPA1-3 dye, which an introduction of two carbazole moieties to form the 2D-D-π-A configuration brought about superior performance, in terms of bathochromically extended the IPCE spectra, enhanced the light harvesting in term of short circuit current density. These organic dyes based on this type of donor moiety or donor molecular architecture are promising candidates for improved performance DSSCs. This suggests that the DSSC devices base on a novel structural modification of the organic dyes strongly influences electron-injection and power conversion efficiencies of the DSSC devices.

4.2.2 Photovoltaic characterization of carbazole-diphenylamine dye for DSSCs

4.2.2.1 Target dye molecular and aim

Due to the promising donor ability of phenylamine, we has designed the target dyes with diphenylamine-encabed with 3,6-di-*tert*-butylcarbazole as double donor, oligothiophene (thiophene unit = 1-3) as π-conjugated linker and cyanoacrylic acid as electron accepter for D-D-π-A sensitizer. The chemical structures of DPA1-3 dye are shown in Figure 4.10.

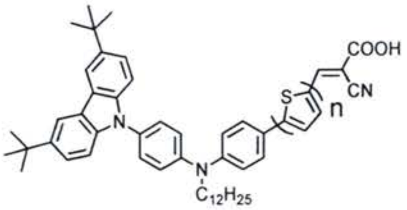

DPA1, n = 1

DPA2, n = 2

DPA3, n = 3

Figure 4.10 The chemical structure of target dyes (DPA1-3).

The DPA1-3 dyes have been also designed by Assoc. Prof. Dr.Vinich Promarak, The compound were synthesized and characterized by Dr. Tanika Khanasa. The physical properties of DPA1-3 dye are listed in Table 4.9 [84].

Therefore, the objectives of this part are to fabrication DSSC devices based on the organic (DPA1-3) dyes and evaluated their photovoltaic characteristic performance.

Table 4.9 The physical properties of DPA1-3 dye [84].

Physical Properties	N3	DPA1	DPA2	DPA3
Chemical formula	$C_{26}H_{16}N_6O_8RuS_2$	$C_{52}H_{61}N_3O_2S$	$C_{56}H_{63}N_3O_2S_2$	$C_{60}H_{65}N_3O_2S_3$
Molecular weight (g/mole)	705.64	792.12	874.25	956.37
Abs_{max} [(a)] (nm)	530	458	463	472
Molar absorptivity[(a)] ($M^{-1}cm^{-1}$)	14,500	5,022	5,485	6,024
Abs_{max} [(b)] (nm)	-	429	435	452
T_{5d} [(c)] (°C)	-	284	336	362
HOMO (eV)	-5.52	-5.22	-5.13	-5.08
LUMO (eV)	-3.84	-2.91	-2.87	-2.84

[(a)] Absorption measured in CH_2Cl_2 solution. [(b)] Absorption of the dyes adsorbed on TiO_2 film. [(c)] Measured by TGA at heating rate of 10°C/min under N_2. [(d)] Calculated using the empirical equation: HOMO = $-(4.44 + E^{ox}_{onset})$. [(e)] Calculated from LUMO = HOMO + E_g.

4.2.2.2 Photovoltaic characteristic of DSSC devices based on DPA1-3 dye

The photovoltaic characteristic of the DSSC devices base on DPA1-3 dyes were measured under simulated sunlight AM 1.5G irradiation (100 mW/cm^2). The DSSC devices were fabricated under the conditions as described in section 4.1. The photograph of complete DSSC devices based on DPA1-3 dye and dye solution are shown in Figure 4.11(a) and Figure 4.11(b), respectively.

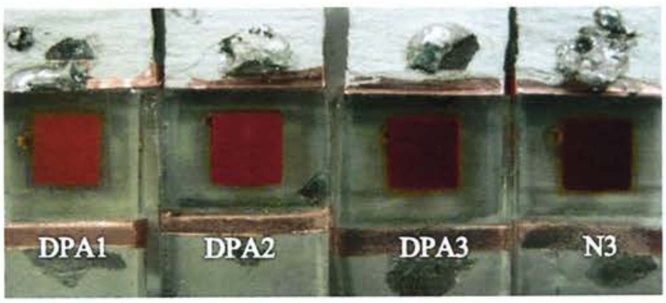

(a)

(b)

Figure 4.11 The photograph of (a) DSSC devices and (b) dye solution based on DPA1-3 dye.

The J-V curves of all dyes are shown in Figure 4.12(a) and IPCE spectra are shown in Figure 4.12(b). The photovoltaic characteristics of DSSC devices base on DPA1-3 dye are listed in Table 4.10.

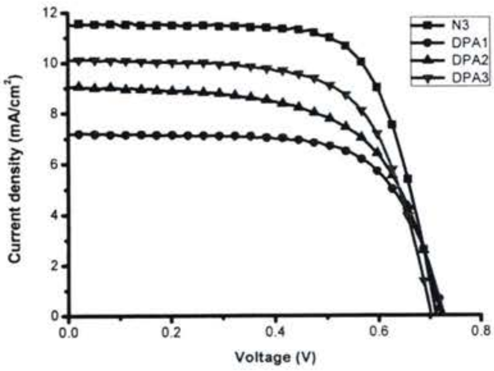

(a)

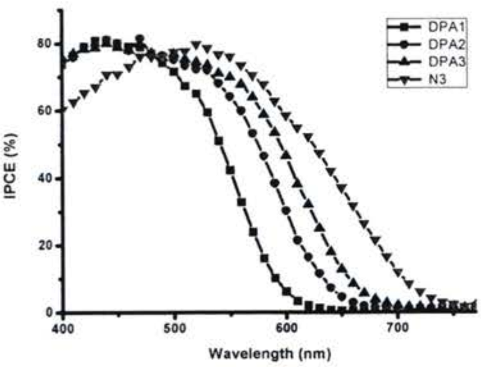

(b)

Figure 4.12 (a) the J-V characteristics (b) photocurrent action spectra of cells based on DPA1-3 sensitizer measured under irradiance of 100 mW/cm^2 AM 1.5G.

The photovoltaic characteristic of DSSC devices base on DPA1-3 dye was increase when increased the extension conjugate length of dye molecule. The π-conjugation in thiophene unit was increased the bathochromic shifted (red shifted) absorption. It was similar occurred in DSSC devices base on TPA1-3 dye in section 4.2.1. The DSSC devices base on DPA3 dye showed the excellent photovoltaic character that exhibits a J_{sc}, V_{oc}, FF and %PCE of 9.40 mA/cm^2, 0.68 V, 0.65 and 4.2%, respectively.

Table 4.10 The photovoltaic characteristic of DSSC devices based on DPA1-3 dye.

Sensitizer	J_{sc} (mA/cm^2)	V_{oc} (V)	**FF**	**PCE (%)**
DPA1	6.60±0.09	0.72±0.00	0.63±0.02	3.0±0.1
DPA2	8.16±1.26	0.70±0.00	0.62±0.03	3.5±0.4
DPA3	9.40±1.24	0.68±0.00	0.65±0.00	4.2±0.5
N3	11.55±0.49	0.69±0.01	0.69±0.02	5.5±0.0

Moreover, comparing photovoltaic characteristic of DSSC devices between TPA1-3 dye (2D-D-π-A in section 4.2.1) and DPA1-3 dye (D-D-π-A). The dye uptakes of DSSC device based on DPA series can adsorbed on TiO_2 film more than TPA series. This because the TPA dyes have two carbazole unit (2D-D-π-A) that increase the steric hindrance of the donor moiety around the carboxylic acid anchoring group whereas DPA dyes (D-D-π-A) have less steric effect from one carbazole moiety resulting in more dye uptake [84]. Therefore, the difference observed in photocurrent and power conversion efficiency of DSSC devices related to molecular volume and how much of dye molecule is absorbs.

The light-harvesting efficiency of DPA1 is expects to be less than those of the other dyes leading to a small incident monochromatic photon to current conversion efficiency for the DPA1 based cell. In contrast, higher IPCE value of DPA3 is probably due to its ε, which enhances the electron-injection yield in comparison with those of the other dyes. Because of their larger molar extinction coefficients, which the IPCE values of DSSC devices based on DPA1-3 dye are higher than that of the N3 dye based cell. However, DSSC devices with N3 dye shows a broader IPCE spectrum, which is consistent with its wide absorption spectrum [84].

These organic (DPA1-3) dyes exhibits power conversion efficiencies of DSSC devices correspond to overall conversion efficiency of 54 - 76% comparing with the N3 dye based cell. These strategies for designing of dyes molecule are proposed significantly simplified chemical structure.

4.2.3 Photovoltaic characterization of carbazole - carbazole dye for DSSCs

4.2.3.1 Target dye molecular and aim

Due to the promising donor ability of carbazole in D-π-A sensitizer, we has designed the target dyes with an organic chromophore based on carbazole as the donor group, with a oligothiophene as linker and a cyanoacrylic acid moiety as acceptor/anchor group for D-D-π-A sensitizer. The molecular structures of target CCT1-3A dye are shown in Figure 4.13.

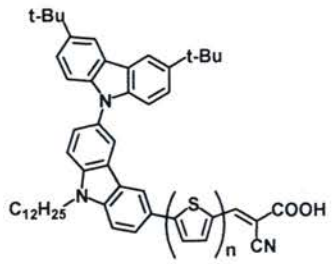

n = 1 – 3

CCT1A n = 1
CCT2A n = 2
CCT3A n = 3

Figure 4.13 The chemical structure of target dyes (CCT1-3A).

The CCT1-3A dyes have been also designed by Assoc. Prof. Dr.Vinich Promarak, The compound were synthesized and characterized by Mr.Sakravee Phunsay. The physical properties of CCT1-3A dye are listed in Table 4.11 [85].

Therefore, the objectives of this part are to fabrication DSSC devices based on the organic (CCT1-3A) dyes and evaluated their photovoltaic characteristic performance.

Table 4.11 The physical properties of CCT1-3A dye [85].

Physical Properties	**N3**	**CCT1A**	**CCT2A**	**CCT3A**
Chemical formula	$C_{26}H_{16}N_6O_8RuS_2$	$C_{52}H_{59}N_3O_2S$	$C_{56}H_{61}N_3O_2S_2$	$C_{60}H_{63}N_3O_2S_3$
Molecular weight (g/mole)	705.64	790.11	872.23	954.36
$Abs_{max}^{(a)}$ (nm)	530	432	457	443
Molar absorptivity$^{(a)}$ ($M^{-1}cm^{-1}$)	14,500	17,461	20,104	27,866
$Abs_{max}^{(b)}$ (nm)	-	420	440	437
$T_{5d}^{(c)}$ (^{o}C)	-	237	263	263
HOMO (eV)	-5.52	-5.33	-5.28	-5.26
LUMO (eV)	-3.84	-3.01	-3.11	-3.23

[a] Absorption measured in CH_2Cl_2 solution. [b] Absorption of the dyes adsorbed on TiO_2 film. [c] Measured by TGA at heating rate of $10^{o}C/min$ under N_2. [d] Calculated using the empirical equation: HOMO = $-(4.44 + E^{ox}_{onset})$. [e] Calculated from LUMO = HOMO + E_g.

4.2.3.2 Photovoltaic characteristic of DSSC devices based on CCT1-3A dyes

The photovoltaic characteristic of the DSSC devices base on CCT1-3A dyes were measured under simulated sunlight AM 1.5G irradiation (100 $mWcm^{-2}$). The DSSC devices were fabricated under the conditions as described in section 4.1. The photograph of complete DSSC devices based on CCT1-3A dye and dye solution are shown in Figure 4.14(a) and Figure 4.14(b) respectively.

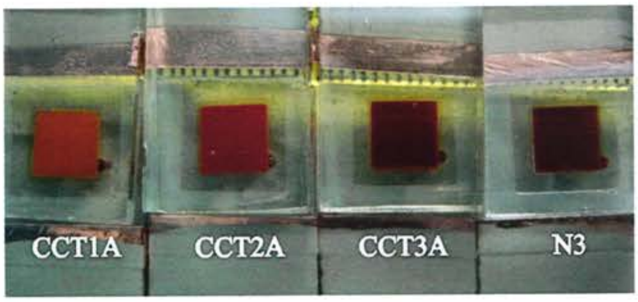

(a)

(b)

Figure 4.14 The photograph of (a) DSSC devices and (b) dye solution based on CCT1-3A dye.

The *J-V* curves of all dyes are shown in Figure 4.15(a) and IPCE spectra are shown in Figure 4.15(b). The photovoltaic characteristics of DSSC devices base on CCT1-3A dye are listed in Table 4.12.

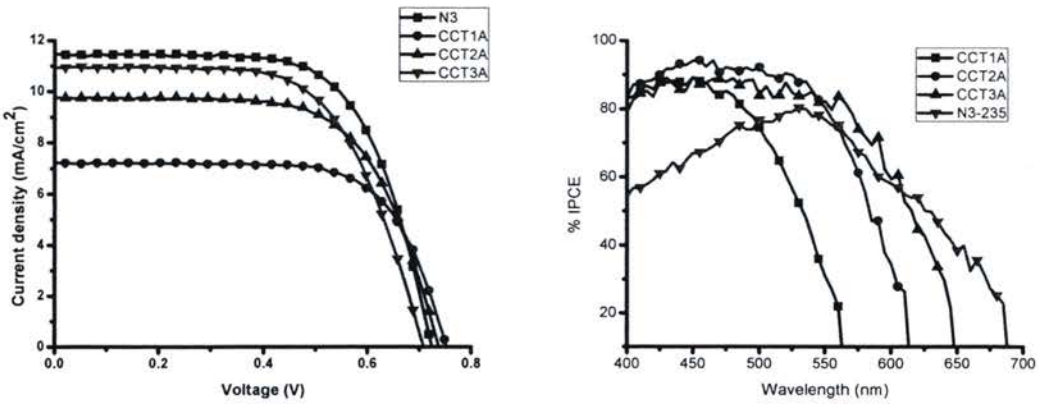

(a) (b)

Figure 4.15 (a) the *J-V* characteristics (b) photocurrent action spectra of cells based on CCT1-3A sensitizer measured under irradiance of 100 mW/cm^2 AM 1.5G.

The photocurrent and power conversion efficiency of device was increase when increased the extension conjugate path length. The π-conjugation length in thiophene unit increased the bathochromic shifted (red shifted) absorption spectra increased. It was similar in DSSC devices based on TPA1-3 dye in section 4.2.1 and DPA1-3 dye in section 4.2.2. Especially, the photovoltaic characteristic of CCT3A dye gave the J_{sc}, V_{oc}, FF and %PCE of 10.66 mA/cm^2, 0.71 V, 0.67 and 5.1%, respectively. It was correspond to overall conversion efficiency of 94% comparing with the N3 dye based cell.

Table 4.12 The photovoltaic characteristic of DSSC devices base on CCT1-3A dye

Sensitizer	J_{sc} (mA/cm^2)	V_{oc} (V)	**FF**	**PCE** (%)
CCT1A	7.06±0.41	0.74±0.01	0.68±0.01	3.6±0.3
CCT2A	9.60±0.09	0.74±0.01	0.67±0.01	4.8±0.1
CCT3A	10.66±0.25	0.71±0.01	0.67±0.03	5.1±0.2
N3	11.40±0.31	0.72±0.01	0.66±0.01	5.4±0.1

The CCT3A based devices with three-thiophene units as electron bridge was exhibit the best maximum IPCE of 86%, which presented the broadest spectra among three dyes and almost cover to 650 nm. It is an indicated the high performance of photon absorption, resulting in high photocurrent and power conversion efficiency. Moreover, the IPCE values of all DSSC devices base on synthesized dyes were higher than that of the N3 dye due to the larger molar extinction coefficients of these organic dyes [85]. However, the N3 dye showed a broader IPCE spectrum, which is consistent with its wider absorption spectrum.

The DSSC devices based on CCT1-3A dye exhibited excellent photovoltaic characteristic and photocurrent action spectrum (IPCE). The red shift and broad in IPCE spectrum was observed when increased conjugation path length by the number of thiophene unit, which cover in the blue/green region of solar light. The CCT3A exhibited the highest solar to electric power conversion efficiency of 94% comparing with commercial available ruthenium complex (N3) dye based cell. The results suggest that the DSSC devices based on double carbazole donor moiety (D-D-π-A) and three-thiophene electron bridge are promising candidates for improvement of the photovoltaic performance of the DSSCs technology.

CHAPTER 5

CONCLUSIONS

In this work, we have been reported the fabrication condition of DSSCs and characterization of the photovoltaic properties of novel organic dye, which including: TPA (2D-D-π-A) dyes, DPA (D-D-π-A) dyes and CCTA (D-D-π-A) dyes.

The 30 μm Dupont ionomer Surlyn® was used as the sealant material. The TiO_2 film thickness was 11 μm, which the screen-printing of 3 layered of a Ti-Nanoxide T/SP as transparent layer and 1 layered of Ti-Nanoxide R/SP as scattering layer. The interfacial-blocking layer TiO_2 film was introduced by immersed FTO conducting glass in 40 mM titanium tetrachloride ($TiCl_4$) at 70°C for 30 min. The square 0.25 cm^2 of masks was place on the front of DSSCs device. The loading of platinum content on counter electrodes was 8.0 $\mu g/cm^2$.

The J_{sc} and %PCE of DSSC devices based on starburst like TPA and DPA organic dye was increased when increased the electron donor by carbazole unit. The bathochromically red shift and broad extended of IPCE spectra were observed when the extension conjugates path length by the thiophene unit. The DSSC device based on DPA3, TPA3 and CCT3A dye exhibited the excellent overall conversion efficiency correspond to 76%, 84% and 94%, respectively, compare with commercial available ruthenium complex (N3) dye based cell. The result indicated that, the strategy capacities of these organic dyes are promising candidates for improvement of the photovoltaic performance in the DSSCs technology.

The further outlook are following as; (1) an increase photocurrent by modified the surface of TiO_2 film, (2) reduce sheet resistance loss by an integrated current correcting grids, (3) eliminate the oxygen and humidity, that degraded almost any electro-active of organic dye, (4) scale up test cell to module, panel and BIPV in term of pilot production line.

REFERENCES

REFERENCES

[1] Green, M. "Third Generation Photovoltaics: Ultra High Conversion Efficiency at Low Cost", Progress in Photovoltaics: Research and Applications. 9(2): 123-135, 2001.

[2] Wikipedia. "Solar Cell", Solar Tracker. http://en.wikipedia.org/wiki/solar_tracker. June 10, 2009.

[3] Sustainable E. "Renewable", Sustainable Biomass. http://sen.asn.au/renewables/biomass. June 10, 2009.

[4] Anoalucia. "Ecological Technology", Wind Power. http://www.andalucia.com/ environment/new-ecological-technology.htm. June 10, 2009.

[5] Solanski, C. "Solar Photovoltaics: Fundamentais Technologies and Application". New Delhi: PHI Learning Prt. Ltd, 2009.

[6] Greg, S. Progress in Next Generation Photovoltaic Devices. Doctor's Thesis: Iowa State University, 2006.

[7] Egat. "Solar Cell Technology", Solar Cell. http://www.egat.co.th/gpo/solar cell.html August 17, 2009.

[8] Grätzel, M. "Photoelectrochemical Cells", Nature. 414(6861): 338-344, 2001.

[9] Gregory, F. and Wu, J. "Third Generation Photovoltaics", Laser & Photon. 4(3): 394-405, 2009.

[10] O'Regan, B., and Grätzel, M. "A Low Cost High Efficiency Solar Cell Based On Dye Sensitized Colloidal TiO_2 Films", Nature. 353(6346): 737-740, 1991.

[11] Festa, P. "Tutte Le Notizie", Summer School Marinella Ferrari. http://www.chimica. unimi.it/ecm/home/aggiornamenti-e-archivi/tutte-le-notizie/ content/summer school-marinella-ferrari.0000.UNIMIDIRE-4434. July 10, 2013.

[12] Ito, S., et al. "Fabrication of Thin Film Dye Sensitized Solar Cells with Solar to Electric Power Conversion Efficiency Over 10%", Thin Solid Films. 516(14): 4613-4619; 2008.

[13] Chiba, Y., et al. "Dye Sensitized Solar Cells with Conversion Efficiency of 11.1%". Japanese Journal of Applied Physics. 45(25): L638-L640, 2006.

[14] Nusbaumer, H., et al. "An Alternative Efficient Redox Couple for the Dye Sensitized Solar Cell System", Chemistry – A European Journal. 9(16): 3756-3763, 2003.

REFERENCES (CONTINUED)

[15] Deng, J., et al. "Solid State Dye Sensitized Hierarchically Structured ZnO Solar Cells", Electrochimica Acta. 56(11): 4176-4180, 2011.

[16] Shen, X., et al. "Quasi Solid State Dye Sensitized Solar Cells Based On Gel Electrolytes Containing Different Alkali Metal Iodide Salts", Solid State Ionics. 179(35-36): 2027-2030, 2008.

[17] Veerappan, G., et al. "Carbon Nanofiber Counter Electrodes for Quasi Solid State Dye Sensitized Solar Cells". Journal of Power Sources. 196(24): 10798-10805, 2011.

[18] Guo, L., et al. "Novel Hydrophobic Ionic Liquids Electrolyte Based On Cyclic Sulfonium Used in Dye Sensitized Solar Cells", Solar Energy. 85(1): 7-11, 2011.

[19] Guo, L., et al. "Ionic Liquid Electrolyte Based On s-propyl Tetra Hydrothiophenium Iodide for Dye Sensitized Solar Cells", Solar Energy. 84(3): 373-378, 2010.

[20] Murai, S., et al. "Quasi Solid Dye Sensitized Solar Cells Containing Chemically Cross Linked Gel: How to Make Gels with a Small Amount of Gelator", Journal of Photochemistry and Photobiology A: Chemistry. 148(1-3): 33-39, 2002.

[21] Suzuki, K., et al. "A New Alkyl Imidazole Polymer Prepared as an Inonic Polymer Electrolyte by In Situ Polymerization of Dye Sensitized Solar Cells", Journal of Photochemistry and Photobiology A: Chemistry. 164(1-3): 81-85, 2004.

[22] Wikipedia. "Solar Cell", Solar Cell. http://en.wikipedia.org/wiki/solar cell. October 27, 2013.

[23] Rühle, S. Electron Transport in Mesoporous TiO_2 Structures and Contact Properties at the TiO_2 /Conductive Substrate Interface. Doctor's Thesis: Rehovot University, 2004.

[24] Moser, J., et al. "Molecular Photovoltaics", Coordination Chemistry Reviews. 171(1): 245-250, 1998.

[25] Grätzel, M. "Conversion of Sunlight to Electric Power by Nanocrystalline Dye Sensitized Solar Cells", Journal of Photochemistry and Photobiology A: Chemistry. 164(1-3): 3-14, 2004.

[26] Grätzel, M. "Perspectives for Dye Sensitized Nanocrystalline Solar Cells", Progress in Photovoltaics: Research and Applications. 8(1): 171-185, 2000.

REFERENCES (CONTINUED)

[27] Zhang, Z. Enhancing the Open Circuit Voltage of Dye Sensitized Solar Cells: CoadSorbents and Alternative Redox Couples. Doctor's Thesis: École Polytechnique Fédérale De Lausanne, 2008.

[28] Bisquert, J., et al. "Physical Chemical Principles of Photovoltaic Conversion with Nano Particulate, Mesoporous Dye Sensitized Solar Cells", The Journal of Physical Chemistry B. 108(24): 8106-8118, 2004.

[29] National Science Foundation. "Solar Radiation at the Earth's Surface", Air mass. http://www.pveducation.org/pvcdrom. June 4, 2010.

[30] National Science Foundation. "Air Mass", Air Mass2.11. http://www.pveducation.org/pvcdrom. November 10, 2010.

[31] Wikipedia. "Air mass", Air mass (solar energy). http://en.wikipedia.org/wiki. June 4, 2010.

[32] Oriel. Oriel Product Training: Solar Simulation. California: Newport Corporation, 2007.

[33] Grätzel, M. "Dye Sensitized Solar Cells", Journal of Photochemistry and Photobiology C: Photochemistry Reviews. 4(2): 145-153, 2003.

[34] Boonyaves, K. Improving Efficiency of Dye senstitized Solar Cell By Modification of TiO_2 Electrode. Doctor's Thesis: Chulalongkorn University, 2006.

[35] Wikipedia. "Quantum Efficiency", Quantum Efficiency. http://en.wikipedia.org/wiki/quantum_efficiency. March 27, 2010.

[36] Tachibana, Y., et al. "Quantitative Analysis of Light Harvesting Efficiency and Electron Transfer Yield in Ruthenium Dye Sensitized Nanocrystalline TiO_2 Solar Cells", Chemistry of Materials. 14(6): 2527-2535, 2002.

[37] Grätzel, M. "Sol-Gel Processed TiO_2 Films for Photovoltaic Applications", Journal of Sol-Gel Science and Technology. 22(1): 7-13, 2001.

[38] Burnside, S., et al. "Deposition and Characterization of Screen Printed Porous Multi Layer Thick film Structures from Semiconducting and Conducting Nanomaterials for Use in Photovoltaic Devices", Journal of Materials Science: Materials in Electronics. 11(4): 355-362, 2000.

REFERENCES (CONTINUED)

[39] Tsoukleris, D., et al. "2-Ethyl-1-Hexanol Based Screen-Printed Titania Thin Film for Dye Sensitized Solar Cells", Solar Energy. 79(4): 422-430, 2005.

[40] Ito, S., et al. "Fabrication of Screen Printing Pastes from TiO_2 Powders for Dye Sensitized Solar Cells", Progress in Photovoltaics: Research and Applications. 15(7): 603-612, 2007.

[41] Han, J., et al. "Dye Sensitized Solid State Solar Cells Fabricated by Screen Printed TiO_2 Thin Film with Addition of Polystyrene Balls", Chinese Chemical Letters. 19(8): 1004-1007,2008.

[42] Nama, J., et al. "Photovoltaic Enhancement of Dye Sensitized Solar Cell Prepared from [TiO_2/Ethyl Cellulose/Terpineol] Paste Employing TRITONTM X Based Surfactant with Carboxylic Acid Group in the Oxyethylene Chain End", Materials Chemistry and Physics. 116(1): 46-51, 2009.

[43] Ito, S., et al. "Facile Fabrication of Mesoporous TiO_2 Electrodes for Dye Solar Cells: Chemical Modification and Repetitive Coating", Solar Energy Materials and Solar Cells. 76(1):3-13, 2003.

[44] Fan, K., et al. "Effects of Paste Components on the Properties of Screen Printed Porous TiO_2 Film for Dye Sensitized Solar Cells", Renewable Energy. 35(2): 555-561, 2010.

[45] Dhungel, S., et al. "Optimization of Paste Formulation for TiO_2 Nanoparticles with Wide Range of Size Distribution for Its Application in Dye Sensitized Solar Cells", Renewable Energy. 35(12): 2776-2780, 2010.

[46] Syrrokostas, M., et al. "Effects of Paste Storage on the Properties of Nanostructured Thin Films for the Development of Dye Sensitized Solar Cells", Renewable Energy. 34(7): 1759-1764, 2009.

[47] Dyesol. "Materials Application", Screens Printer Large. ttp://www.dyesol.com/products/equipments/materials-application/screen-printers/screen-printer-large.html. January 19, 2012.

[48] Toby, M. Solaronix Catalogue. Aubone Switzerland: Solaronix, 2010.

[49] Tulloch, G. Dyesol Catalogue. Queanbeyan Australia: Dyesol Global HQ, 2010

REFERENCES (CONTINUED)

[50] Libre, I. "Sustainable Colorado", Irish Company Solar Print. http://sustainable colorado. blogspot.com/2011_01_01_archive.html. July 22, 2012.

[51] Takurou, N., et al. "Counter Electrodes for DSC: Application of Functional Materials as Catalysts", Inorganica Chimica Acta. 361(3): 572–580, 2008.

[52] Jinmaol, C., et al. "A Novel Method for Preparing Platinized Counter Electrode of Nano Crystalline Dye Sensitized Solar Cells", Chinese Science Bulletin. 50(1): 11-14, 2005.

[53] Khelashvili, G., et al. "Preparation and Characterization of Low Platinum Loaded Pt:SnO_2 Electrocatalytic Films for Screen Printed Dye Solar Cell Counter Electrode", Thin Solid Films. 515(7-8): 4074-4079, 2007.

[54] Li, P., et al. "Improvement of Performance of Dye Sensitized Solar Cells Based on Electrodeposited Platinum Counter Electrode", Electrochimica Acta. 53(12): 4161-4166, 2008.

[55] Fang, X., et al. "Performances Characteristics of Dye Sensitized Solar Cells Based on Counter Electrodes with Pt Films of Different Thickness", Journal of Photochemistry and Photobiology A: Chemistry. 164(1): 179-182, 2004.

[56] Fang, X., et al. "Effect of the Thickness of the Pt Film Coated on a Counter Electrode on the Performance of a Dye Sensitized Solar Cell", Journal of Electroanalytical Chemistry. 570(2): 257-263, 2004.

[57] Hagfeldt, A., et al. "Dye Sensitized Solar Cells", Chemical Reviews. 110(11): 6595-6663, 2010.

[58] Jena, A., et al. "Dye Sensitized Solar Cells: a Review", Transactions of the Indian Ceramic Society. 71(1): 1-16, 2012.

[59] Wu, J., et al. "Progress on the Electrolytes for Dye Sensitized Solar Cells", Pure and Applied Chemistry. 80(11): 2241-2258, 2008.

[60] Yu, Z. Liquid Redox Electrolytes for Dye Sensitized Solar Cells. Doctor's Thesis: Kth Chemical Science and Engineering, 2012.

[61] Kong, F., et al. "Review of Recent Progress in Dye Sensitized Solar Cells", Advances in OptoElectronics. 2007(1): 1-13, 2007.

REFERENCES (CONTINUED)

[62] Li, B., et al. "Review of Recent Progress in Solid State Dye Sensitized Solar Cells", Solar Energy Materials and Solar Cells. 90(5): 549-573, 2006.

[63] Tennakone, K., et al. "A Dye Sensitized Nano Porous Solid State Photovoltaic Cell", Semiconductor Science and Technology. 10(12): 1689-1693, 1995.

[64] Kumara, G., et al. "Dye Sensitized Solar Cell with the Hole Collector p-CuSCN Deposited from a Solution in N-Propyl Sulphide", Solar Energy Materials and Solar Cells. 69(2): 195-199, 2001.

[65] Regan, O., et al. "Large Enhancement in Photocurrent Efficiency Caused by UV Illumination of the Dye Sensitized Heterojunction TiO_2/RuLL'NCS/CuSCN: Initiation and Potential Mechanisms", Chemistry of Materials. 10(6): 1501-1509, 1998.

[66] Tennakone, K., et.al. "Dye Sensitized Solid State Photovoltaic Cell Based On Composite Zinc Oxide/tin (IV) Oxide Films", Journal of Physics D. 32(4): 374, 1999.

[67] Kong, F. T., et al. "Review of Recent Progress in Dye Sensitized Solar Cells", Advances in OptoElectronics. 2007(01): 1-13, 2007.

[68] Kim, S. "Molecular Engineering of Organic Sensitizers for Solar Cell Application", Journal of the American Chemical Society, 128(51): 16701-16707, 2006.

[69] Kazuhiro, K. "Photo Sensitization of a Porous TiO_2 Electrode with Meroyanine Dyes Containing a Carboxyl Group and a Long Alkyl Chain", Chemical Communications. 261(13): 1173-1174, 2000.

[70] Hara, K., et al. "Oligothiophene Containing Coumarin Dyes for Efficient Dye Sensitized Solar Cells", The Journal of Physical Chemistry B. 109(1): 15476-15482, 2005.

[71] Solaronix. "Buying Guide for Newcomers" How to Start with Dye Solar Cells . http://www.solaronix.com/products/device bulid - up. June 7, 2011.

[72] Martineau, D. Dye Solar Cells for Real. Aubonne Switzerland: Solaronix, 2010.

[73] Papageorgiou, N. "On the Relevance of Mass Transport in Thin Layer Nanocrystalline Photoelectrochemical Solar Cells", Solar Energy Materials and Solar Cells. 44(1): 405-438, 1996.

REFERENCES (CONTINUED)

[74] Nelson, J., et al. "Mass Transport of Poly Pyridyl Cobalt Complexes in Dye Sensitized Solar Cells with Meso Porous TiO_2 Photo Anodes", The Journal of Physical Chemistry C. 112(46): 18255-18263, 2008.

[75] Desilvestro, H. What Physical Factors Affect Current Voltage Characteristics of Dye Solar Cells. Queanbeyan Australia: Dyesol, 2008.

[76] Bisquert, J., et al. "Determination of Rate Constants for Charge Transfer and the Distribution of Semiconductor and Electrolyte Electronic Energy Levels in Dye Dye Sensitized Solar Cells by Open Circuit Photo voltage Decay Method", Journal of the American Chemical Society. 126(41): 13550-13559, 2004.

[77] Wang, M., et al. "Enhanced Light Harvesting Amphiphilic Ruthenium Dye for Efficient Solid State Dye Sensitized Solar Cells", Advanced Functional Materials. 20(11): 1821-1826, 2010.

[78] Baglio, V., et.al. "Influence of TiO_2 Film Thickness on the Electrochemical Behavior of Dye Sensitized Solar Cells", International Journal of Electrochemical Science. 6(1): 3375-3384, 2011.

[79] Brian C., et al. "Influence of the $TiCl_4$ Treatment on Nanocrystalline TiO_2 Films in Dye Sensitized Solar Cells. 2. Charge Density, Band Edge Shifts, and Quantification of Recombination Losses at Short Circuit", The Journal of Physical Chemistry C. 111(37): 14001-14010, 2007.

[80] Ito, S., et al. "Photovoltaic Characterization of Dye Sensitized Solar Cells: Effect of Device Masking on Conversion Efficiency", Progress in Photovoltaics: Research and Applications. 14(7): 589-601, 2006.

[81] Won, J., et al. "Dye Sensitized Solar Cells: Scale Up and Current Voltage Characterization", Solar Energy Materials & Solar Cells. 91(18): 1676-1680, 2007.

[82] Khelashvili, G., et al. "Catalytic Platinum Layers for Dye Solar Cells: A Comparative Study", Thin Solid Films. 512(1): 342-348, 2006.

REFERENCES (CONTINUED)

[83] Khanasa, T., et al. "Synthesis and Characterization of 2D-D-π-A-Type Organic Dyes Bearing Bis(3,6-di-tert-butylcarbazol-9-ylphenyl)aniline as Donor Moiety for Dye-Sensitized Solar Cells", European Journal of Organic Chemistry. 2013(13): 2608-2620, 2013.

[84] Namuangruk, S., et al. "D-D-π-A-Type Organic Dyes for Dye-Sensitized Solar Cells with a Potential for Direct Electron Injection and a High Extinction Coefficient: Synthesis, Characterization, and Theoretical Investigation", The Journal of Physical Chemistry C. 116(49): 25653-25663, 2012.

[85] Phansay, S. Synthesis and Characterization of Carbazole Derivatives for Optoelectronic Devices. Master's Thesis: Ubon ratchathani University, 2011.

APPENDIX


International Congress
for Innovation in Chemistry
(PERCH-CIC Congress VII)
"Chemistry, Environment and Society"
May 4-7, 2011
Jomtien Palm Beach Hotel & Resort, Pattaya, Thailand
Abstract Submission Deadline: January 31, 2011
Registration Online at www.perch-cic.org
Topics
• Alternative Energy
• Analytical Technologies
• Catalysis
• Chemical Biology and Biophysical Chemistry
• Chemical Education
• Computational and Theoretical Chemistry
• Cosmeceuticals, Nutraceuticals and Pharmaceuticals
• Environmental Chemistry
• Food Safety
• Materials Science and Nanotechnology
• Natural Products and Synthesis
PERCH-CIC Center of Excellence for Innovation in Chemistry
PERDO
For more information, please contact the Center of Excellence for Innovation in Chemistry
Tel: +66(0)2-201-5180, +66(0)2-644-5126 Fax: +66(0)2-644-5126 Email: scvrt@mahidol.ac.th Website: http://www.perch-cic.org

Effect of Large Particle TiO_2 Content in Light Scattering Layer on the Efficiency of Dye-sensitized Solar Cell

__Somphop Morada__, **Siriporn Jungsuttiwong, Tinnagon Keawin, Sayant Saengsuwan, Vinich Promarak, Taweesak Sudyoadsuk**

Center for Organic Electronics and Alternative Energy, Department of Chemistry and Center of Excellence for Innovation in Chemistry, Faculty of Science, Ubon Ratchathani University, Warinchumrap, Ubon Ratchathani 34190, Thailand.

Introduction and Objective

Dye-sensitized solar cells (DSC) have recently emerged as a promising inexpensive alternative to conventional p–n junction solar cells. Light management is some choices to optimization the DSC. In preliminary study, the effect of large particle TiO_2 content in scattering layer (SL) on the DSC efficiency was investigated.

Methods

The multilayered TiO_2 nanostructure films for DSC were fabricated by screen-printing method. The nanocrystalline TiO_2 (nc-TiO_2) paste was prepared as reference [1] by using 21-nm TiO_2 powder (P-25, Evonik). The mixture of 21 nm-TiO_2 and 400 nm-TiO_2 (Fluka) powers were used for light scattering (SL) paste preparation. The measurement are carried out in sealed cell with the glass/SnO_2:F/nc-TiO_2/SL-TiO_2/I^-/I_3^-/SnO_2:F (Pt)/glass composition under AM1.5 G (100 mW/cm^2) illumination.

Results

Figure 1 shows the dependence of power conversion efficiency (PCE) on the 400 nm-TiO_2 particle content in the light scattering layer, which varied in the rage from 10-40 wt%. The PCE is decreased by increase in large particle TiO_2 content. The highest PCE of 3.2±0.3 % was achieved when using the 10 wt% 400 nm-TiO_2 particle as a light scattering layer.

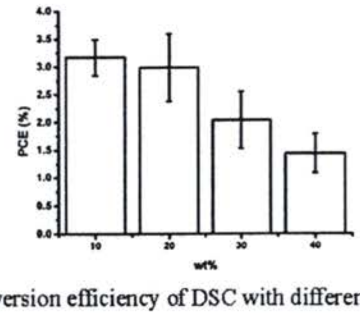

Figure 1. Power conversion efficiency of DSC with difference 400 nm-TiO_2 content.

Conclusion

In this preliminary studied, it found that the 10wt% 400 nm-TiO_2 particle is suitable for the light scattering layer of DSC. The improvement DSC performance is under investigated.

Keywords: DSC, Light Scattering layer

Selected References:

1. Ito, S.; Murakami, T.N.; Comte, P. *Thin Solid Films*, **2008**, *516*, 4613-4619.
2. Koo, H.J.; Park, J.; Yoo, B. *Inorganica Chimica Acta*, **2008**, *361*, 677-683.

Mr.Somphop Morada M.Sc. Student
b 1984 in Bangkok, Thailand
Ubon Ratchathani University, Thailand, Chemistry, B.Sc. 2006
Research field: Dye-sensitized solar cell, Photovoltaic cell, Optoelectronics

PERCH-CIC Congress VII (CONTINUED)

Effect of Large Particle TiO_2 Content in Light Scattering Layer on the Efficiency of Dye-sensitized Solar Cell

Somphop Morada, Siriporn Jungsuttiwong, Tinnagon Keawin, Sayant Saengsuwan, Vinich Promarak, Taweesak Sudyoadsuk
PERCH-CIC PERDO
Center for Organic Electronics and Alternative Energy, Department of Chemistry and Center of Excellence for Innovation in Chemistry, Faculty of Science, Ubon Ratchathani University, Warinchamrap, Ubon Ratchathani 34190, Thailand

Introduction

Dye-sensitized solar cells (DSCs) have recently emerged as a promising inexpensive alternative to conventional p–n junction solar cells. The highly efficient photovoltaic conversions, combined with ease of manufacturing and low production costs, make the DSCs technology an attractive approach for large-scale solar energy conversion [1].

In DSCs, the dye-adsorbed TiO_2 film plays an important role in converting photons to electrical energy since dyes generate photo excited electrons and the TiO_2 film serves as a pathway for photo-injected electrons.

Light management and optical engineering of TiO_2 were some choices to optimization the DSCs.

The research focused attractive on the effect of large particle TiO_2 content in scattering layer (SL) on the DSCs efficiency.

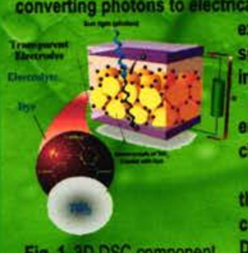

Fig. 1. 3D DSC component.

Experimental

The modified TiO_2 paste was prepared as reference [1] by using the nanocrystalline-TiO_2 (21 nm, P-25, Evonik Degussa) and mixture submicron-size (21 : 400 nm) of TiO_2 powders to make the transparent and light scattering paste, respectively.

The commercial available TiO_2 paste (20T/SP and R/SP, Solaronix) and modified paste was deposited on SnO_2:F glass for fabricated photo anode electrodes by screen-printing method and sintered at 500°C and then immerse in strain solution to completed dye sensitizer uptake.

The measurement are carried out in sandwich sealed cell with the glass/SnO_2:F/nc-TiO_2/SL-TiO_2/I^-/I_3^-/(Pt)/SnO_2:F/glass composition under AM1.5 G (100 mW/cm²) illumination [2].

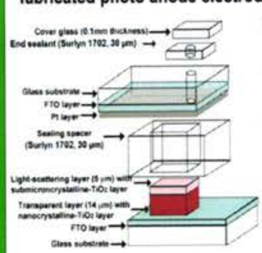

Fig. 2. The configuration of DSC device.

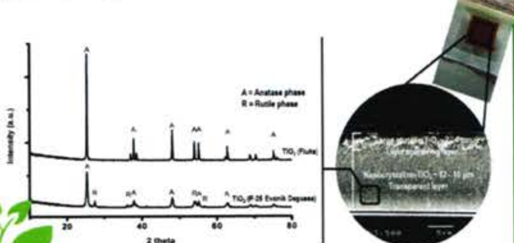

Fig. 3. XRD and SEM photograph of DSCs photo anode electrode.

Results and Discussion

Fig. 4 shows the I-V curve of two different TiO_2 structure of photo anode electrode. The TiO_2 electrode consisting of microcrystalline light-scattering gave photo current (J_{sc}) greater than that only transparent nanocrystalline electrode. The result indicated that, large particle in top layer was promoted to recapture a part of the light, which to enhance the light harvesting of the DSCs device [3].

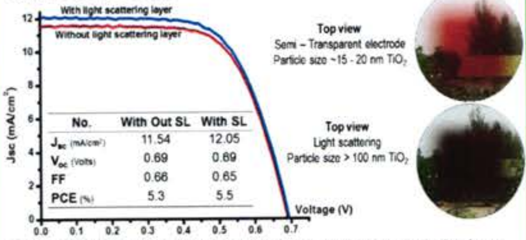

No.	With Out SL	With SL
J_{sc} (mA/cm²)	11.54	12.05
V_{oc} (Volts)	0.69	0.69
FF	0.66	0.65
PCE (%)	5.3	5.5

Fig. 4. The I–V curves of DSC device with and with out scattering layer, film thickness 14.68±0.16 μm, base on N3 dye.

Fig. 5 shows the dependence of power conversion efficiency (%PCE) base on the 400 nm-TiO_2 particle content for the light scattering layer, varied in the rage from 10-40 wt%. The PCE was decreased as increased in large particle TiO_2 content.

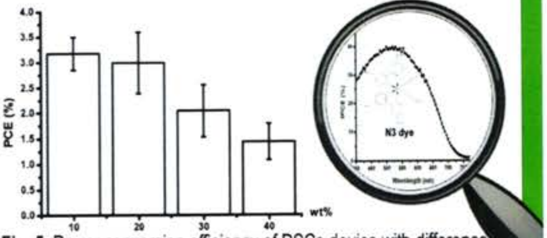

Fig. 5. Power conversion efficiency of DSCs device with difference 400 nm-TiO_2 content (n=3).

In this preliminary studied, it found that the modified paste 10wt% 400 nm-TiO_2 particle is suitable for the light scattering layer of DSCs. The improvement device performance is under investigated.

References

1. Ito, S.; Chen, P.; Khaja, M. *Prog. Photovolt: Res. Appl.*, 2007, DOI: 0.1002/pip
2. Ito, S.; Murakami, T.N.; Comte, P. *Thin Solid Films*, 2008, *516*, 4613-4619.
3. Koo, H.J.; Park, J.; Yoo, B. *Inorganica Chimica Acta*, 2008, *361*, 677-683.

Acknowledgements

Center of Excellence for Innovation in Chemistry (PERCH – CIC)
Center for Organic Electronics and Alternative Energy, Department of Chemistry
Faculty of Science, Ubon Ratchathani University

RESEARCH INTEGRATION for ASEAN COMMUNITY

ประชุมวิชาการ มอบ.วิจัย ครั้งที่ 5

เอกสารสืบเนื่องจากการประชุม

สาขา วิทยาศาสตร์และเทคโนโลยี

4 - 5 สิงหาคม 2554

ณ โรงแรมสุนีย์ แกรนด์ แอนด์ คอนเวนชั่น เซ็นเตอร์ จังหวัดอุบลราชธานี

Investigation Assembly Process And Application Of Low Cost Carbonaceous Materials For Counter Electrode In Dscs

Somphop Morada*, Siriporn Jungsuttiwong, Tinnagon Keawin, Sayant Saengsuwan, Vinich Promarak, Taweesak Sudyoadsuk
Center for Organic Electronics and Alternative Energy, Department of Chemistry Faculty of Science, Ubon Ratchathani University
E-mail : Bangrang.pri@gmail.com

บทคัดย่อ

งานวิจัยนี้ทำการศึกษาเทคนิคการเตรียมฟิล์มไททาเนียมไดออกไซด์สำหรับขั้วไฟฟ้าทำงานในเซลล์แสงอาทิตย์ชนิดสีย้อมไวแสง ประกอบไปด้วยการศึกษาการปรับสภาพขั้วไฟฟ้าทำงานด้วยไททาเนียมเตตระคลอไรด์ การออกแบบและความหนาของฟิล์มไททาเนียมไดออกไซด์ที่เหมาะสม การติดหน้ากากสำหรับเซลล์แสงอาทิตย์ในขณะวัดประสิทธิภาพ และการประยุกต์ใช้งานผงคาร์บอนสำหรับขั้วไฟฟ้าช่วยงานในเซลล์แสงอาทิตย์ชนิดสีย้อมไวแสง ผลการศึกษาพบว่าการปรับสภาพขั้วไฟฟ้าทำงานด้วยไททาเนียมเตตระคลอไรด์ช่วยเซลล์แสงอาทิตย์ให้กระแสไฟฟ้าและประสิทธิภาพการเปลี่ยนพลังงานแสงเพิ่มขึ้น การออกแบบและความหนาของชั้นไททาเนียมไดออกไซด์ พบว่าทั้งสองปัจจัยส่งผลต่อค่ากระแสและศักย์ไฟฟ้าของเซลล์ และการติดหน้ากากสำหรับเซลล์แสงอาทิตย์ในขณะวัดประสิทธิภาพช่วยให้ลดการประมาณค่ากระแสไฟฟ้าที่เกินความเป็นจริงช่วยให้ได้รับข้อมูลของเซลล์ที่มีความแม่นยำมากกว่า เซลล์แสงอาทิตย์ชนิดสีย้อมไวแสงที่ใช้กราไฟต์และคาร์บอนแบล็ค ในการประยุกต์ใช้ในขั้วฟ้าช่วยงานให้ประสิทธิภาพการเปลี่ยนพลังงานแสงที่ 4.2% เทียบเคียงได้กับการใช้งานขั้วไฟฟ้าช่วยโดยทั่วไปภายใต้แสงอาทิตย์จำลองที่ความเข้มแสง AM1.5 (1000 W/m^2)

คำสำคัญ : เซลล์แสงอาทิตย์ชนิดสียอมไวแสง ขั้วไฟฟ้าช่วยชนิดคาร์บอน กระบวนการขึ้นรูป

Abstract

In this research, techniques of TiO_2 film fabrication technologies consist of pre-treatment of the working electrode by $TiCl_4$, variations in design and layer thickness of nano-crystalline TiO_2, device masking and application of carbon material as counter were investigated. The result was found that the J_{sc} and PCE of DSCs increases with $TiCl_4$ treatments. Optimization of the design and thickness of the TiO_2 layer as the working electrode, influence both the J_{sc} and V_{oc} of the devices. DSCs device with solid mask were eliminated the overestimated the photocurrents, provide more accurate cell performance data. DSCs employing graphite carbon black composite as counter electrode achieve efficiency as 4.2% which quite attractive to conventional counter electrode under illumination of AM1.5 (1000 W/m^2) simulated sunlight

Keywords : Dye-sensitized solar cells (DSCs), Carbon Counter Electrode, Fabrication process

Introduction

Dye-sensitized solar cells (DSCs) have recently emerged as a promising inexpensive alternative to conventional p–n junction solar cells. The highly efficient photovoltaic conversions,

Investigation of assembly process and application of low cost carbonaceous materials for counter electrode in DSCs

Somphon Morada, Siriporn Jungsuttiwong, Tinnagon Keawin, Sayant Saengsuwan, Vinich Promarak, Taweesak Sudyoadsuk

Center for Organic Electronics and Alternative Energy, Department of Chemistry and Center of Excellence for Innovation in Chemistry, Faculty of Science, Ubon Ratchathani University, Warinchamrap, Ubon Ratchathani 34190, Thailand.

Bangrang.sri@gmail.com

RESEARCH INTEGRATION for ASEAN COMMUNITY

Introduction

In this research, techniques of TiO_2 film fabrication technologies consist of pre-treatment of the working electrode by $TiCl_4$, variations in design and layer thickness of nano crystalline TiO_2 and application of carbon material as counter were investigated.

Experimental

The commercial available TiO_2 paste (20T/SP and R/SP, Solaronix) and modified paste was deposited on SnO_2:F glass as a photo anode electrodes by screen-printing method [1].

The measurement are carried out in sandwich sealed cell with the glass/SnO_2:F/nc-TiO_2/SL-TiO_2/I^-/I_3^-/(Pt)/SnO_2:F/glass (Fig.1) composition under AM1.5 G (100 mW/cm²) illumination [2].

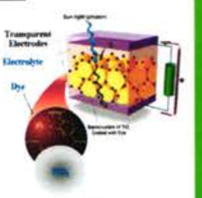

Fig. 1. 3D DSC component.

Results and Discussion

Optimum thickness

The thin film TiO_2 layer was in sufficient TiO_2 would not adsorb enough dye and thus the cell would not absorb sufficient light resulting in low photocurrents.

The thick film TiO_2 layer were increased the length of the electron pathways, recombination and diffusion length of I^-/I_3^- species. Which effect to decrease ff and Voc and in extreme cases even Jsc. Therefor, the optimum TiO_2 thickness was approximately 11 µm (Fig. 2).

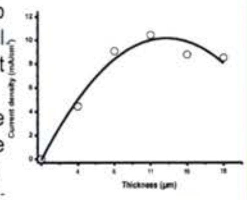

Fig. 2. The current density as a function of TiO_2 thickness.

Optimum structural design

Fig. 3 shows the photograph of two different TiO_2 photo anode electrode. The DSCs device consisting of nano crystalline TiO_2 cover with light scattering layer gave photo current (12.05 mA/cm²) greater than that only nano-crystalline electrode (8.88 mA/cm²) . The result indicated that, large particle in top layer was promoted to recapture a part of the light, which to enhance the light harvesting of the DSCs device.

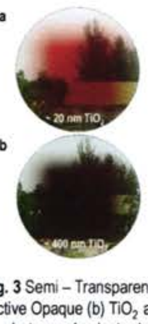

Fig. 3 Semi – Transparent (a) Active Opaque (b) TiO_2 as a photo anode electrode.

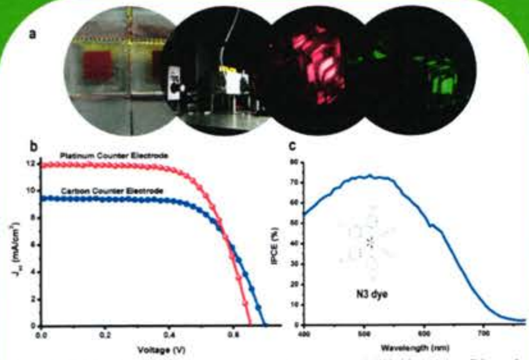

Fig. 4. DSCs device and measurements process (a) I–V curves (b) and IPCE curves (c) of DSC device with platinum and graphite carbon black composites counter electrodes.

Carbon counter electrode

The DSCs device with graphite carbon black composites as counter electrodes was shown surprising potential (~ 80%) comparison with platinum counters electrodes. Which function of the graphite was electronic conduction as well as catalytic activity, the high-surface area carbon black was added for increased catalytic effect. The result was enhancing of DSCs technology in three areas such as costs applicability and sustainability, which attractive to conventional PV technologies.

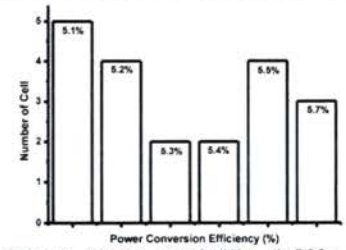

Fig. 5. Histogram depicting reproducibility of DSCs conversion efficiencies. Reported values of 20 DSCs devices produced with same condition.

Reproducibility of fabrication process

The conversion efficiencies greater than 5.3±0.2% were obtained with optimum fabrication condition. The statistical graph shows convincingly the excellent reproducibility of the method elaborated here for the fabrication of moderate efficient dye sensitized solar cells.

References

1. Ito, S.; Chen, P.; Khaja, M. *Prog. Photovolt: Res. Appl.*, 2007, DOI: 0.1002/pip. 768
2. Ito, S.; Murakami, T.N.; Comte, P. *Thin Solid Films*, 2008, *516*, 4613-4619.

Acknowledgements

1. Center of Excellence for Innovation in Chemistry (PERCH – CIC)
2. Center for Organic Electronics and Alternative Energy, Department of Chemistry Faculty of Science, Ubon Ratchathani University

PERCH-CIC PERDO

COER

Journal article I

THE JOURNAL OF
PHYSICAL CHEMISTRY

Article

pubs.acs.org/JPCC

D−D−π−A-Type Organic Dyes for Dye-Sensitized Solar Cells with a Potential for Direct Electron Injection and a High Extinction Coefficient: Synthesis, Characterization, and Theoretical Investigation

Supawadee Namuangruk,[†] Ryoichi Fukuda,[‡,§] Masahiro Ehara,[*,‡,§] Jittima Meeprasert,[†] Tanika Khanasa,[‖] Somphob Morada,[‖] Tinnagon Kaewin,[‖] Siriporn Jungsuttiwong,[‖] Taweesak Sudyoadsuk,[‖] and Vinich Promarak[*,‖,⊥]

[†]National Nanotechnology Center (NANOTEC), Thailand Science Park, Patumthani 12120, Thailand

[‡]Institute for Molecular Science and Research Center for Computational Science, 38 Nishigo-naka, Myodaiji, Okazaki 444-8585, Japan

[§]Japan Science and Technology Agency CREST, Sanboncho-5, Chiyoda-ku, Tokyo 102-0075, Japan

[‖]Center for Organic Electronic and Alternative Energy, Department of Chemistry and Center for Innovation in Chemistry, Faculty of Science, Ubon Ratchathani University, Warinchumrap, Ubon Ratchathani 34190, Thailand

Supporting Information

ABSTRACT: A series of organic sensitizers with the direct electron injection mechanism and a high molar extinction coefficient comprising double donors, a π-spacer, and anchoring acceptor groups (D−D−π−A type) were synthesized and characterized by experimental and theoretical methods for dye-sensitized solar cells. (*E*)-2-Cyano-3-(5″-(4-((4-(3,6-di-*tert*-butylcarbazol-9-yl)phenyl)dodecylamino)-phenyl)-[2,2′:5′,2″-terthiophene]-5-yl)acrylic acid showed performance with a maximal incident photon to electron conversion efficiency of 83%, J_{sc} value of 10.89 mA cm^{-2}, V_{oc} value of 0.70 V, and fill factor of 0.67, which correspond to an overall conversion efficiency of 5.12% under AM 1.5G illumination. The molecular geometry, electronic structure, and excited states were investigated with density functional theory, time-dependent density functional theory, and the symmetry-adapted cluster-configuration interaction method. The double donor moieties not only contribute to enhancement of the electron-donating ability, but also inhibit aggregation between dye molecules and prevent iodide/triiodide in the electrolyte from recombining with injected electrons in TiO_2. Detailed assignments of the UV−vis spectra below the ionization threshold are given. The low-lying light-harvesting state has intramolecular charge transfer character with a high molar extinction coefficient because of the long π-spacer. Our experimental and theoretical findings support the potential of direct electron injection from the dye to TiO_2 in one step with electronic excitation for the present D−D−π−A sensitizers. The direct electron injection, inhibited aggregation, and high molar extinction coefficient may be the origin of the observed high efficiency. This type of D−D−π−A structure with direct electron injection would simplify the strategy for designing organic sensitizers.

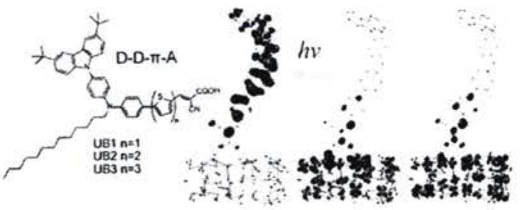

■ INTRODUCTION

Since the report on dye-sensitized solar cells (DSSCs) with a dramatic increase in the light-harvesting efficiency by O'Reagan and Grätzel in 1991,[1] this type of solar cell has attracted considerable and sustained attention as it offers the possibility of low-cost conversion of the photoenergy.[2] To date, a DSSC with a validated efficiency (η) record of >11% has been obtained with ruthenium complex dyes such as the black dye.[3] Though there is still room for improvement of the efficiency of ruthenium-based DSSCs,[4] ruthenium dyes are nevertheless costly and hardly attained and normally have a moderate absorption intensity.[5] Enormous effort is also being dedicated to developing efficient dyes suitable for their modest cost, ease of synthesis and modification, large molar extinction coefficient, and long-term stability. Ruthenium-free dyes or organic dyes meet all these criteria; therefore, there has been remarkable development in organic dye-based DSSCs in recent years,[6] and efficiencies exceeding 12% have been achieved using dyes which have broad, red-shifted, and intense spectral absorption in the visible light region, 400−800 nm.[7]

Although remarkable progress has been made in the organic dyes as sensitizers for DSSCs, optimization of their chemical

Received: May 9, 2012
Revised: November 15, 2012
Published: November 20, 2012

dx.doi.org/10.1021/jp304489t | J. Phys. Chem. C 2012, 116, 25653−25663

Journal article II

Tetrahedron Letters 54 (2013) 2435–2439

Contents lists available at SciVerse ScienceDirect

Tetrahedron Letters

journal homepage: www.elsevier.com/locate/tetlet

Synthesis and characterization of β-pyrrolic functionalized porphyrins as sensitizers for dye-sensitized solar cells

Kanokkorn Sirithip [a], Somphob Morada [a], Supawadee Namuangruk [b], Tinnagon Keawin [a], Siriporn Jungsuttiwong [a], Taweesak Sudyoadsuk [a], Vinich Promarak [c,*]

[a] Center for Organic Electronic and Alternative Energy, Department of Chemistry and Center for Innovation in Chemistry, Faculty of Science, Ubon Ratchathani University, Ubon Ratchathani 34190, Thailand

[b] National Nanotechnology Center (NANOTEC), 130 Thailand Science Park, Klong Luang, Pathumthani 12120, Thailand

[c] School of Chemistry and Center for Innovation in Chemistry, Institute of Science, Suranaree University of Technology, Muang District, Nakhon Ratchasima 30000, Thailand

ARTICLE INFO

Article history:
Received 19 October 2012
Revised 22 February 2013
Accepted 8 March 2013
Available online 15 March 2013

Keywords:
Porphyrin
β-Pyrrolic position
Donor–π-acceptor
Thiophene
Dye-sensitized solar cell

ABSTRACT

New β-pyrrolic functionalized porphyrins with donor–π–acceptor character were synthesized and characterized as dye sensitizers for dye-sensitized solar cells. Two types of π-conjugated spacers, namely benzene and thiophene rings, with cyanoacrylic acid as an acceptor were linked to the porphyrin ring at the β-pyrrolic position. These porphyrins showed high thermal and electrochemical stability. As sensitizers, the porphyrin dye bearing a thiophene ring as the π-conjugated spacer gave better cell performance with a short-circuit photocurrent density (J_{sc}) of 4.57 mA cm^{-2}, an open-circuit voltage (V_{oc}) of 0.59 V, and a fill factor (ff) of 0.59, corresponding to an overall conversion efficiency (η) of 1.94%.

Dye-sensitized solar cells (DSSCs) have attracted considerable and sustained attention as they offer the possibility of low-cost conversion of photoenergy.[1] To date, DSSCs with a validated efficiency record of >11% have been obtained with Ru complex dyes.[2] More recently, a DSSC submodule of 17 cm^2 consisting of eight parallel cells with conversion efficiency of >9.9% was fabricated by Sony.[3] Though there is still room for improvement of the efficiency of Ru-based DSSCs, Ru dyes are nevertheless costly, hard to obtain, and normally have moderate absorption intensity.[2,4] Significant effort is being dedicated to develop new and efficient dyes being suitable for their modest cost, ease of synthesis and modification, large molar extinction coefficients, and long-term stability.[5] Organic dyes with donor–π–acceptor (D–π–A) character meet all these criteria. Remarkable progress has been made in the pursuit of organic dyes as sensitizers for DSSCs[6] and efficiencies exceeding 11% have been achieved.[7] Most of the efficient dyes have a cyanoacrylic acid unit as acceptor and anchoring groups.[6]

Among these dyes, porphyrin has attracted a great deal of attention because of its natural role in photosynthesis, its intense absorption in the visible region, its high stability and the relative ease with which functional groups can be attached to its framework.[8] Furthermore, its inherent LUMO level is situated above the conduction band of TiO_2, and its HOMO level is below the redox couple of the electrolyte solution required for charge separation at the semiconductor-dye-electrolyte surface, which makes it a good donor moiety.[9] A large number of porphyrins have been developed as sensitizers for DSSCs such as carboxyphenyl metalloporphyrins,[10] thiophene-, olefin-, and acetylene-linked porphyrins,[11] quinoxaline-fused porphyrins,[12] a Zn–Zn porphyrin dimer,[13] oligo(phenylethynyl)-linked porphyrins,[14] and bacteriochlorin.[15]

From the Goutermann orbital model of porphyrin (Fig. 1), in the ground state, the HOMOs (a_{1u} or a_{2u}) have the orbital density mostly on the porphyrin *meso*-positions and the nitrogens with a small amount of electron density on the β-pyrrolic positions. In the excited state, the electrons go into the LUMO orbitals (E_g) which have electron density on the β-pyrrolic and *meso*-positions. This means that a porphyrin functionalized at the β-pyrrolic positions would be expected to show strong excited state communication. Therefore, incorporation of π-conjugated spacers with cyanoacrylic acid as an acceptor at the β-pyrrolic position of porphyrin would potentially offer strong excited state electron transfer from the porphyrin dye to TiO_2, consequently resulting in a highly efficient dye for DSSCs.

In this work, we present the synthesis and characterization of new functionalized porphyrins bearing two types of π-conjugated spacers, namely benzene and thiophene rings, with cyanoacrylic

* Corresponding author. Tel.: +66 44 224 207; fax: +66 44 224 185.
E-mail address: pvinich@sut.ac.th (V. Promarak).

0040-4039/$ - see front matter © 2013 Elsevier Ltd. All rights reserved.
http://dx.doi.org/10.1016/j.tetlet.2013.03.037

Journal article III

FULL PAPER

EurJOC European Journal of Organic Chemistry

DOI: 10.1002/ejoc.201201479

Synthesis and Characterization of 2D-D-π-A-Type Organic Dyes Bearing Bis(3,6-di-*tert*-butylcarbazol-9-ylphenyl)aniline as Donor Moiety for Dye-Sensitized Solar Cells

Tanika Khanasa,[a] Nittaya Jantasing,[a] Somphob Morada,[a] Nararak Leesakul,[b] Ruangchai Tarsang,[a] Supawadee Namuangruk,[c] Tinnagon Kaewin,[a] Siriporn Jungsuttiwong,[a] Taweesak Sudyoadsuk,[a] and Vinich Promarak*[d]

Keywords: Donor–acceptor systems / Dyes / Sensitizers / Conjugation

A series of novel 2D-D-π-A-type organic dyes, namely CCTTnA (n = 1–3), bearing bis(3,6-di-*tert*-butylcarbazol-9-ylphenyl)aniline as an electron-donor moiety (2D-D), oligothiophene segments with a number of thiophene units from one to three units as π-conjugated spacers (π), and cyanoacrylic acid as the electron acceptor (A) were synthesized and characterized as dye sensitizers for dye-sensitized solar cells (DSSCs). These compounds exhibit high thermal and electrochemical stability. Detailed investigations of these dyes reveal that both peripheral carbazole donors (2D) have beneficial influence on the red-shifted absorption spectrum of the dye in solution and dye adsorbed on TiO_2 film, and the broadening of the incident monochromatic photon-to-current conversion efficiency (IPCE) spectra of the DSSCs, leading to enhanced energy conversion efficiency (η). Among these dyes, CCTT3A shows the best photovoltaic performance, and a maximal incident monochromatic photon-to-current conversion efficiency (IPCE) value of 80 %, a short-circuit photocurrent density (J_{sc}) of 9.98 mA cm^{-2}, open-circuit voltage (V_{oc}) of 0.70 V, and fill factor (FF) of 0.67, corresponding to an overall conversion efficiency η of 4.6 % were achieved. This work suggests that organic dyes based on this type of donor moiety or donor molecular architecture are promising candidates for improved performance DSSCs.

Introduction

Since the report by O'Reagan and Grätzel in 1991 on dye-sensitized solar cells (DSSCs) with dramatically increased light harvesting efficiency,[1] this type of solar cell has attracted considerable and sustained attention because it offers the possibility of low-cost conversion of photoenergy.[2] To date, DSSCs with a validated efficiency record of more than 11% have been obtained with Ru complexes such as the black dye.[3] More recently, a DSSC submodule of 17 cm^2 consisting of eight parallel cells with a conversion efficiency of more than 9.9% was fabricated by Sony.[3] Although there is still room for improvement of the efficiency of Ru-based DSSCs,[4] Ru dyes are nevertheless costly, difficult to attain, and normally have only moderate absorption intensity.[5] Enormous effort is also being dedicated to the development of new and efficient dyes that are suitable with respect to their modest cost, ease of synthesis and modification, large molar extinction coefficient, and long-term stability. Organic dyes meet all these criteria. Thus, there have been remarkable developments in organic dye-based DSSCs in recent years,[6] and efficiencies exceeding 10% have been achieved by using dyes that have broad, red-shifted, and intense spectral absorption in the visible light region.[7] Although remarkable progress has been made in the development of organic dyes as sensitizers for DSSCs, their chemical structures still require optimization for further improvement in performance. Most of the developed organic dyes are composed of donor, π-conjugation, and acceptor moieties, thereby forming a D-π-A structure, and broad ranges of conversion efficiencies have been achieved.[6–8] Most of the highly efficient DSSCs based on organic dyes have long π-conjugated spacers between the donor and acceptor, resulting in broad and intense absorption spectra, aromatic amines as donor moieties, a strong electron-withdrawing group (cyanoacrylic acid) as acceptor, and anchoring moieties. However, the introduction of long π-conjugated segments results in rod-like molecules, which can lead to recombination of the electrons to the triiodide and magnify

[a] Center for Organic Electronic and Alternative Energy, Department of Chemistry, Faculty of Science, Ubon Ratchathani University, Ubon Ratchathani 34190, Thailand
[b] Department of Chemistry, Faculty of Science, Prince of Songkhla University, Hat Yai, Songkhla 90110, Thailand
[c] National Nanotechnology Center, 130 Thailand Science Park, Paholyothin Rd., Klong Luang Pathumthani 12120, Thailand
[d] School of Chemistry and Center of Excellence for Innovation in Chemistry, Institute of Science, Suranaree University of Technology, Muang District, Nakhon Ratchasima 30000, Thailand
Fax: +66-44-224648
E-mail: pvinich@sut.ac.th

Supporting information for this article is available on the WWW under http://dx.doi.org/10.1002/ejoc.201201479.

Journal article IV

Tetrahedron Letters 54 (2013) 4903–4907

Contents lists available at SciVerse ScienceDirect

Tetrahedron Letters

journal homepage: www.elsevier.com/locate/tetlet

An organic dye using *N*-dodecyl-3-(3,6-di-*tert*-butylcarbazol-*N*-yl) carbazol-6-yl as a donor moiety for efficient dye-sensitized solar cells

Taweesak Sudyoadsuk[b], Janeeya Khunchalee[b], Sakrawee Pansay[b], Pongsathorn Tongkasee[b], Somphob Morada[b], Tinnagon Kaewin[b], Siriporn Jungsuttiwong[b], Vinich Promarak[a,*]

[a] School of Chemistry and Center of Excellence for Innovation in Chemistry, Institute of Science, Suranaree University of Technology, Muang District, Nakhon Ratchasima 30000, Thailand

[b] Center for Organic Electronic and Alternative Energy, Department of Chemistry and Center of Excellence for Innovation in Chemistry, Faculty of Science, Ubon Ratchathani University, Ubon Ratchathani 34190, Thailand

ARTICLE INFO

Article history:
Received 12 March 2013
Revised 14 June 2013
Accepted 28 June 2013
Available online 4 July 2013

Keywords:
Organic dye
D–D–π–A
Carbazole
Oligothiophene
Dye-sensitized solar cell

ABSTRACT

New organic dyes, namely **CCTA** and **CFTA** using *N*-dodecyl-3-(3,6-di-*tert*-butylcarbazol-*N*-yl)carbazol-6-yl and 2-(3,6-di-*tert*-butylcarbazol-*N*-yl)-9,9-bishexylfluoren-7-yl as donor moieties, respectively, were synthesized, characterized, and employed as a dye sensitizer in dye-sensitized solar cells (DSSCs). The **CCTA**-sensitized solar cell produces higher device performance with an overall conversion efficiency of 5.69% [a short circuit current (J_{sc}) = 11.31 mA cm^{-2}, an open-circuit voltage (V_{oc}) = 0.71 V, and a field factor (FF) = 0.71] reaching >96% of the reference N719-based device (overall conversion efficiency = 5.92%).

Dye-sensitized solar cells (DSSCs) have attracted considerable and sustained attention due to the potential of low-cost conversion of the photoenergy that they offer.[1] To date, a DSSC with a validated efficiency of >11% has been obtained with Ru complex dyes.[2] More recently, a DSSC submodule of 17 cm^2 made up of eight parallel cells possessing a conversion efficiency of >9.9% was fabricated by Sony.[3] Though there is still room for improvement of the efficiency of Ru-based DSSCs, Ru dyes are nevertheless costly, are difficult to prepare and normally have moderate absorption intensity.[2,4] Significant effort is also being dedicated to develop new and efficient dyes which are suitable for their modest cost, ease of synthesis and modification, large molar extinction coefficient, and long-term stability.[5] Ru-free dyes or organic dyes meet all these criteria. Although remarkable progress has been made in the field of organic dyes as sensitizers for DSSCs,[6] efficiencies exceeding 11% have been achieved,[7] optimization together with simplification of their chemical structures for further improvement in their performance is still necessary. To this end, we have prepared a new, simple donor–π–acceptor (D–π–A) type organic dye, namely (*E*)-5″-(*N*-dodecyl-3-(3,6-di-*tert*-butylcarbazol-*N*-yl)carbazol-6-yl)-2,2′:5′,2″-terthiophene-5-cyanoacrylic acid (**CCTA**), bearing an *N*-dodecyl-3-(3,6-di-*tert*-butylcarbazol-*N*-yl)carbazol-6-yl as a donor moiety for DSSCs (Fig. 1). In our design, 3,6-di-*tert*-butylcarbazole is employed as an additional donor to *N*-dodecylcarbazole, thereby forming a donor–donor moiety (D–D). Recently, many groups have reported that DSSCs using carbazole-based dyes have shown a conversion efficiency (η) up to 9.1%, indicating the importance of their further investigations in DSSCs.[8]

In addition, carbazole derivatives have stimulated interest in their excellent hole-transport ability and have become classic hole-transporting materials.[9] Moreover, the bulky, nonplanar structure of the designed moiety may prove to be valid in solving

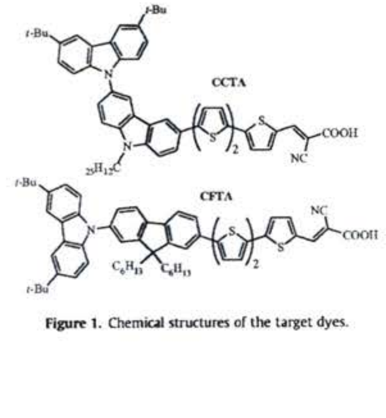

Figure 1. Chemical structures of the target dyes.

* Corresponding author. Tel.: +66 44 224 277; fax: +66 44 224 648.
E-mail address: pvinich@sut.ac.th (V. Promarak).

0040-4039/$ - see front matter © 2013 Elsevier Ltd. All rights reserved.
http://dx.doi.org/10.1016/j.tetlet.2013.06.143

Journal article V

EurJOC European Journal of Organic Chemistry

FULL PAPER

DOI: 10.1002/ejoc.201300373

Synthesis and Characterization of D–D–π–A-Type Organic Dyes Bearing Carbazole–Carbazole as a Donor Moiety (D–D) for Efficient Dye-Sensitized Solar Cells

Taweesak Sudyoadsuk,[a] Sakravee Pansay,[a] Somphob Morada,[a] Rattanawalee Rattanawan,[a] Supawadee Namuangruk,[b] Tinnagon Kaewin,[a] Siriporn Jungsuttiwong,[a] and Vinich Promarak*[c]

Keywords: Dyes / Dye-sensitized solar cell / Sensitizers / Photochemistry / Energy conversion / Oligothiophenes

A series of new D–D–π–A-type organic dyes – **CCTnA** (n = 1–3), **CCT3N** and **CCT2PA**, bearing the 3-(3′,6′-di-*tert*-butylcarbazol-*N*′-yl)-*N*-dodecylcarbazol-6-yl system as an electron donor moiety (D–D) – were synthesized by convenient methods and successfully utilized as dye sensitizers for dye-sensitized solar cells (DSSCs). The central π-conjugated bridges were made of oligothiophene and oligothiophene-phenylene units, whereas the acceptor groups were either cyanoacrylic acid or cyanoacrylamide. Detailed investigation into the relationship between the structures, spectral and electrochemical properties, and performances of the DSSCs is described. The DSSC devices performed remarkably well, with typical overall conversion efficiencies of 3.60–5.69 %, and optimal incident photon-to-current conversion efficiencies (IPCEs) exceeding 80 %. The devices containing oligothiophene bridging groups performed better than those with oligothiophene-phenylene bridging groups. Of solar cells based on these dyes, the **CCT3A**-based one gave a maximum IPCE value of 84 %, a short-circuit photocurrent density (J_{sc}) of 11.31 mA cm^{-2}, an open-circuit voltage (V_{oc}) of 0.71 V and a fill factor (FF) of 0.71, corresponding to an overall conversion efficiency (η) of 5.69 % (>96 % of that of the reference N719-based cell, η = 5.92 %). This work suggests that the organic dyes based on donor moieties or donor molecular architectures of this type are promising candidates for improvement of the performances of DSSCs.

Introduction

Dye-sensitized solar cells (DSSCs) have attracted considerable, sustained attention because they offer the possibility of low-cost conversion of photoenergy.[1] To date, DSSCs with validated efficiency records of >11% have been obtained with Ru complex dyes.[2] More recently, a 17 cm^2 DSSC submodule consisting of eight parallel cells and displaying a conversion efficiency of >9.9% was fabricated by Sony.[3] Although there is still room for efficiency improvement in Ru-based DSSCs, Ru dyes are costly, difficult to produce and normally display only moderate absorption intensity.[2,4] Enormous effort is also being dedicated to the development of new and efficient dyes featuring modest cost, ease of synthesis and modification, large molar extinction coefficients, and long-term stability.[5]

Ru-free organic dyes meet all of these criteria. Although remarkable progress has been made in the use of organic dyes as sensitizers for DSSCs, with efficiencies exceeding 11% having been achieved,[6] the optimization and simplification of their chemical structures for further improvements in performance is still needed. In terms of electronic structure, the LUMO energy level of a dye has to be higher than the energy of the conductive band (CB) of a TiO_2 electrode for efficient electron injection, whereas the LUMO energy level of the dye has to be lower than the iodide/triiodide (I^-/I_3^-) redox potential for oxidation and regeneration of dye, respectively. Additionally, a high absorption coefficient over a wide range of visible light wavelength is required for light-harvesting efficiency.

In terms of molecular structure, avoidance of unfavourable aggregation of dyes is also necessary to achieve high efficiency. π–π Aggregation can lead not only to self-quenching and reduction of electron injection into TiO_2, but also to instability of the organic dye, due to the formation of excited triplet states and unstable radicals under light irradiation conditions.[7] Stability of the dye in its ex-

[a] Department of Chemistry and Center of Excellence for Innovation in Chemistry, Faculty of Science, Ubon Ratchathani University,
Ubon Ratchathani, 34190 Thailand
[b] National Nanotechnology Center (NANOTEC),
130 Thailand Science Park, Klong Luang, Pathumthani 12120 Thailand
[c] School of Chemistry and Center of Excellence for Innovation in Chemistry, Institute of Science, Suranaree University of Technology,
Nakhon Ratchasima, 30000 Thailand
Fax: +66-44224648
E-mail: pvinich@sut.ac.th
pvinich@gmail.com

Supporting information for this article is available on the WWW under http://dx.doi.org/10.1002/ejoc.201300373.